NSWC/WOL MP 76-15

WAVE MAKING BY AN UNDERWATER EXPLOSION

By Gregory K. Hartmann

SEPTEMBER 1976

NAVAL SURFACE WEAPONS CENTER
WHITE OAK LABORATORY

UNCLASSIFIED

SECURITY CLASSIFICATION OF THIS PAGE (When Data Entered)

REPORT DOCUMENTATION PAGE

READ INSTRUCTIONS BEFORE COMPLETING FORM

(14) REPORT NUMBER: NSWC/WOL/MP-76-15

2. GOVT ACCESSION NO.

3. RECIPIENT'S CATALOG NUMBER

4. TITLE (and Subtitle): (6) Wave Making by an Underwater Explosion

5. TYPE OF REPORT & PERIOD COVERED

6. PERFORMING ORG. REPORT NUMBER

7. AUTHOR(s): (10) Gregory K. Hartmann

8. CONTRACT OR GRANT NUMBER(s)

9. PERFORMING ORGANIZATION NAME AND ADDRESS
Naval Surface Weapons Center
White Oak Laboratory
White Oak, Silver Spring, Maryland 20910

10. PROGRAM ELEMENT, PROJECT, TASK AREA & WORK UNIT NUMBERS
0; 0;
0; 0;

11. CONTROLLING OFFICE NAME AND ADDRESS

(11) 12. REPORT DATE: September 1976

13. NUMBER OF PAGES: 159

14. MONITORING AGENCY NAME & ADDRESS (if different from Controlling Office)
(12) 164

15. SECURITY CLASS. (of this report): UNCLASSIFIED

15a. DECLASSIFICATION/DOWNGRADING SCHEDULE

16. DISTRIBUTION STATEMENT (of this Report)

Approved for public release; distribution unlimited

17. DISTRIBUTION STATEMENT (of the abstract entered in Block 20, if different from Report)

18. SUPPLEMENTARY NOTES

19. KEY WORDS (Continue on reverse side if necessary and identify by block number)

Underwater explosions
Wave making
Explosion bubble containment
Explosion bubble blowout

20. ABSTRACT (Continue on reverse side if necessary and identify by block number)

This paper is a historical account of wave making experiments made during and immediately after World War II, from the smallest to the largest scale including the Atom Baker Bikini. The various theories of explosive wave making are discussed and comparisons are made between the observations and the theoretical expectations. Scaling laws are examined for the two distinct cases: explosion bubble containment (deep case) and explosion bubble blowout (shallow case).

DD FORM 1 JAN 73 1473 EDITION OF 1 NOV 65 IS OBSOLETE
S/N 0102-014-6601

UNCLASSIFIED
SECURITY CLASSIFICATION OF THIS PAGE (When Data Entered)

391576

4/1

The influence of the sea bottom is considered. A general conclusion is reached that it is possible to reconcile theory and experiment within a factor of two with regard to wave amplitude and within a few percent with regard to wave period. The number of experiments which are directly applicable to the conditions imposed by theory is limited. Theory in some cases assumes the presence of a rigid bottom, and in other cases no bottom at all; whereas in most experiments a non rigid bottom is present. A synthesis of all these results is made leading to a semi-empirical prescription by which explosively generated waves may be predicted.

The conclusions are not inconsistent with later work in this field done in the last decade.

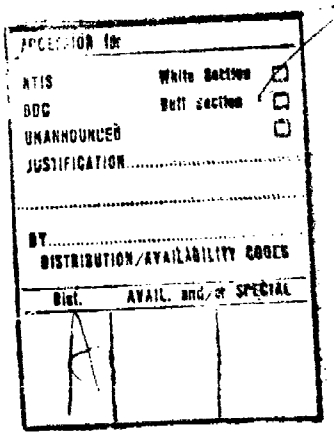

TABLE OF CONTENTS

ILLUSTRATIONS

TABLES

WAVE MAKING BY AN UNDERWATER EXPLOSION

Foreword

Chapter I of this report was written in October 1944. The data had been analyzed and the results had joined the list of possible countermeasures for use against the newly deployed German pressure mine. However, the experiments and their results were not published, partly because they were not very useful for sweeping pressure mines, and partly because of the constraints of security at the time and the demands of other work. During a trip to England in late August 1944 to discuss the results of the experiments with Admiralty officials, J. G. Kirkwood, who was a member of the party, put to paper his general theory of explosion wave making, and this was first published in the British Undex series as No. 94 under the title "Memorandum on the Generation of Surface Waves by an Underwater Explosion." This theory was immediately used for the analysis of the experimental results obtained in the Bureau of Ordnance tests which had been conducted at Solomons, Maryland, in early August, and in later tests conducted by the Underwater Explosion Research Laboratory, at Woods Hole, Massachusetts. The theory, containing numerical evaluations of the necessary integrals made by the Mathematics Tables Project under the Applied Mathematics

Panel of the NDRC, and certain suggestions made by R. J. Finkelstein, J. von Neumann, and F. J. Weyl of the Bureau of Ordnance Research Group on the theory of explosions, was submitted to the Compendium of British and American Reports on Underwater Explosion Research in 1947. The same article minus the tables was published in the Journal of Applied Physics Vol. 19, 346-360, April 1948 under the title "Surface Waves from an Underwater Explosion" by J. G. Kirkwood and R. J. Seeger.

The purpose of the present report is to describe the results obtained in those early experiments which represented a considerable effort and which would be difficult to repeat. It is also of interest that questions concerning the size of waves made by large explosions have arisen from time to time, an early example being in the Crossroads Baker shot at Bikini in August 1946. The results herein reported were of use in the planning for Baker although the data were not originally obtained for that purpose. The production of waves by explosions and their effects in harbours or ports will doubtless continue to be a matter of tactical or strategic interest. The British researches reported in the UER Compendium Volume II, dated early in 1945, were designed in part to calculate or predict the wave effects following the explosion of a ship-load of munitions.

In this report I have used the draft essentially as originally written for the description of the Solomons' experiments and results

(i.e., Chapter I). The discussions of other early experimental data, and of the various early theories and scaling laws have been added. I have only recently seen some of the work done by Tetra Tech, Incorporated and by Scripps Institution of Oceanography described in the "Handbook of Explosion-Generated Waves" TC-130, Oct 1968. I believe that the data given in the present report may be useful though belated addition to their work in the shallow water regime.

In those urgent days of World War II it goes without saying that the Bureau of Ordnance had the advice and counsel of many distinguished men. A meeting was called on 14 August 1944 to discuss the results of the wave making work done up to that time for possible use in mine sweeping. I have a draft memo of that date entitled "Tentative Conclusions" which notes that the optimum charge weight would be such that the depth of water is approximately ten times the radius of the charge, this being roughly the equilibrium bubble radius; that larger charges than that are wasteful: that experiments on large charges indicate that distance has more effect on period than does weight; that the effect of weight if any is masked by errors; that the effect of depth is uncertain. Appended to the memo in longhand is the notation; Present: Brunauer (Commander S.), E. B. Wilson, J. von Neumann, J. G. Kirkwood, J. Keithly, J. Bardine, P. M. Fye, and G. K. Hartmann.

There were many others who participated in this effort: from NOL (hydrophones and photography); from DTMB (photography); from the Applied Explosives Group, BuOrd; from NMWTS Solomons, and other segments of the Navy; and from UERL Woods Hole. Their contributions, although perhaps forgotten by them, may, we hope, be recalled by this belated account and this belated expression of appreciation.

With regard to this current report I would like to express appreciation and thanks to several at the Naval Surface Weapons Center for their help: to Dr. W. C. Wineland for agreeing to publish the report, to Drs. George Hudson, Joel Rogers and George Young for corrections and helpful suggestions, and to Grace Couldren for administrative assistance, and to the Center generally for placing its splendid resources in illustrations and typing at the disposal of this work.

The urgency of these experiments made it impossible to plan them in such a manner that subsequent tests could profit from information learned in earlier tests. It is only in the light of later insights (and in this case much later) that a reasonably unified view of these complex phenomena has been achieved. We must also remember that in this practical world urgency is frequently the spur to get something done. If a problem is not born in a crisis it frequently cannot command the priority to obtain the necessary resources. But in a crisis there is frequently no time to pursue

all questions to a solution. There are therefore some questions which remain open. The role of the bottom and its characteristics has not been theoretically dealt with when the charge is on the bottom or when the depth is shallow. The phenomena shaping the water cavity for shallow explosions in either deep or shallow water have been treated only in gross approximations. The problem of making reliable predictions of wave phenomena caused by large explosions or of scaling from one experiment to another may still be a subject of disagreement or at best of uncertainty. The making of unambiguous predictions should be a part of the repertoire of any explosion phenomena expert. Perhaps in these less urgent days it will be possible to complete the missing information and put this subject to the continued rest that is undoubtedly deserves.

BuOrd Experiments at Solomons	22 Jul - 4 Aug 1944
Conference on Conclusions	14 Aug 1944
Trip to England	Aug - Sep 1944

Kirkwood's memo on "Generation of Surface Waves by an Underwater Explosion" written on this trip and published as Undex-94 by the British.

Shot #6 at Solomons in 100 ft water	6 Sep 1944
Writing on Experimental Results (GKH)	8 - 24 Oct 1944 (Interrupted)
Writing on Theory - Kirkwood & Seeger drafted between	Oct 1944 and Feb 1945
Production of Surface Waves by Underwater Explosion (Distributed and Lumped Charges)	UERL draft by R. W. Spitzer 29 Nov 1944
"Gravity Waves Produced by Surface and Underwater Explosions"	W. G. Penney Imperial College of Science & Technology, London Mar 1945

"Waves in Baker" W. G. Penney (Joint Task Force)	24 Jul 1946
Baker Event Bikini Atoll	25 Jul 1946
"Surface Waves from an Underwater Explosion" J. G. Kirkwood and R. J. Seeger.	submitted to Underwater Explosion Research British-American Compendium. 27 May 1947

Identical article minus tables appeared in Journal of Applied Physics Vol. 19, pp 346-360 Apr 1948.

Writing on Experimental Results and Analysis (G. K. H.) resumed and completed Jan - Feb 1976.

I. TESTS AT SOLOMONS, (1944)

1. Introduction

In the summer of 1944 tests were planned and conducted to produce gravity waves in water by explosions, and to determine their suitability for sweeping pressure mines. Although it is well known from casual observations of underwater explosions that the detonation of conventional charges, say depth charges, produces practically no observable wave system, nevertheless it was felt desirable to try larger charges and to make specific preparations to observe whatever surface waves were formed.

2. Site

A site for this series of experiments was chosen in the Patuxent River at the Naval Mine Warfare Test Station (NMWTS) Solomons, Maryland. The depth of water at this spot off Sotterley's Point was about 40 feet over an area at least 2,000 feet by 1,000 feet. The bottom was a soft mud into which for example a mine would sink about three feet. This mud probably influenced the magnitude of the waves, but the first requirement was to find a large uniform area sufficiently remote to allow the experiments to be done.

3. Experimental Arrangement

Observations on the waves produced were made in three ways: by aerial photography to determine wavelengths and velocities; by surface photography to measure surface wave amplitudes and periods; and by pressure recording systems placed on the bottom. The aerial photography was accomplished from a blimp. In order to measure the surface amplitudes a range of telephone poles was set up. Each pole was 30 feet long and was submerged in the water by a 300 pound anchor so that about 7 feet of the pole extended into the air. The top portion of the pole was painted with alternate black and white strips 6 inches wide. The range consisted of about a dozen poles in a straight line about 140 feet apart.

The wave motion was found to have very little effect on the poles, except at distances less than about 300 feet from the explosion where the outward rush of water caused the poles to sway, rotating more or less about their anchors and thereby submerging themselves. The pressure recording systems consisted of units each composed of a NOL Mk 1 hydrophone, a bridge network and an Estraline Angus recorder. The hydrophone was protected from explosive shock by a rigid bronze cone which allowed slow seepage through a small hole but which screened out very sharp changes in pressure. This protective device was tried out in a preliminary series of shots made 22 July (reported by J. F. Moulton, BuOrd memorandum) in which it was found that the pressure sensitive diaphragm would operate

successfully if the shock impulse from the explosion, making allowance for surface reflection, was less than 0.25 lb sec/in^2.

The main shots were carried out under Explosive Investigation Memorandum No. 62 under BuOrd forwarding letter S68 005316 of 22 July 1944. The schedule of shots fired is shown in Table 1.

Note to Table 1.

The bombs LC, AN, M56 were initiated by filling the nose fuze seat liner with Comp C-2 and detonating this statically by means of an Army Engineer Special detonator. The Demolition charges used were the Mk 14 Mod 1 approximately 50 plus pounds Cast TNT no booster, 13" x 13" x 6½" in cardboard box. Mk 9 approximately 115 pounds cast TNT with 63 grams auxiliary booster Mk 4 (1.6" diameter, 3" length granular TNT) 13" x 13" x 13" in steel container. For shot 4, the charges were crated in cubical boxes approximately 5 feet on a side. In each crate a Mk 9 charge was set in the middle and an electric detonator was used to initiate it. Each crate contained 180 Mk 14 Mod 1 demolition charges and one Mk 9, making about 9,200 pounds of charge in each box.

4. Shot 1

The size of charge for the first shot was chosen by considering that the bubble radius of the expanded gases should be at least

Table 1 Schedule of Shots

Date	Solomons Shot No.	Local Number	Wt. lbs (TNT)	Blimp	Surface Photography	Pressure Recorder	Water Depth
	494	1	3362 (1 block buster)	Yes	Yes	No	~40 ft
	495	2	6724 (2 block busters)	Yes	Yes	Yes (one distance)	~40 ft
	497	3	23,534 (7 block busters)	No	Yes	Yes (one distance)	~40 ft
4 Aug 1944	501	4	45,575 (Dem. Charges)	No	Yes	Yes (two distances)	~40 ft
	502	5	2,034 (Dem. Charges)	No	Yes (?)	Yes (two distances)	~40 ft
6 Sep		6	2.025 (Dem. Charges)	No	No	Yes (one distance)	~100 ft

equal to the depth of the water. For convenience the charges were placed on the bottom although it was realized that this might not be the most efficient use of the explosive. Since the wave making process is so inefficient from the standpoint of energy, the question as to the best possible position for the charge does not seem to be of prime importance. The maximum bubble radius for an underwater explosior of TNT at depth D is given in the absence of free or rigid surfaces by

$$r_{max} = 13.5 \frac{W^{1/3}}{(33 + D)^{1/3}} \text{feet}$$

where W is the weight of charge in pounds. This assumes that 45% of the total explosive energy is retained in the bubble. Putting r_{max} = 40 feet gives W = 1,900 pounds. The unit chosen for the first shot was a 4,000-pound bomb containing 3,362 pounds of TNT. This choice yielded a charge which was presumably large enough and at the same time easy to handle.

For Shot No. 1 the range of poles was photographed by means of especially mounted aircraft cameras having a field of view of 40^{o}, and capable of taking a picture every 2/5 second. In order to save film an estimate of the time of arrival of the waves at the various

poles was made using the velocity expected for waves of length great compared to the depth, i.e., $V = \sqrt{gh} = 36$ ft/sec. For a pole at a distance of say 1,000 feet from the explosion, the earliest possible time of arrival of waves would be 28 seconds. At this time and thereafter, however, on Shot 1 there were observed no waves at all at these distances and consequently the cameras were turned off or in some cases not started and consequently no records of any value were obtained. However, a subsequent examination of the aerial pictures taken from the blimp at altitude 1,500 feet showed unmistakably a system of ring waves extending at least 1,400 feet from the explosion and with wavelength increasing with increasing distances. Consideration of these pictures shows that the long slow swell of the outer rings would not be observable except under very calm surface conditions and only then by an observer with some experience . Figure 1 shows a sequence of photographs taken at t = 0, 27, 45 and 71 seconds after the explosion.

5. Camera Arrangement and Details

Consideration of these aerial photographs made it necessary to investigate somewhat more in detail the wave system produced. Accordingly, on Shot 2 the camera setup was changed so that long focus narrow field lenses were used with one camera on each pole. The number of poles photographed was considerably reduced. A special 70 mm Mitchell camera was supplied and operated by the David Taylor Model Basin, which could photograph two poles simultaneously.

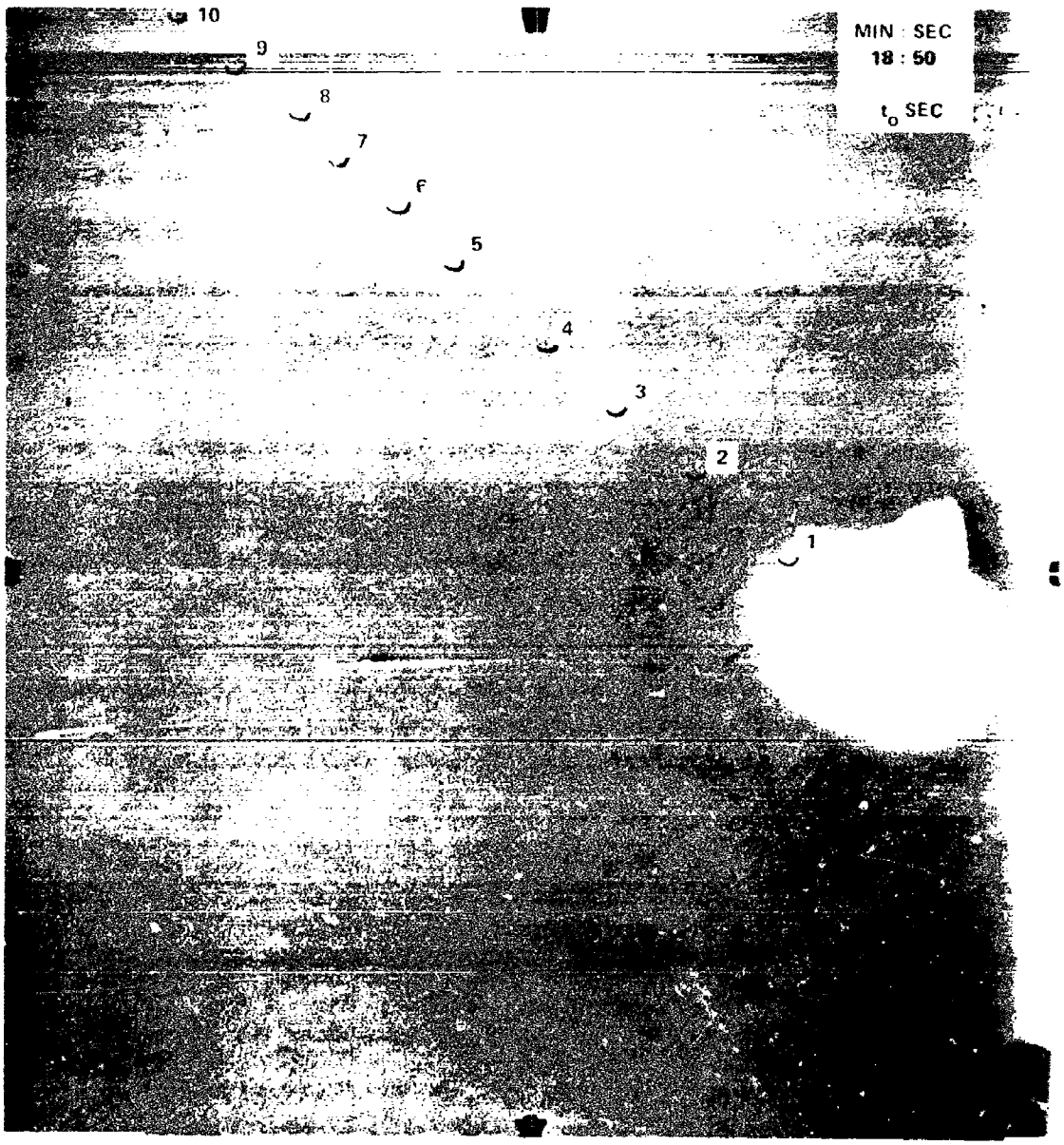

Approximate Pole Distances with Explosion at 0

Pole Number	Distance	Pole Number	Distance
1	142 Ft.	7	976 Ft.
2	284	8	1096
3	399	9	1264
4	546	10	1425
5	714	11	1575
6	849	12	1669

Figure 1(a) Shot Number 1 – 3362 Lbs. TNT on Bottom – Water Depth ~40 Ft.

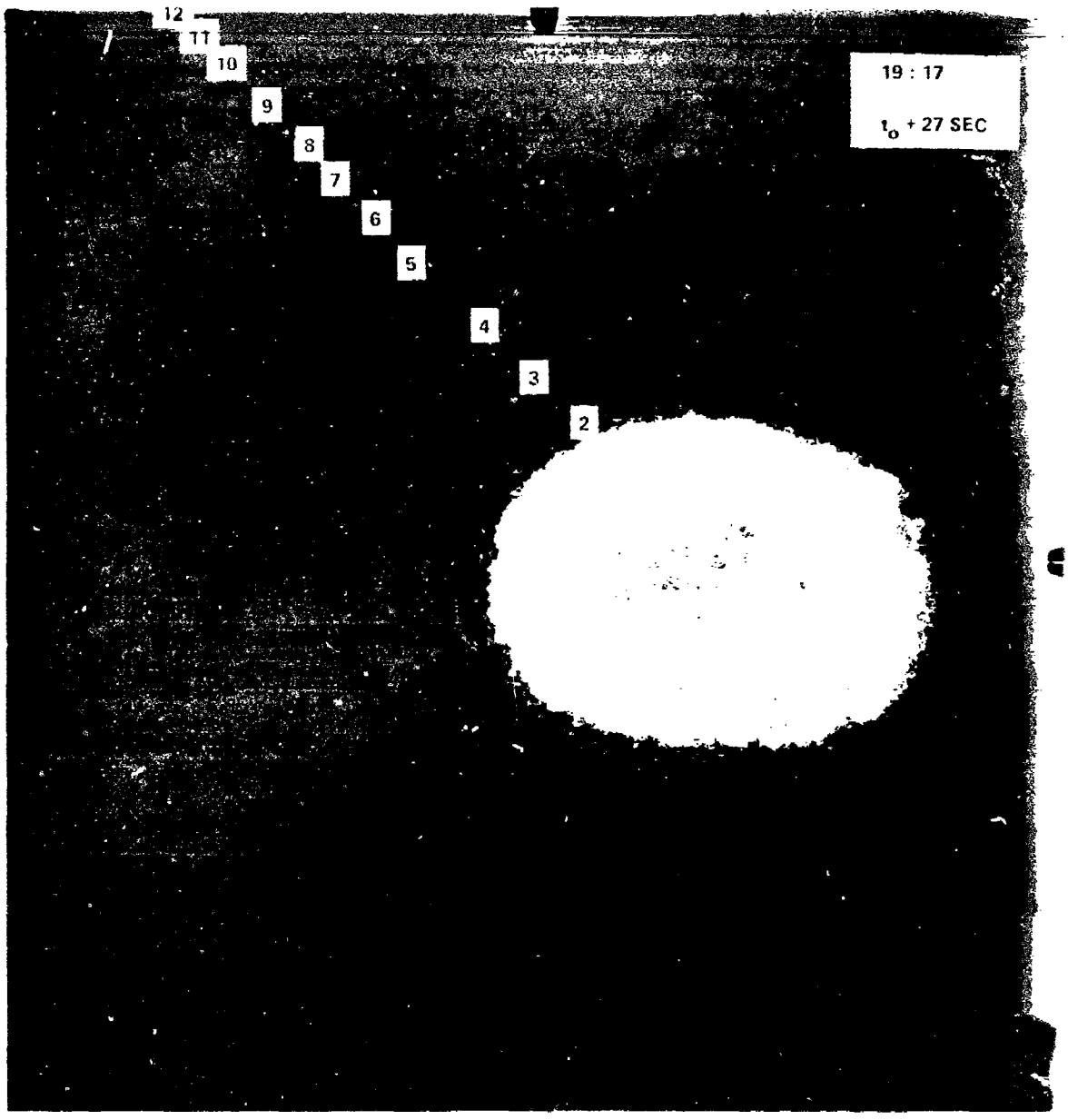

Approximate Pole Distances with Explosion at 0

Pole Number	Distance	Pole Number	Distance
1	142 Ft.	7	976 Ft.
2	284	8	1096
3	389	9	1264
4	546	10	1425
5	714	11	1575
6	849	12	1669

Figure 1(b) Shot Number 1 – 3362 Lbs. TNT on Bottom – Water Depth ~40 Ft.

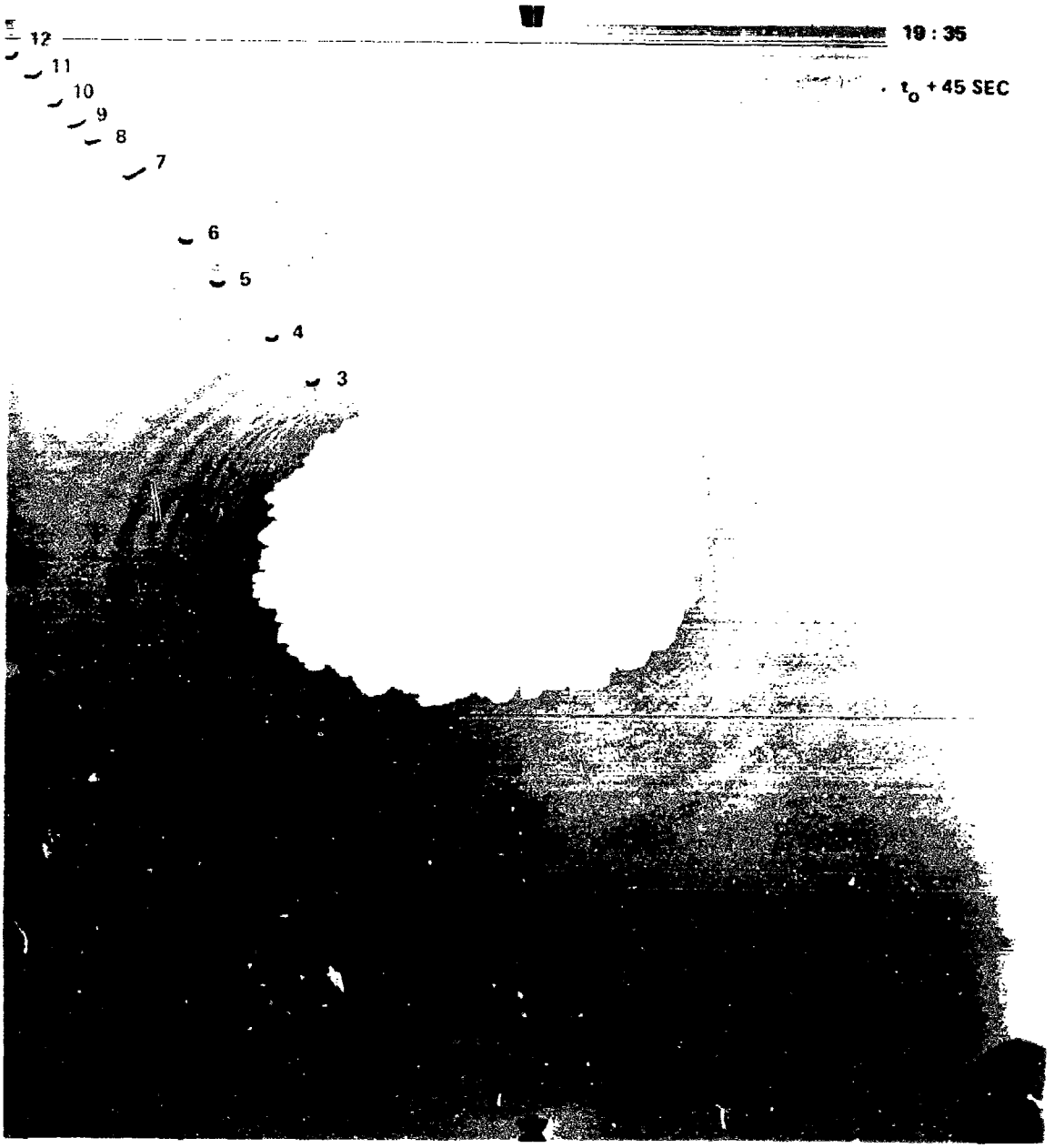

Approximate Pole Distances with Explosion at 0

Pole Number	Distance	Pole Number	Distance
1	142 Ft.	7	976 Ft.
2	284	8	1096
3	389	9	1264
4	546	10	1425
5	714	11	1575
6	849	12	1669

Figure 1(c) Shot Number 1 – 3362 Lbs. TNT on Bottom – Water Depth ~40 Ft.

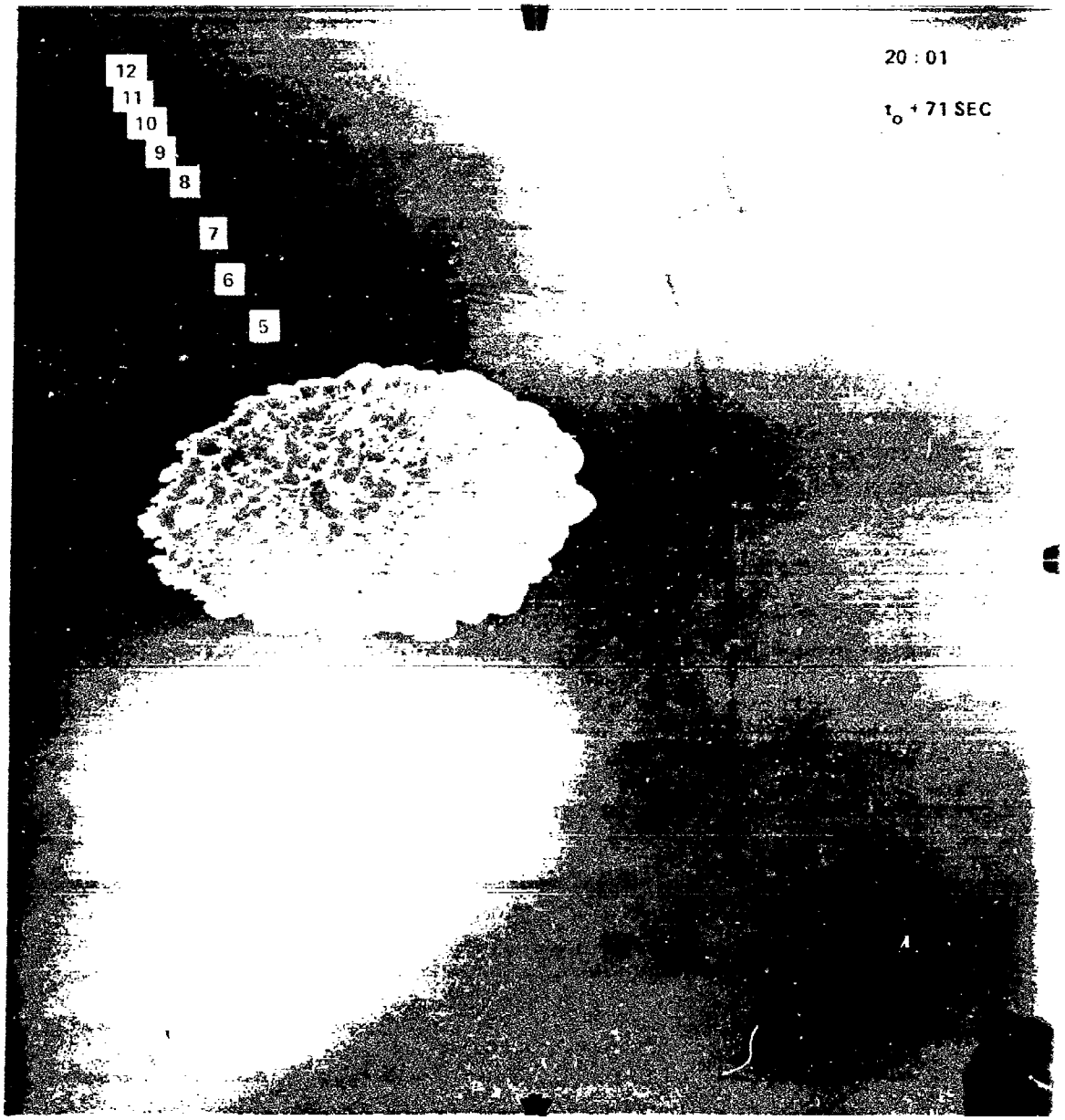

Approximate Pole Distances with Explosion at 0

Pole Number	Distance	Pole Number	Distance
1	142 Ft.	7	976 Ft.
2	284	8	1096
3	389	9	1264
4	546	10	1425
5	714	11	1575
6	849	12	1669

Figure 1(d) Shot Number 1 – 3362 Lbs. TNT on Bottom – Water Depth ~40 Ft.

The records obtained by this camera were used to determine wavelength by measuring the difference in phase between waves at the two poles. In all the photographic work due attention was paid to getting optimum resolution by reducing the circle of confusion and the optical diffraction to a value less than the resolving power of the film. Details as to the various cameras used are given for the sake of completeness in Table 2. Wave amplitudes could be estimated to about ± ½ inch with the lenses of longest focal length.

6. Distances

The range of poles was set out at the beginning of the series and the positions of the poles were determined before each shot by means of a range finder (1 meter base) and a crude azimuth (polaris) circle graduated in degrees. The distances and angles were plotted out for each shot and give rise to the following table of distances.

The various interpolar distances obtainable from this table permit an estimate to be made of the precision of measurement of distance. It turns out that if σ^2 is the variance associated with the mean distance, m, between poles, then $\sigma = \pm 0.085m$. This means for example that the best distance between pole 11 and 12 on all shots is 109 feet ± 6 feet, using probable error equal to 2/3 σ.

Table 2 Details as to Cameras

Camera	Focal length	Speed	Stop =n	p_∞	Field of View	Distance	6" at this distance appears on film as
F54 in blimp 7" film	10"	Every 2 sec	--	--	40°	2000'	.0025"
K25	6 3/8"	2½ frames/sec	16	335'	40°	380'-680'	.0095"-.0049"
35 mm Mitchell	17"	24 frames/sec	16	2390'	3.5°	430'	.020"
70 mm Mitchell	6"	10 frames/sec	16	298'	19°	360'	.0069"

Where $n = f/d$

Resolving power of the film $\tilde{=}$ 50 lines/mm = .0008"

Resolving power of lens = $f0 = 1.22 \lambda n$ = .0004" if n = 16 for all lenses.

C = Diameter of circle of confusion $\leq$ .00063"

Corresponding hyperfocal distance = $p_\infty = f^2/cn$,.

Table 3 Distances from Explosions to Poles in feet

Pole Number	Shot 1	Shot 2	Shot 3	Shot 4*	Shot 5*
0	Charge	-	-	-	-
1	142	-	-	-	-
2	284	-	-	-	-
3	389	-	-	-	-
4	546	-	charge	-	-
5	714	charge	-	-	-
6	849	168	-	-	-
7	976	299	412	879	636
8	1096	419	517	1028(H)	771(H)
9	1264	581	659	1170	927
10	1425	753	801	-	-
11	1575	895	928	-	-
12	1669	1007(H)	1048(H)	1579	1330
13	-	-	-	-	-
14	-	-	-	-	-
15	-	-	-	2000	1760
16	-	-	-	2140(H)	1896(H)
17	-	-	-	2363	2120

(H) indicates hydrophone placed on bottom near pole.
* charge not at pole.

7. Wavelength vs. Velocity (aerial data)

On Shot 2, photographs from the air were also obtained. The average interval between pictures was 2.5 seconds. From these pictures in which a scale was provided by a barge 110 feet long, the distances between some of the outer poles was determined. These compare well with the average interpolar distances obtained by range finder and circle. Thus:

Distance Between Poles	Range Finder Method Ave.	Aerial Photograph
9 and 10	158 feet	165 feet
10 and 11	140 feet	138 feet
11 and 12	109 feet	112 feet

From these photographs a plot was made of the distance travelled versus time since the explosion for the first three troughs in the wave pattern (Figure 2). The troughs were identified by the presence of shadow. There is, however, some question as to whether the first trough observable is really the first trough in

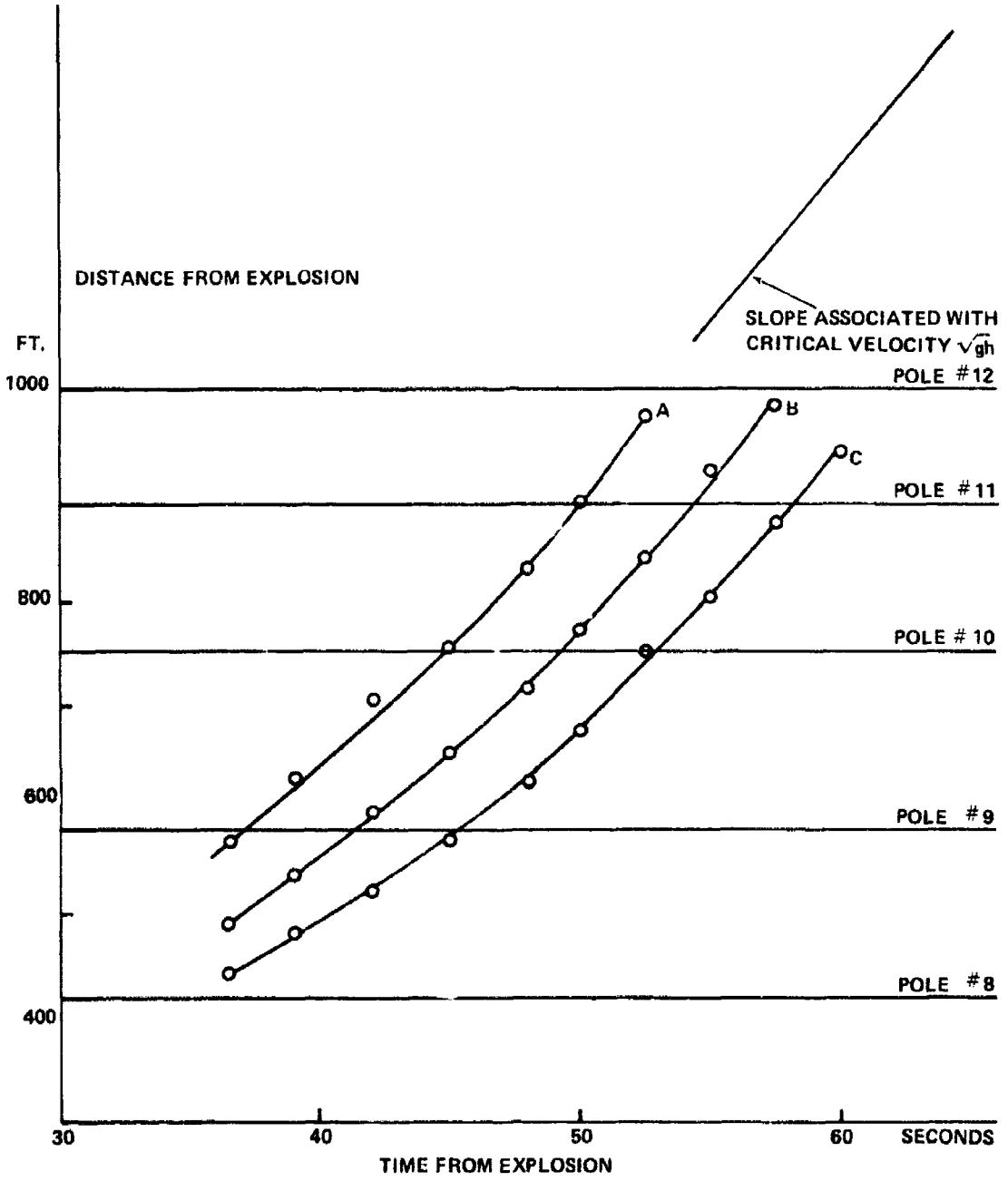

FIG. 2 TIME - DISTANCE PLOT FOR TROUGHS A, B, AND C OF SHOT 2
(FROM AERIAL PHOTOGRAPHS)

the series since the glare from the sun makes that part of the water surface uniformly light in the region into which any rapidly travelling leading wave would advance. This is illustrated in the photograph, Figure 3. This is mentioned as a caution in the application of the aerial technique for measuring wavelength. Indeed the hydrophone record appended to Figure 3 shows that the first section has already arrived at pole 12 before a wave disturbance shows itself from the air.

Various wavelengths in the pattern resulting from Shot 2 reveals that the first one has been missed. The first visible trough is called A, the second B and the third C.

In Figure 2 it is seen that the slopes of the three curves increase with distance and that the velocity $\sqrt{gh}$ = 35 ft/sec, is approached. It is also apparent that the separation between successive troughs increases with distance, which is to say that the wavelength is increasing with distance. Thus the separation between A and B varies as follows with distance:

Figure 3 Shot Number 2 At this time the hydrophone record at Pole 12 showed the first suction maximum. The first visible trough (between Poles 10 and 11) appears to be the second suction (labeled A).

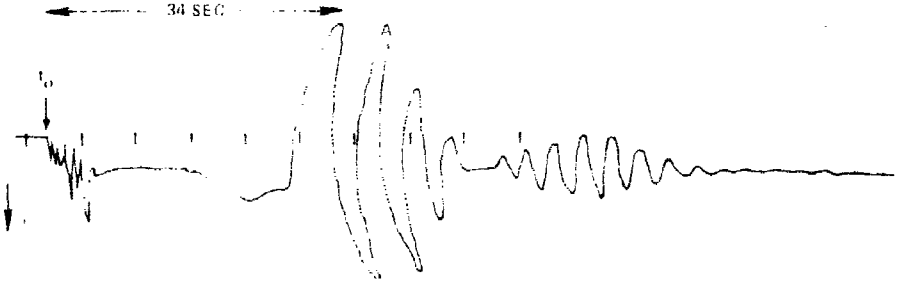

Pole	Distance from explosion of crest between A and B	Distance from A to B = λ	Velocity of crest between A and B	V computed from λ
9	581 ft	95 ft	22 ft/sec	22 ft/sec
10	753 ft	112 ft	22 ft/sec	24 ft/sec
11	895 ft	119 ft	29 ft/sec	24 ft/sec
12	1007 ft	123 ft	31 ft/sec	25 ft/sec

The values in the last column are computed from:

$$V = \frac{\lambda}{T} = \left(\frac{g\lambda}{2\pi} \tanh \frac{2\pi h}{\lambda}\right)^{\frac{1}{2}}, \text{ (See Appendix A),}$$

taking $h = 38$ feet. It is noted that at this depth and at these wavelengths the value of V according to the ordinary monochromatic theory increases very slowly with λ in this range. It is of course not surprising that the simple theory does not agree exactly with the observed velocities.

8. Wavelength vs. Velocity (surface data)

On Shot 2 the 70 mm Mitchell camera was trained on poles 11 and 12. The distance between these poles is taken as 109 feet. The surface records obtained are reproduced in Figure 4. The pressure record obtained near pole 12 is also shown. The correspondence between the surface amplitude measurements and the bottom pressure measurements is very good. It is possible to number the positive pressure peaks after the first suction, and the surface crests after the first trough and to put these into one to one correspondence. The camera was set to run at 8 frames/second, but comparison of the times of arrival of corresponding peaks at the bottom and at the surface, assuming that the Esterline-Angus timescale was correct, reveals that the camera was running a little fast. To correct intervals the following factor must be used

$$\Delta t_{true} = .87\ (\Delta t_{70\text{ mm camera}})$$

Even this does not provide a perfect correction because of local variations of speed in the camera.

The wavelengths were measured from the film record as follows: Let Δt_{70} = time of arrival at pole 12 -- time of arrival at pole 11. The resulting velocities, periods and wavelengths are listed in Table 4.

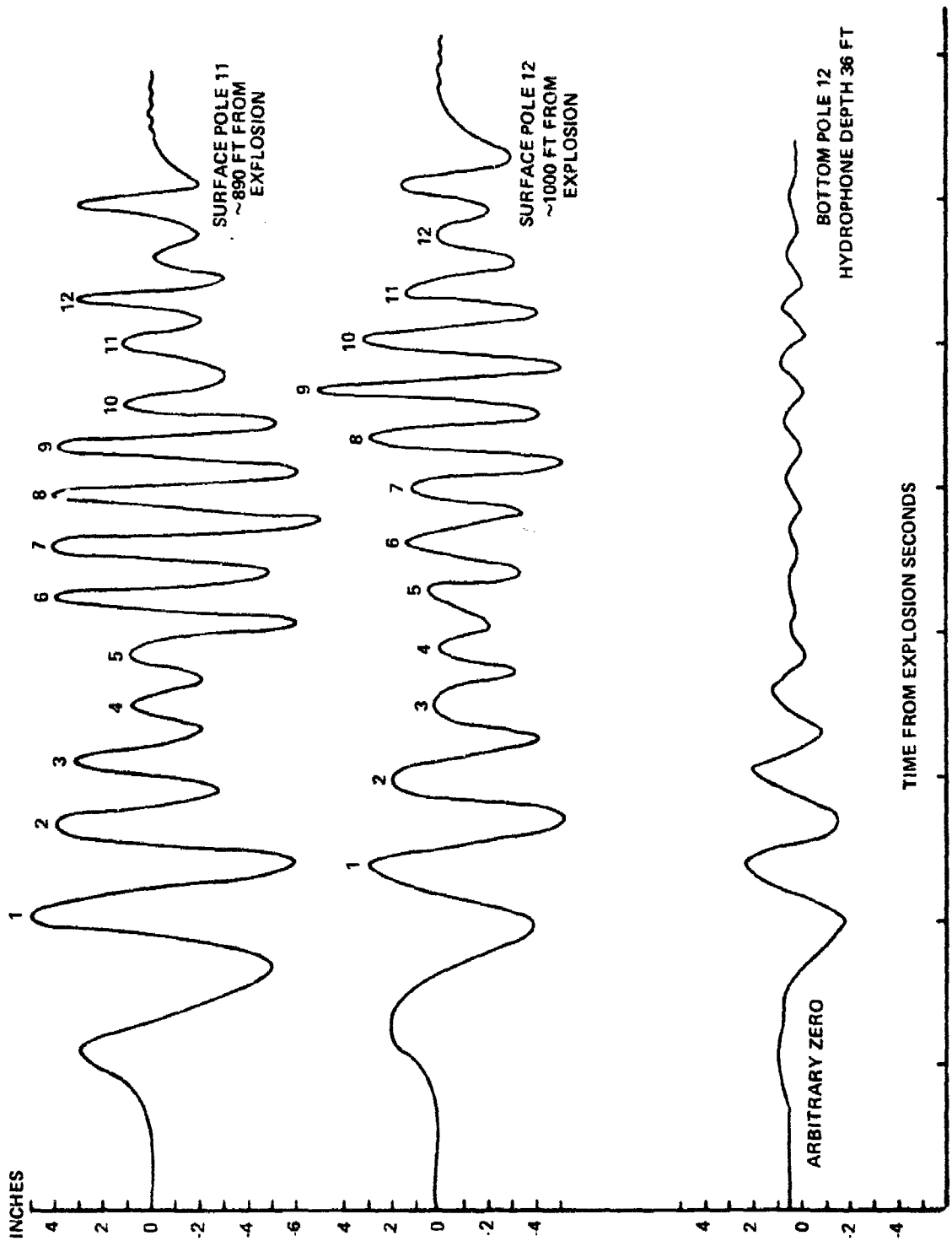

FIG. 4 COMPARISON BETWEEN SURFACE WAVES AND PRESSURES AT THE BOTTOM
SHOT 2 6724 LBS TNT DEPTH OF WATER 37.5 ON BOTTOM

Table 4 Wavelengths and Velocities, Shot 2

Number of Crest After First Trough	1	2	3	4	5	6	7	8	9	10	11	12
Δt_{70}	3.4 sec	3.66	4.50	4.40	4.86	4.77	4.68	4.82	4.82	5.32	4.50	5.35
Δt_{true}	2.96	3.18	3.92	3.83	4.22	4.15	4.07	4.19	4.19	4.64	3.92	4.65
vel = $\frac{109}{\Delta t_{true}}$	37 ft/sec	35	28	29	26	26	27	26	26	24	28	24
True Period = .87 x Measured Period at pole 12	5.95 sec	5.14	3.9	3.9	3.7	3.5	3.6	3.4	3.5	3.4	37	
ave. vel. ft/sec	36	31.5	29.5	27.5	26	26.5	26.5	26	25	26	26	
λ = ave. vel. x period, (ft)	214	162	116	108	97	92	94	88	87	88	95	

These wavelengths are not comparable with those measured from aerial photographs, since those were measured from trough to trough, whereas these are measured from crest to crest. Further, as has been mentioned, it is uncertain whether the first trough was visible at all from the air.

Schematically the situation is thus:

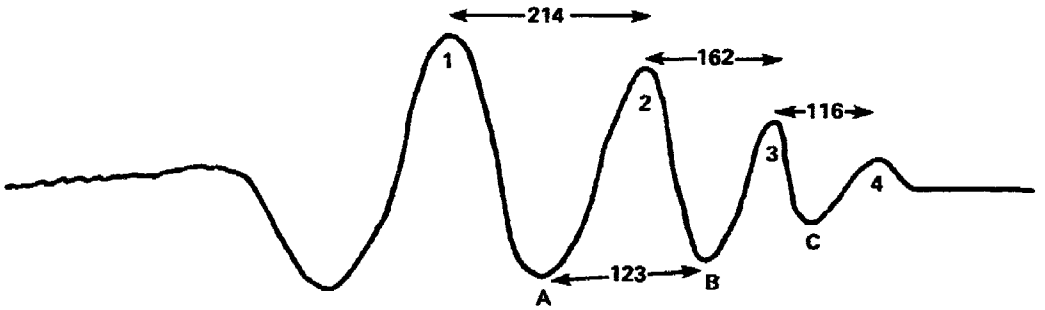

This might suggest that perhaps A is really the third trough. This possibility is not ruled out by the comparison of the velocities. It is certainly true that difficulties of observation make the measurements from aerial photographs much less reliable than direct measurements on the surface. In subsequent shots the aerial photography was dispensed with.

9. Addendum (1976)

The consistency of these measurements may be checked as follows: If Δt = time taken for a given crest to travel from pole 11 to pole 12, i.e., 110 feet then,

$$\text{velocity} = \frac{110}{\Delta t} \qquad \text{- - - - - -} \qquad (1)$$

T = period from one crest to the next at pole 12. Hence, λ = velocity x T. Having found the value for λ we ask what velocity does this require, from

$$v^2 = \frac{g\lambda}{2\pi} \tanh \frac{2\pi h}{\lambda} \qquad \text{- - - - - -} \qquad (2)$$

(See Figure 5)

λ=	214 ft	162	116	108	97	92	94	88	87	88	95
average vel from (1)	36 ft/sec	31.5	29.5	27.5	26	26.5	26.5	26	25	26	26
velocity from (2)	30	27	24	23.4	22	21	21	21	21	21	21

The discrepancy in velocity can be largely eliminated by eliminating the correction made for the speed of the camera. If in fact the camera was accurate and the recorder was inaccurate, (and there is no way to be sure now) then the systematic bias can be relieved. This means that the values for the periods and durations as

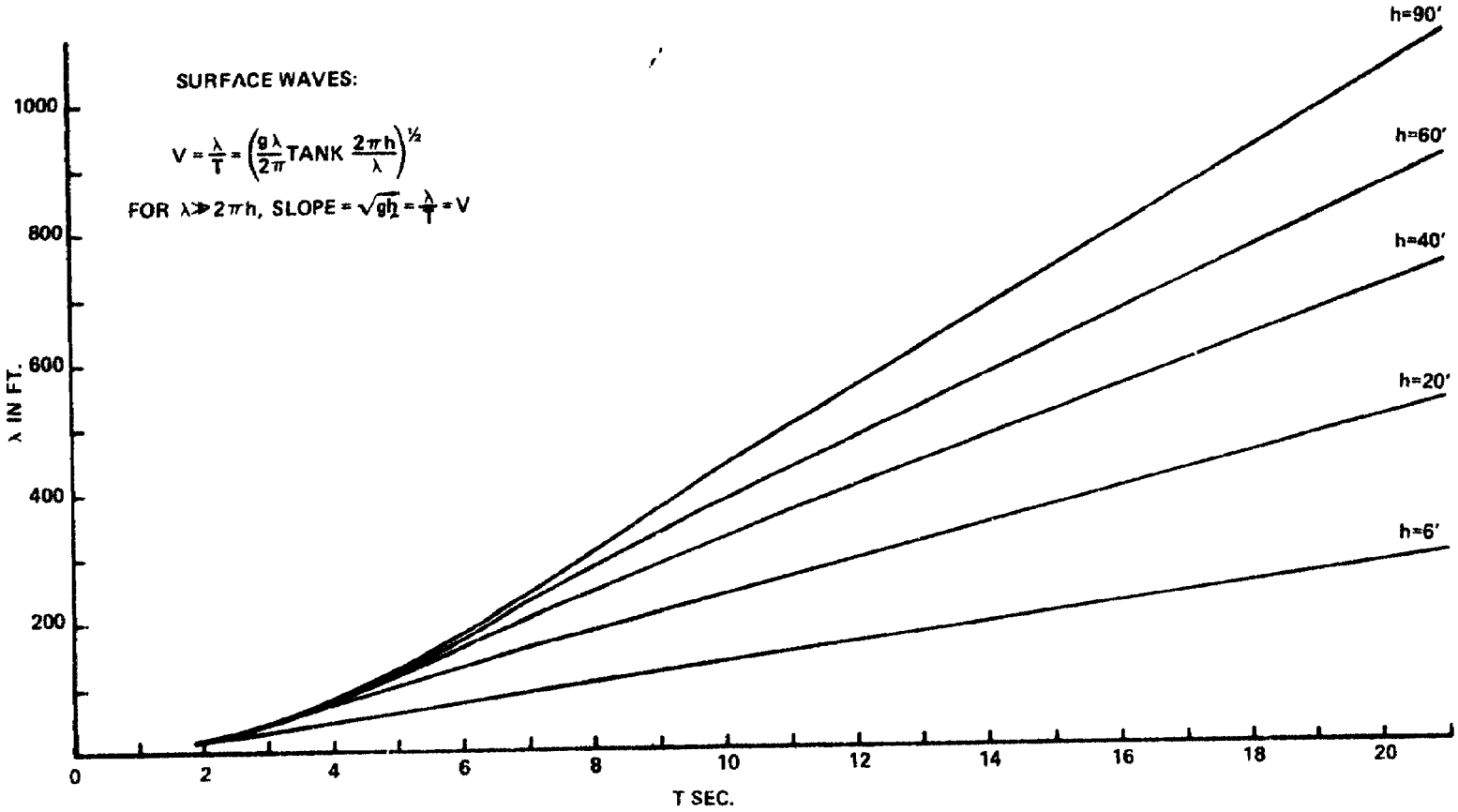

FIG. 5 WAVE LENGTH VS. PERIOD FOR VARIOUS DEPTHS.

determined by the hydrophone at least on this shot should be increased by about 15%. Rather than indulge in such a correction program I will leave the numbers as originally noted with a caution as to the general accuracy of all the measurements. Figure 6 shows the surviving aerial photographs from Shot 2, taken at 11, 27, 46 and 57 seconds after the explosion. In the two earlier pictures the waves had not appeared whereas in the last picture the earliest swells have gone beyond the range of poles. The picture taken at 46 seconds, however, lets one with a little imagination list the distances from the outermost dark ring (beyond pole 12) to the next one inside and so on. These distances are wavelengths and are approximately 178, 113, 97, 86, and 59 feet which brings us just inside pole 9. This is an instantaneous view of the wave pattern. The longer waves travel faster than the shorter ones and consequently the pattern spreads out creating longer waves which then travel faster. The whole pattern will spread out until all the waves are long enough to travel at the same maximum speed. By that time however the waves will have vanished. Even in this photograph at 46 seconds, the "first" wave has a wavelength which is somewhat shorter than the wavelength of the first wave obtained from pole photography. It is therefore concluded that the waves of very long length (and hence very slight slopes) cannot be reliably detected by aerial photography.

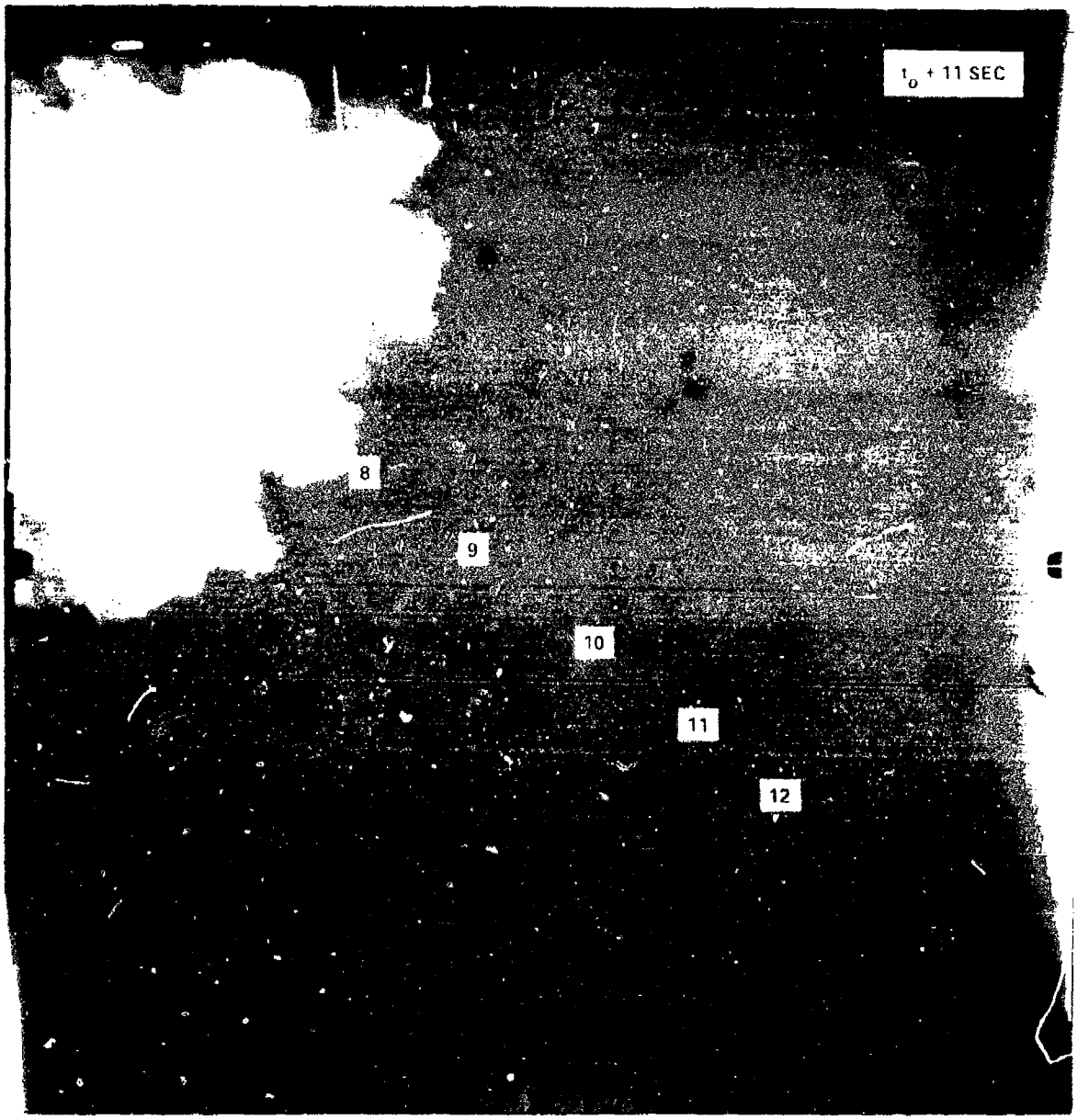

Approximate Pole Distances with Explosion at 0

Pole Number	Distance	Pole Number	Distance
6	168 Ft.	10	753 Ft.
7	299	11	895
8	419	12	1007
9	581		

Explosion Occurred at t_0 = 16:37:09

Figure 6(a) Shot Number 2 – 6724 Lbs. TNT on Bottom – Water Depth ~40 Ft.

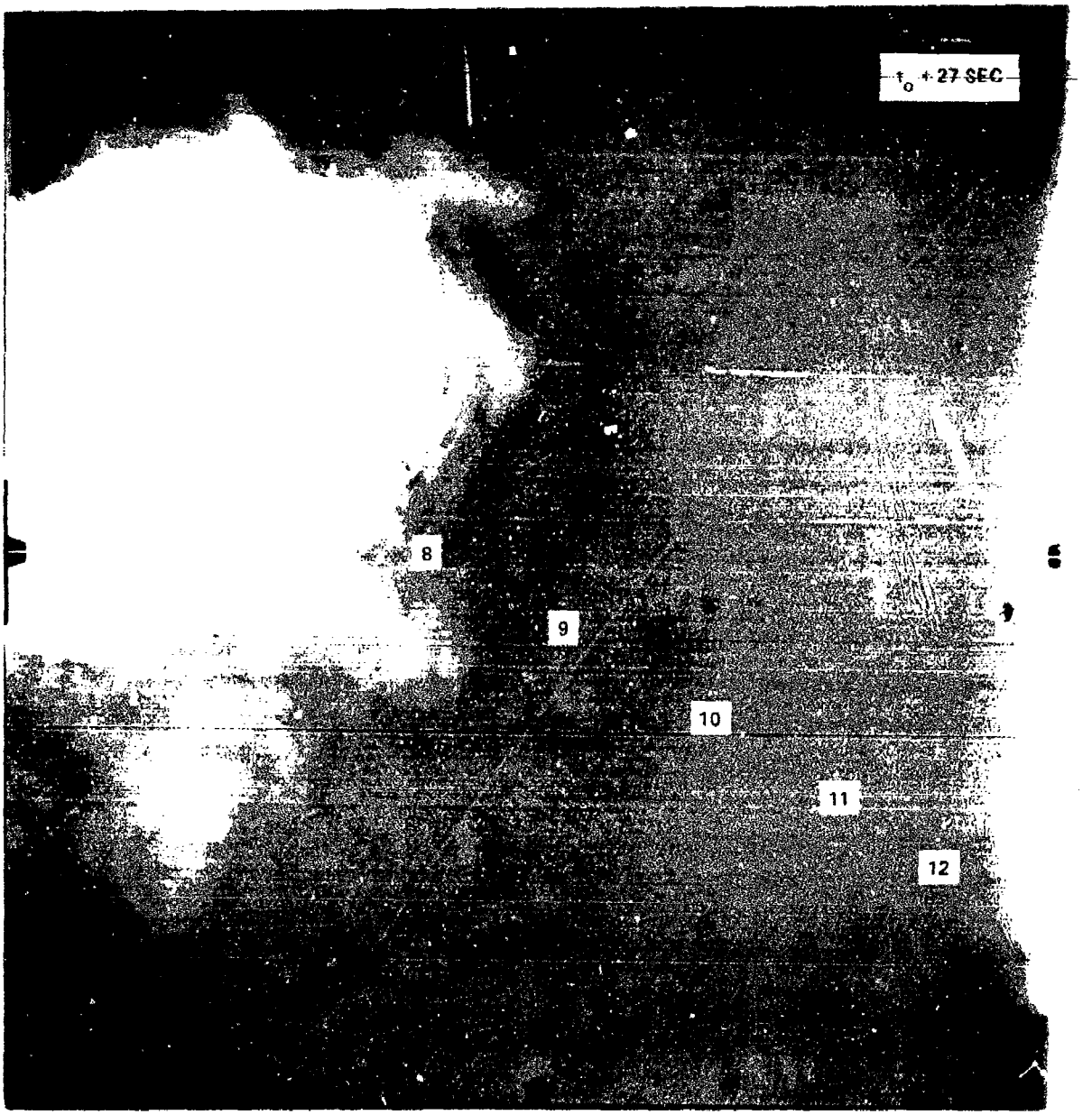

Approximate Pole Distances with Explosion at 0

Pole Number	Distance	Pole Number	Distance
6	168 Ft.	10	753 Ft.
7	299	11	895
8	419	12	1007
9	581		

Explosion Occurred at t_o = 16:37:09

Figure 6(b) Shot Number 2 – 6724 Lbs. TNT on Bottom – Water Depth ~40 Ft.

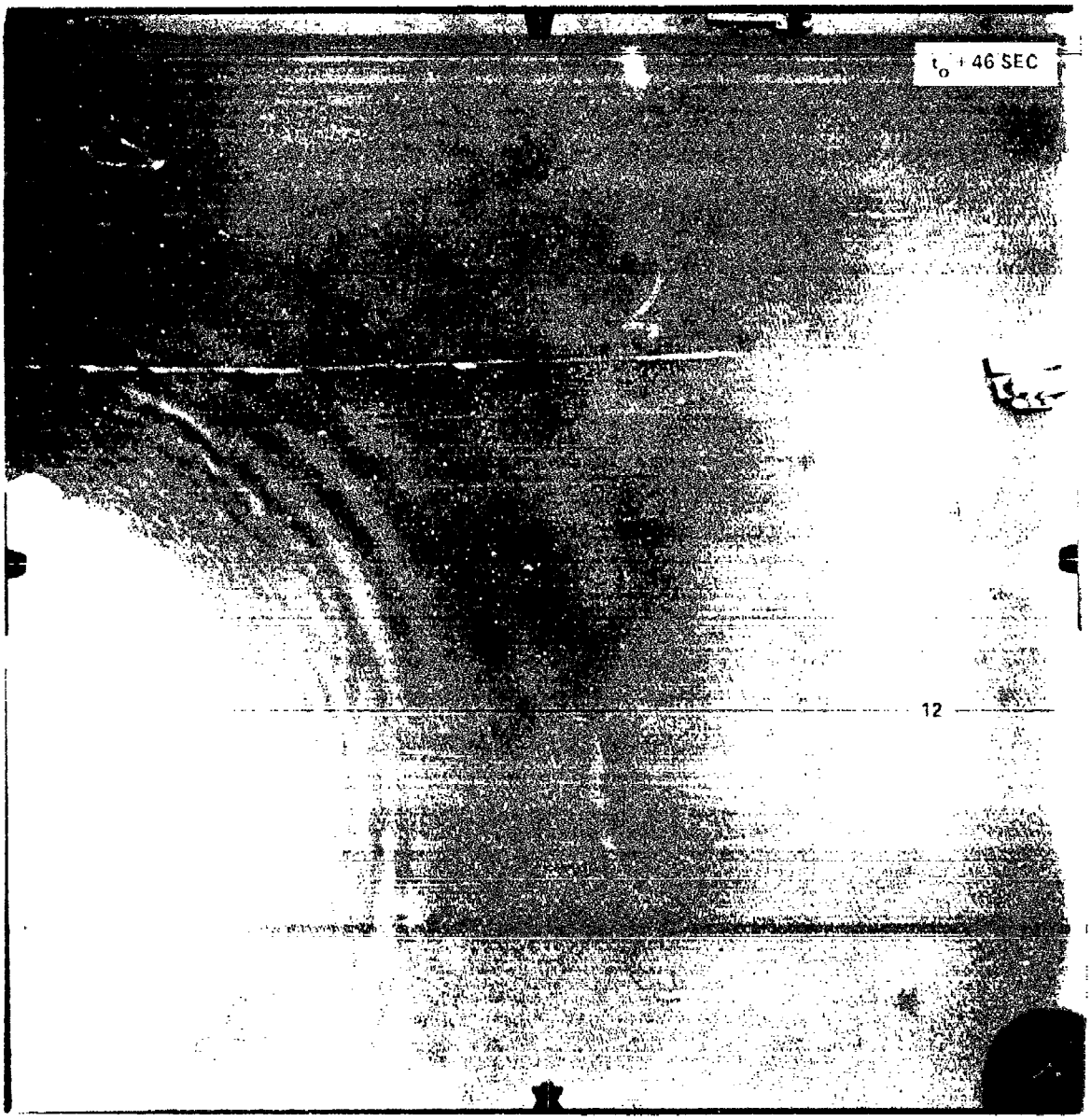

Approximate Pole Distances with Explosion at 0

Pole Number	Distance	Pole Number	Distance
6	168 Ft.	10	753 Ft.
7	299	11	895
8	419	12	1007
9	581		

Explosion Occurred at t_o - 16:37:09

Figure 6(c) Shot Number 2 6724 Lbs. TNT on Bottom Water Depth ~ 40 Ft.

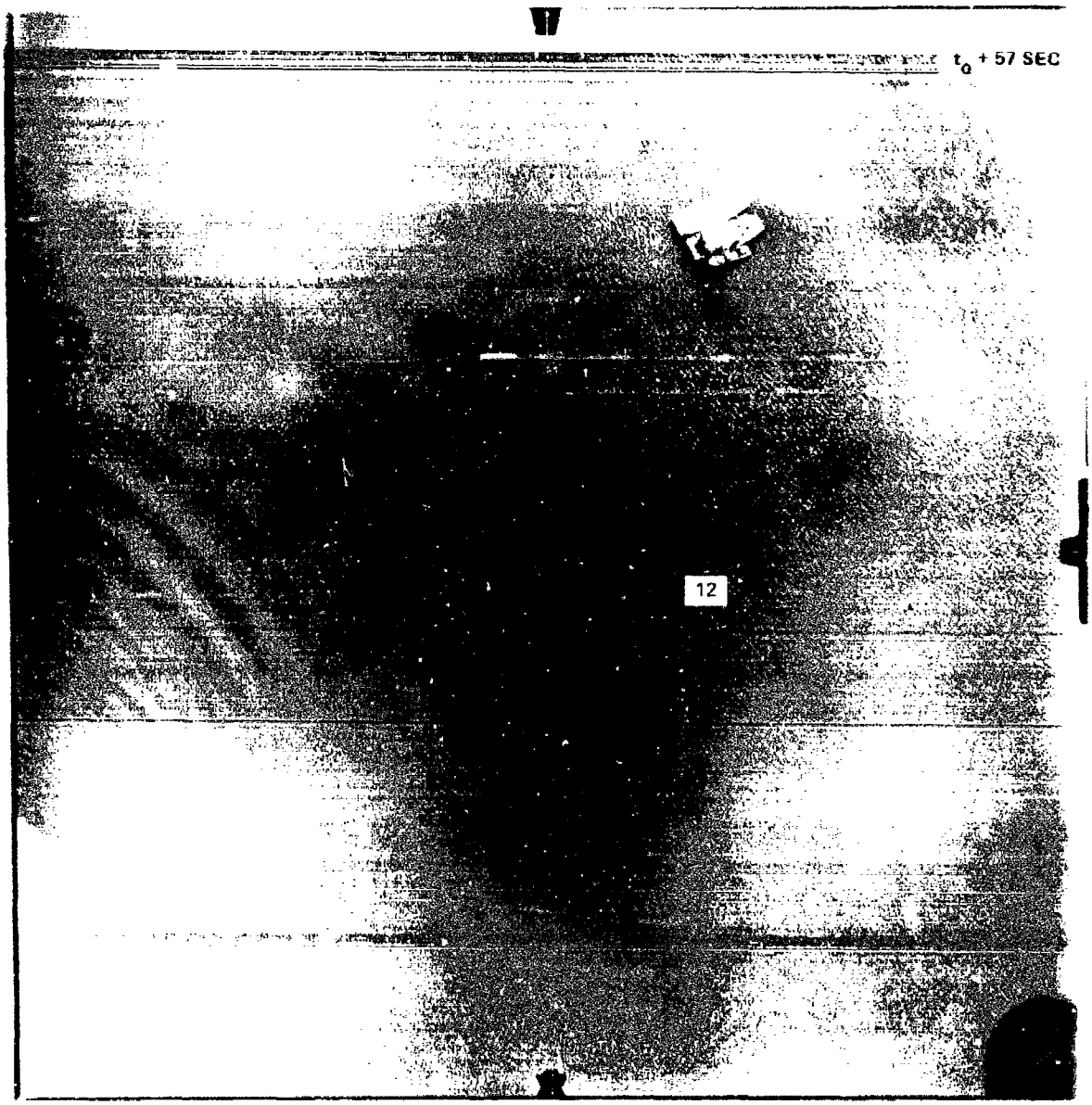

Approximate Pole Distances with Explosion at 0

Pole Number	Distance	Pole Number	Distance
6	168 Ft.	10	753 Ft.
7	299	11	895
8	419	12	1007
9	581		

Explosion Occurred at t_0 - 16:37:09

Figure 6(d) Shot Number 2 – 6724 Lbs. TNT on Bottom – Water Depth ~40 Ft.

10. Comparison of Surface and Bottom Measurements

The pressure record obtained in the vicinity of pole 12 is also shown in Figure 4. A comparison between the surface and bottom amplitudes can be made by use of the simple monochromatic theory. It has already been seen that the surface and bottom amplitudes keep in phase very well. This is to be expected from the simple theory.

It can be shown (Appendix A) that if η is the surface amplitude in inches, and Δp is the excess pressure in inches of water at a height z above the bottom, then

$$\eta = \Delta p \frac{\cosh kh}{\cosh kz}$$

where h = depth of the water and $k = 2\pi/\lambda$. This relation holds for either plane waves or cylindrical waves. In the present case the pressures were measured at a distance of 1.5 feet from the bottom. The depth of the water on Shot 2 of the hydrophone was 37½ feet. Hence z = 1.5 feet, h = 37½ feet.

In order to apply this relationship it is necessary to know or estimate λ.

We associate with each peak and crest a wavelength which is the average distance to the two neighboring peaks on either side. (See Table 4). In Table 5 we compare the measured surface amplitudes with those calculated from the bottom amplitudes. The agreement is reasonable.

Figure 7 reproduces all the existing hydrophone records obtained in the Solomons series.

Figure 8 displays the only other measurements of surface and bottom amplitude over a series of many waves. (For Shot 4.) Although there are no nearby measurements as in the case of Shot 2 from which the wavelength may be inferred, it is possible here to measure the periods between successive peaks and determine wavelength assuming that the wave train is at least locally monochromatic. This assumption does not always apply. The period P is given by

$$V = \frac{\lambda}{P} = \left[\frac{g\lambda}{2\pi} \tanh \frac{2\pi h}{\lambda}\right]^{\frac{1}{2}}$$

Furthermore, at the bottom the pressure change, Δp, in linear units is related to the surface amplitude η by

Table 5 Surface and Bottom Amplitudes, Shot 2

Average λ	188 ft	139	112	103	94.5	93	91	87.5	87.5	91.5
pertaining to peak number	2	3	4	5	6	7	8	9	10	11
Δp measured	1.65"	.8	.02	.03	.14	.27	.37	.46	.37	.10
η calculated	3.10"	2.25	.08	.15	.86	1.72	2.50	3.44	2.78	.67
η measured (= ½ wave height)	3.35"	2.20	.6	1.0	2.0	2.6	3.75	5.0	3.75	2.2

The agreement between the last two rows is rather good for the first two (long) waves, but fails thereafter. The calculated surface amplitudes for the shorter wavelengths underestimate the actual amplitudes. Since for shorter wavelengths the ratio between surface and bottom amplitudes becomes much larger, the effect of errors in measurement becomes magnified.

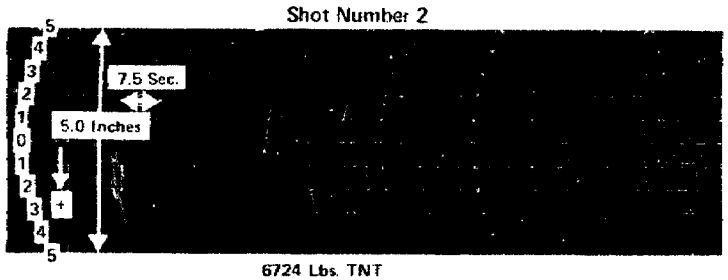

6724 Lbs. TNT
1007 Ft.
Depth of Phone 36 Ft.
Depth of Water 37.5 Ft.

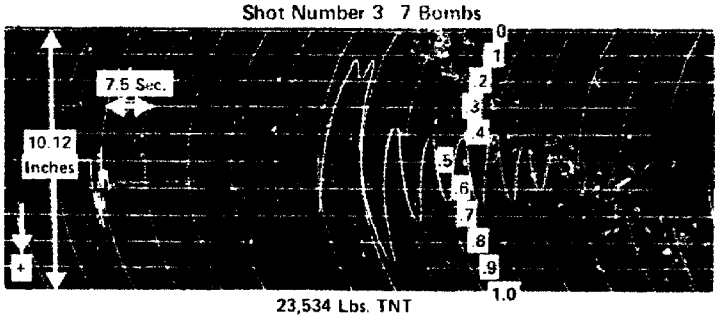

23,534 Lbs. TNT
1050 Ft.
Depth of Phone 37 Ft.
Depth of Water 39 Ft.

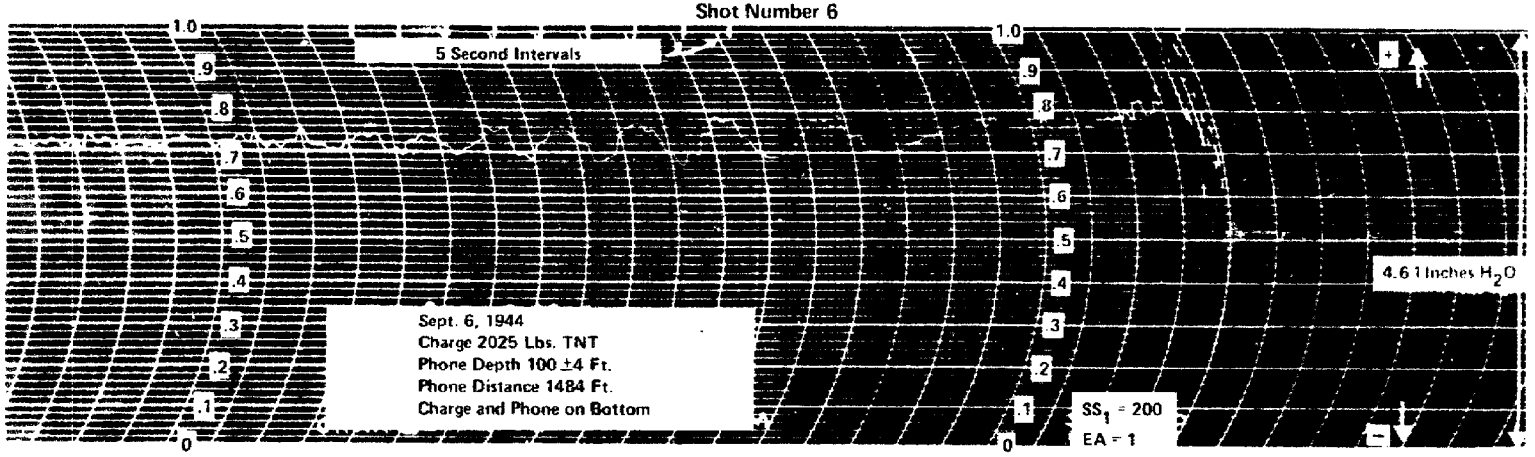

Figure 7(a) Hydrophone Records at Solomons

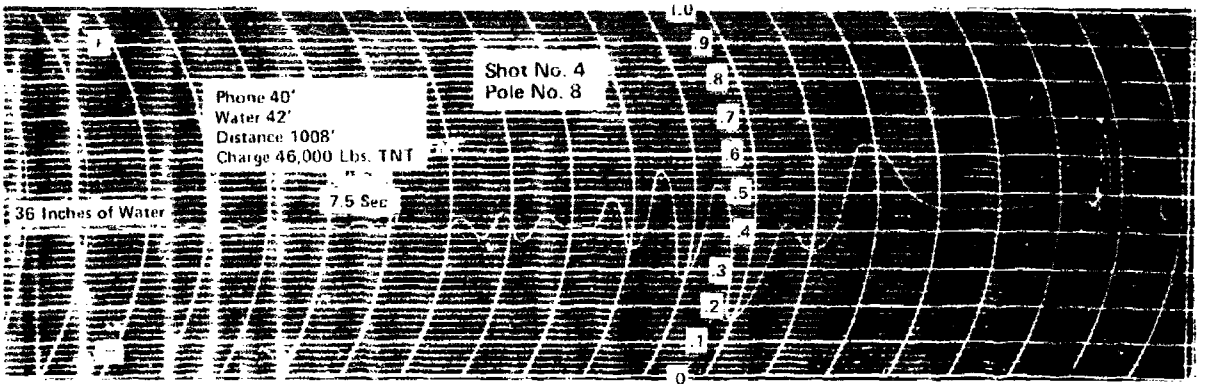

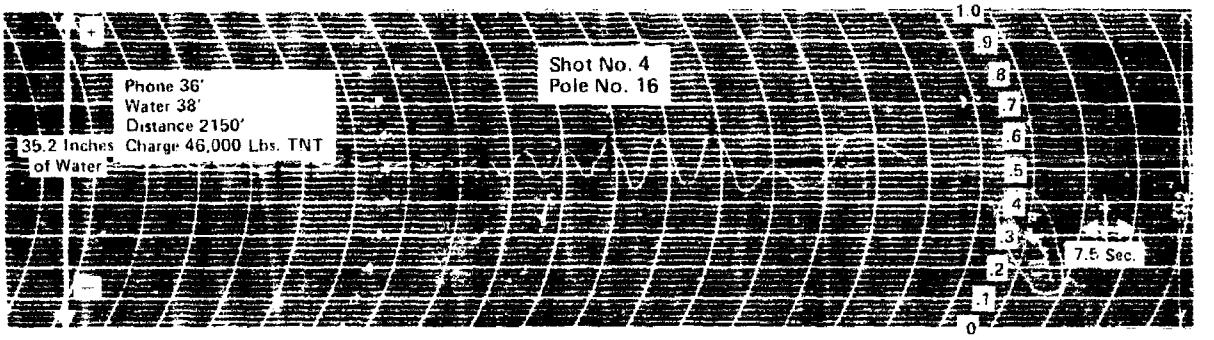

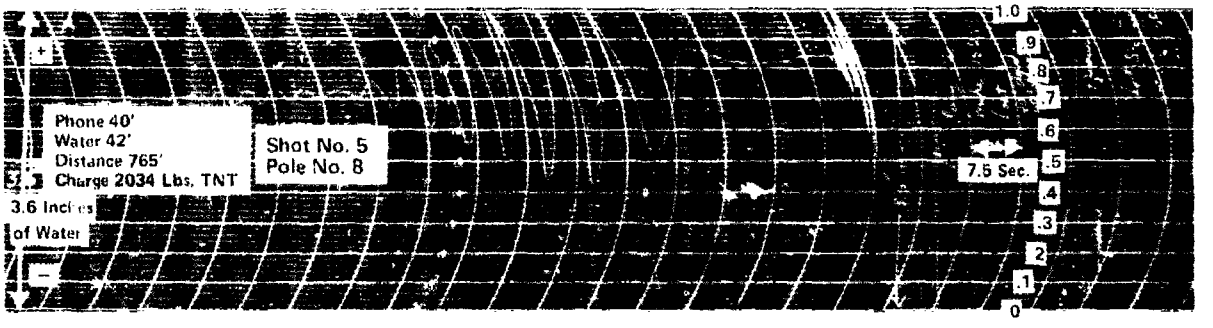

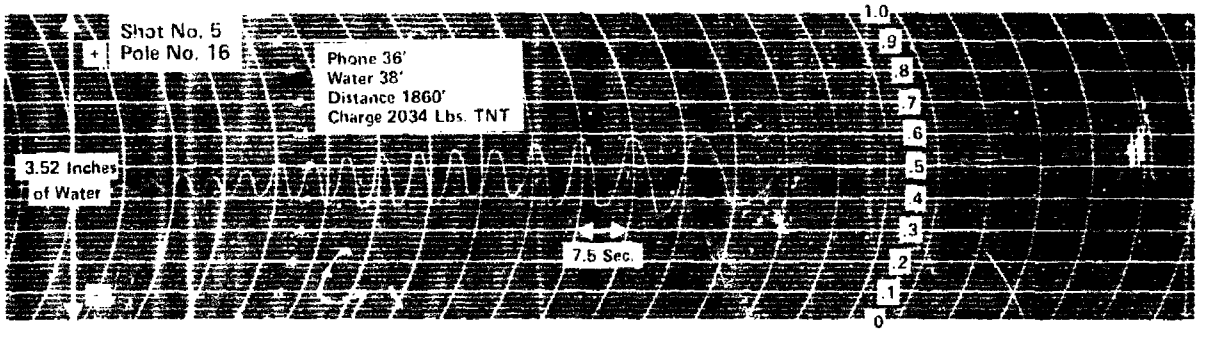

Figure 7(b) Hydrophone Records at Solomons

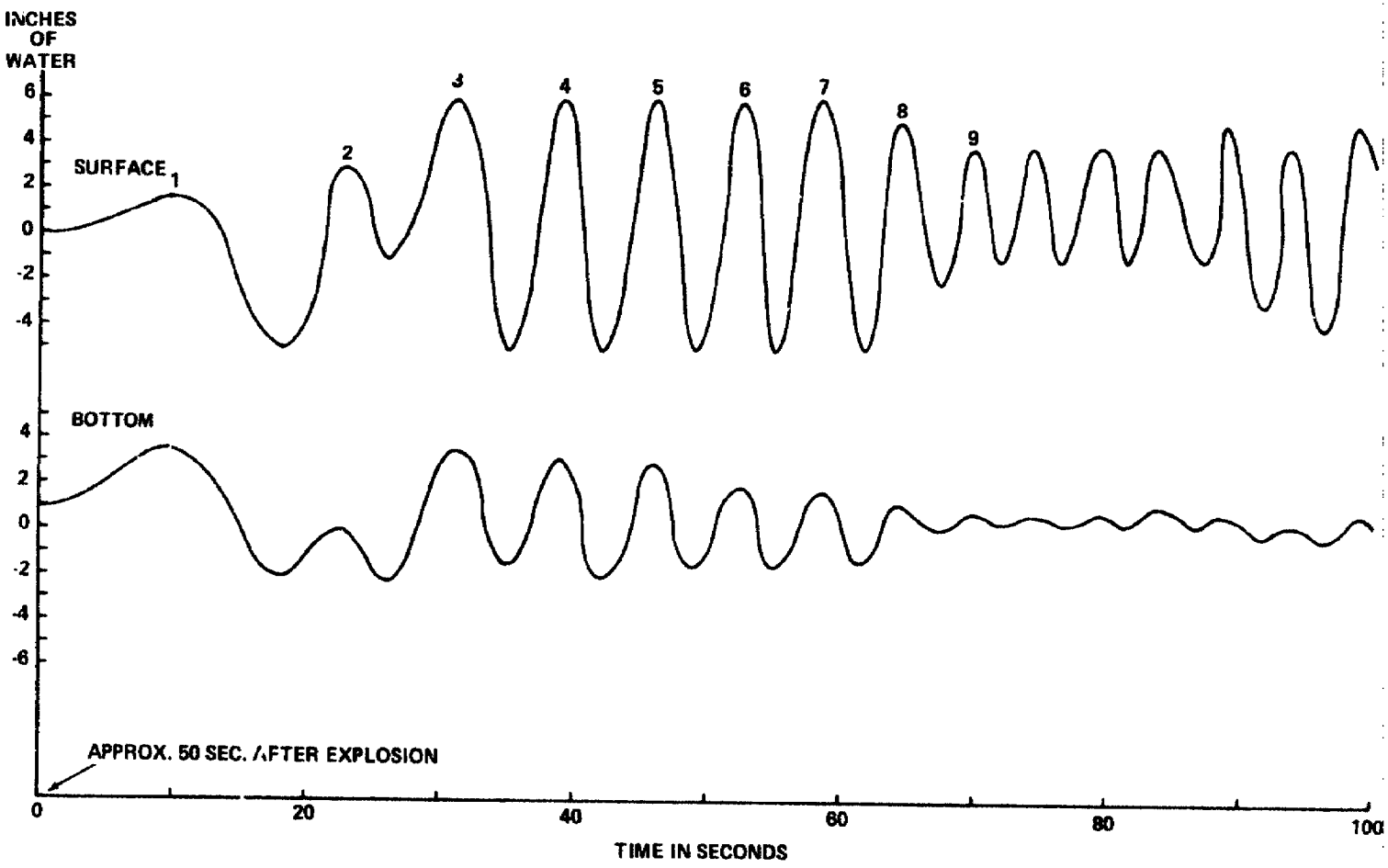

FIG. 8 COMPARISON OF SURFACE AND BOTTOM WAVES GENERATED AT 2140 FT. FROM A 23 TON EXPLOSION OF TNT IN ~40 FT. OF WATER (SHOT 4)

$$\eta = \Delta p \cosh \frac{2\pi h}{\lambda}$$

Using these relations it is possible to construct the curves of Figure 9.

Referring to Figure 8, the times between successive wave crests, P, are:

Wave Number	1	2	3	4	5	6	7	8
Period (sec)	12	8	8	7	6.7	6.0	6.0	5.7
From Figure 9:								
$\Delta p/\eta$ at 40 ft	.83	.65	.65	.55	.50	.41	.41	.37
η = ½ (crest + trough)	3.3"	2	5.5	5.5	5.5	5.5	5.5	3.5
Calculated Δp	2.7"	1.3	3.6	3.0	2.7	2.2	2.2	1.3
Measured Δp	2.8"	1.1	2.6	2.6	2.2	1.8	1.6	0.6

The agreement is reasonable.

The other cases where comparison is possible between bottom and surface measurements give similar results, namely for Shot 3 at 1048

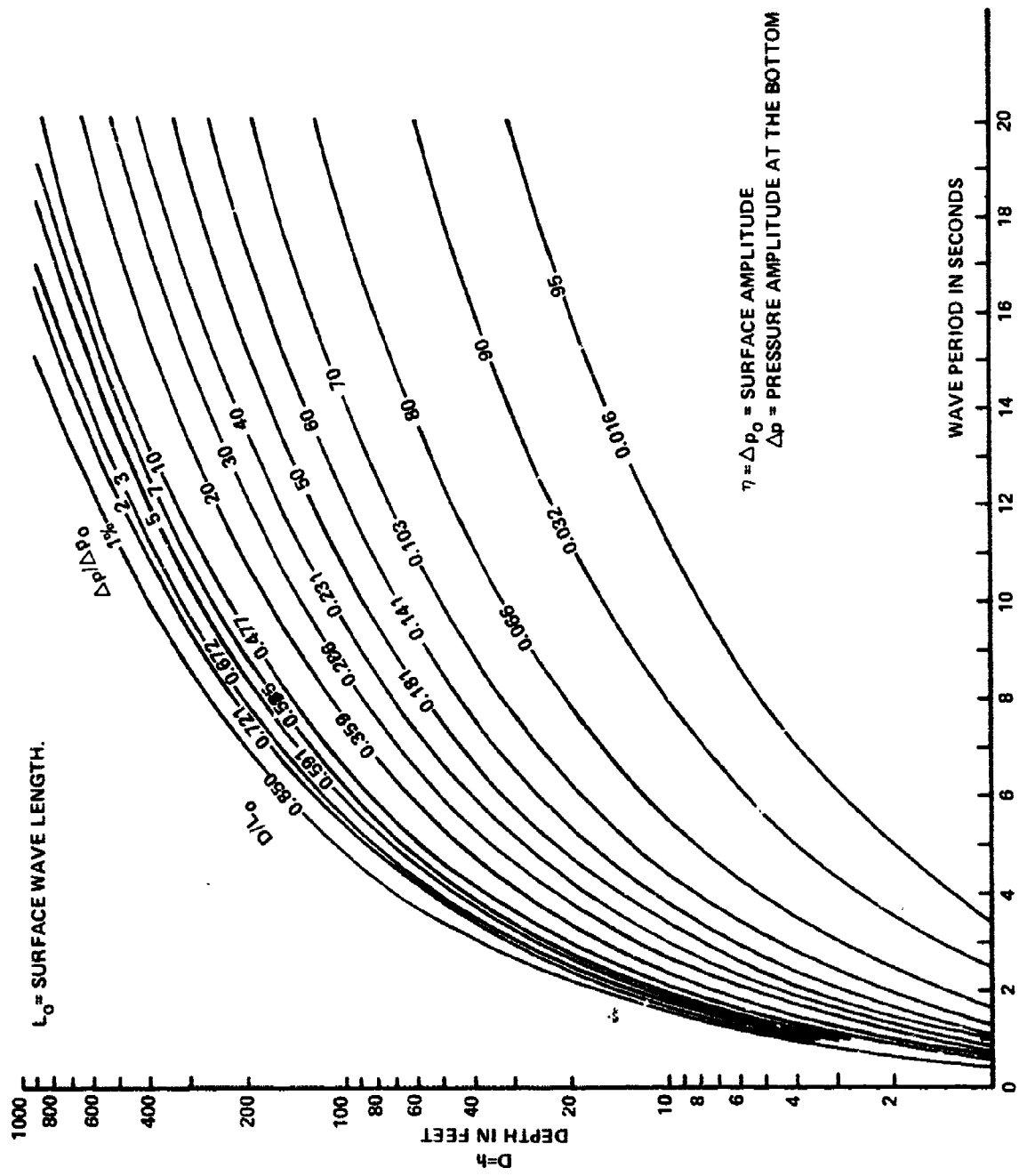

FIG. 9 $\Delta p/\Delta p_o$ IN% REDUCTION OF PRESSURE FLUCTUATION WITH DEPTH.

feet and for Shot 4 at 1028 feet. As already indicated, if the slight elevation of the hydrophones above the bottom is neglected, then under the assumption that the wave motion is monochromatic, i.e., consists of a set of waves all having the same wavelength (which is not the case) then $\eta = \Delta p \cosh 2\pi h/\lambda$. If h is taken to be 40 feet, the factor to be applied to Δp in order to calculate η depends on wavelength λ in the following manner:

λ feet	400	300	200	150	100	80
$\eta/\Delta p$	1.21	1.37	1.89	2.78	6.19	11.7

If λ is small, a small error in λ will produce a larger change in the factor. For this reason and others, one would not expect very close agreement between measured η and η estimated from bottom pressure measurements, at short wavelengths.

11. Summary of Data

The original data on the Solomons tests consisted of hydrophone records and films. The originals and the films have long since disappeared, but measurements were made from the films at the time.[1] These results, wave heights, periods, pressures and distances are all summarized in Table 6, which pertains to the 40-foot sites.[2]

Table 6 Data Summary

Shot	Pole	Records	Distance from Explosion	Suction Phase: Duration	Suction Phase: Pressure on bottom	Suction Phase: Surface Amplitude	Suction Phase: Subsurface Amplitude	First Positive Phase: Time of Arrival	First Positive Phase: Pressure	First Positive Phase: Wavelength in ft.	First Positive Phase: Wave Velocity
2	8	35mm Film	419 ft.	3.2 sec		-12"	7"	20.2 sec [b]		80 [c]	
	9	35mm Film	581	2.8 sec		-3.6"	4.8"	21.3 sec [b]		95 [d] 135 [c]	22.1 [d] ft/sec
	10	35mm Film	753							112 [d]	22.0 [d]
	11		895	6.0 sec		-5.2"	4.8"	35.4 sec		119 [d] 185 [c]	29.0 [d]
		70mm Film									
	12		1007	5.6" (Pressure Record)		-2.5" to -3.8"	4.0" inches	39.0 sec	+1.9	177 171 [d] 195 [c]	30.6 30.7 [d]
		FM Pressure Record		for 5.0 sec [b] 4.0 sec (70mm)	-2.2 inches		4.6" [a]	77.1 sec [a]		93.2 [a] 81 [c]	23.9 [a]
3	9	35mm Film	659	4.9 sec		-11"	15.5"	36.8 sec [b]		162 [c]	
	10		801	6.4 sec		-7"	12"	43.9 sec		160 205 [c]	
		70mm Film									
	11		928	4.0 sec		-7" [b]	11.5"	49.4 sec		132 169 220 [c]	25.4
	12	35mm Film	1048	5.0 sec		-5.5"	13" 4.5" [a]	47.6 sec [b] 100.3 sec [b]		210 [c] 55 [a,c]	
		FM Pressure Record		6.6 sec	-5.06"			48.2 [b] 101.2 [b]	3.2"	160 [c] 55 [a,c]	9.1
4	7		879	4.5 sec 12.4 sec*		-9"	12"	48.8 sec		240 [c]	30.4 [c]
		70mm Film									
	8		1028	6.8 sec 13.9 sec*		-6.5"	13.5"	51.0 sec		536 [b] 240 [c]	67.8 30.4
		FM Pressure Record		5.0 sec 13.1 sec*	+ -8.6" -4.3 10.0"*			48.5 sec [b]	3.0" +4.3"	220 [c]	29.2 [c]
	9	35mm Film	1170	7.3 sec 15.8 sec*		-8"	12"	59.8 sec [b]		245 [c]	30.2 [c]
	12	35mm Film	1579	6.3 sec 12.6 sec*		-4.5"	5.5"	53.9 sec [b]		186 [c]	28.2 [c]
	15	35mm Film	2000								
	16	35mm Film	2140	9.1 sec 18.1 sec*		-5"	6.5" 4.0" [a]	89.4 sec [b] 162.1 sec [b]		229.0 209.2 [a]	24.1 18.8 [a]
		FM Pressure Record		8.3 14.2 sec*	-2.8" -2.1"			81.8 sec [b] 142.1 sec [b]	+2.8" +3.6"	295 [c] 150 [1,c]	
	17	35mm Film	2363	9.0 sec 18.2 sec*		-4.5"	5"	98.6 sec [b] 173.9 sec [b]		290 [c]	31.6 [c]
5	8	Pressure Record	771	7.8 sec	-.94"			38 sec [b]	+.94		20 (dist/time) [b]
	16	Pressure Record	1860	8.5 sec	-.36"			66 sec [b]	+.38		28 (dist/time) [b]

Remark: *On Shot 4 the suction was divided into two shallow parts. Surface Records indicate a brief positive phase between them, the pressure record does not. The starred times concern the duration of both parts, the unstarred that of the first part.

Key: (a) data for some member of second wave group.
(b) unreliable data.
(c) computed from $\frac{1}{T^2} \frac{g}{2\pi\lambda} \tanh \frac{2\pi h}{\lambda}$.
(d) blimp data.

Before these data are subjected to analysis (in Chapter III), it will be useful to review in the next chapter some of the theoretical concepts to be used.

Except for Figure 4 and Figure 8 there are no extant records from photography. Shot 1 yielded no data except from aerial photographs. Shot 6 done in 100 feet of water and only with hydrophone data is listed in Table 7 (Chapter III). Figure 7 reproduces the only hydrophone data, namely: Shot 2 at 1007 feet, Shot 3 at 1050 feet, Shot 4 at 1008 and 2150, Shot 5 at 765 and 1860, and Shot 6 at 1485 in 100 feet of water. Figure 8 reproduces film and hydrophone data from Shot 4 at 2140 feet.

II DISCUSSION OF THEORY

1. Historical Introduction

The literature of gravity waves is extensive starting in 1776 with Laplace who considered water motion in a rectangular canal. Results obtained by Lagrange a few years later for shallow water stated that the velocity of travel depended only on the water depth and not as Laplace found on the wavelength. As Thorade says in his "Problems in Water Waves " 1931[1] in the Historical Side Lights page 4, "At the end of the 18^{th} Century there had been put forth two different theories in regard to waves, the mutual relation between which had never been explained, so in 1802 Gerstner put forth a new theory which assumed that the water was infinitely deep, while the scientific study of waves was again promoted by Poisson and Cauchy (1815), two savants of high rank. Both blamed their predecessors for having studied only fully developed waves, and they dealt with the creation of the waves by citing the following illustration: submerge a solid object, not too large, in water of unlimited depth; wait until the water has become calm and then suddenly withdraw the object. What kind of waves will be formed?" Of course both Laplace and Lagrange were right. If the wavelength was small compared with the depth, Laplace was right. If wavelength was long compared with

depth, then Lagrange was right. Poisson and Cauchy introduced greater complexity as well as insight to the subject by initiating the wave motion with a mixture of wavelengths needed to describe their initial conditions. Thorade's book contains much historical information. The subject of waves is discussed in a few short paragraphs by Landau and Lifshitz "Fluid Mechanics"[2] starting with a deceptively simple introduction: "The free surface of a liquid in equilibrium in a gravitational field is a plane. If, under the action of some external perturbation, the surface is moved from its equilibrium position at some point, motion will occur in the liquid. This motion will be propagated over the whole surface in the form of waves, which are called gravity waves, since they are due to the action of the gravitational field. Gravity waves appear mainly on the surface of the liquid, they affect the interior also, but less and less at greater and greater depths."

2. General Considerations

The gravity waves considered by Cauchy,[3] Poisson,[4] Penney,[5] Kirkwood and Seeger[6] occur in a medium which is irrotational, nonviscous, incompressible and of uniform density. A very short and useful book by C. A. Coulson[7] "Waves, a Mathematical Account of the Common Types of Wave Motion," Oliver and Boyd, Ltd. 1941, divides the types of wave motion in liquids into two groups. One group has been called tidal waves or better long waves in shallow water and arises when the wavelength is much

greater than the depth of the liquid. With waves of this type the vertical acceleration of the particles is neglected in comparison with the horizontal acceleration. Coulson refers to the second group as surface waves in which the vertical acceleration is no longer negligible and the wavelength is much less than the depth of the liquid.

The various treatments all use a linear equation of motion, neglecting the square of the particle velocity, and assume that the amplitude is small compared with the water depth. Of course each treatment insists on the conservation of mass, and requires the pressure to be constant at the free surface and the normal component of the velocity at a rigid boundary to be zero. The differences in treatment then relate to the method of prescribing the initial conditions or of dealing with the explosion gas bubble. The solution is made up by a synthesis of individual solutions such that at $t = 0$ the function is made to fit the initial surface contour (or an initial set of velocities on a flat surface, the impulsive case). Thereafter, if t is allowed to vary, the solution which was made to fit initially continues to evolve its own description of what happens which fits all the conditions and is also unique. The waves produced depend on the volume of the cavity.

3. Cauchy, Poisson, and the Explosion Problem

Note that in the first memoires on the theory of waves (Cauchy, Poisson) it was seen that a complete solution could be achieved from one of two possible initial conditions. The problem was initially treated only for plane waves, i.e., waves that do not spread -- for example, in a canal.

The variables are distance, height, and time. For these first papers the medium was infinitely deep and infinitely extended in directions + x. See Lamb[8], sections 238 and 239.

Case 1. Initial elevation of the free surface around the origin.

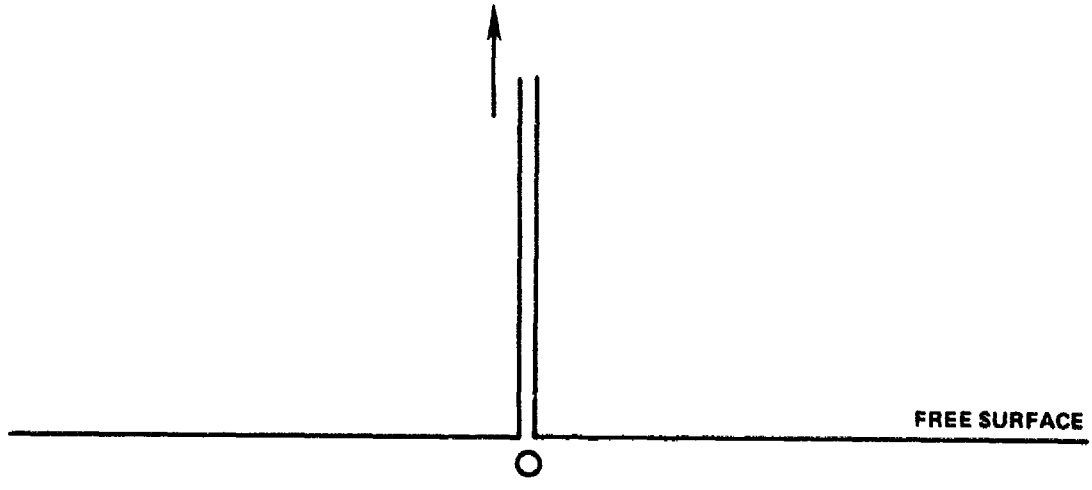

The initial elevation is confined to the immediate neighborhood of the origin. The initial elevation is given by f(x) = 0 for all but infinitesimal values of x, but

$$\int_{-\infty}^{\infty} f(x)\,dx = 1,$$

a so called δ function. The subsidence of this initial elevation produces a train of waves at a distance, the first arrival of which is a positive wave, a crest. The assumption of a delta function here is mathematically the simplest but physically quite unreal in that it calls for an infinitely tall infinites simally thin column of water at the origin which descends under gravity with constant acceleration to feed the wave system. Poisson preferred to start with an initial depression in the water formed by a paraboloid which at $t = 0$ was suddenly removed. He solved this problem for the case of propagation in two dimensions.

If one were to start from rest with a crater in the surface, which is otherwise at the undisturbed level, the first thing to arrive would be a trough. However, an explosion near the surface, blowing out, cannot produce a pure cavity. There has to be an edge of water piled up above the undisturbed level at the same time the cavity reaches its maximum. Further, at this instant the maximum radius of the cavity may be at rest, but the lower parts of it are already filling in and the outer parts of the annular edge are moving outward. It might be possible to obtain a solution using the Cauchy-Poisson method if one could assume the proper "stationary" contour for the water surface in the blowout case. This would be a cavity surrounded by an annulus all taken to be at rest at a time

t = zero. It would be necessary to obtain an analytic expression for this contour, assuming cylindrical symmetry, as a function of r and z, and depending on the parameters charge weight, charge depth and water depth. Penney, in fact, achieved this approximately, but its validity is limited to depths just short of blowout.

Case 2. The other solvable situation is that of an initially flat surface with a limited part of it endowed at t = 0 with a distribution of vertical velocities, i.e., initial impulses are applied to the surface supposed undisturbed. In the case of a deep explosion, the underwater shock wave is reflected almost immediately from the free surface imparting upward velocity to successively deeper layers. The resulting spray dome is flung into the air and descends much later, in some cases, after the waves have already left the area. Consequently the velocity imparted upward has negligible effect on wave formation. The removal of water in the form of spray by the shock wave reflection leaves a slight depression in the remaining surface which could contribute to wave formation but will be neglected. The only remaining cause for wave formation is then the expanding gas globe which increases to a maximum size and then decreases in a time equal to the bubble period. This situation is treated in Kirkwood and Seeger's paper and is not applicable to the blowout situation. On the other hand, an explosion in air over water at rest does reproduce the condition pertaining to the second Cauchy calculation. The initial impulse is downward into the water as in Cauchy's case. The resulting wave

train again begins with a positive pulse. The water surface initially having to move downward requires the adjacent surface to move upward, the water being incompressible. It is this elevated annulus which again causes the initial wave train to proceed. Because of the poor impedance match between air and water, even for air compressed in shock, the fraction of the air blast energy impinging on the water surface which could be taken up by the water in kinetic energy is small, probably less than 4% or perhaps 1% of the total explosion energy. (See Appendix B for Energy in Surface Waves.) On the other hand, the energy in the nonventing underwater explosion retained in the gas globe is approximately 45% of the total explosion energy, and all of this energy is available for moving the water. One therefore expects that an underwater explosion would be more efficient at making waves than an air burst. However, if a charge is exploded deep enough, the bubble expansion will have very little effect on the surface height. Waves are produced only by a local variation in surface height, not by a gradual or general slight increase in height. As the deep gas globe oscillates and rises, it emits pulses at each minimum, causes turbulence and otherwise dissipates its energy so that no surface waves are made.

As we shall see later, the efficiency of the wave making process is very low even in the underwater case where the actual wave energy is only a fraction of a percent of the total energy.

Clearly a key question is at what position above or below the surface are the greatest waves made. It seems reasonable that this is at some point below the surface rather than above. It is important to see how the cavity or crater formation varies with depth near the surface. This question will be considered in a later section.

It is apparent from Lamb's discussion of wave propagation in two dimensions (reference (8), Section 255) that Cauchy and Poisson worked this problem and also that the latter considered the formation of waves from "an initial paraboloidal depression." If we start with a limited initial displacement, then the description of this contour will be a superposition of all wavelengths. As these waves travel outward, the longer ones will travel faster than the shorter ones so that after a while the original harmonic content of the disturbance is spread out and displayed on the water surface. This is true as long as the medium is dispersive, i.e., for those waves which are short compared with the depth. However, the asymptotic solution for diverging (cylindrical symmetry) waves in an unlimited sheet of water of uniform depth (reference (8), Section 194, 195) shows that the amplitude of these waves ultimately varies inversely as the square root of the distance from the origin. This is readily seen from the fact that at a large distance the wavelengths are large compared with the depth and consequently all travel at the same speed. Therefore, the total energy of a wave is proportional to the amplitude squared and to the circumference of

the circle which the wave has reached, but not to the wavelength which now is constant as distance is further increased. Assuming there is no energy dissipation, the result follows. This is mentioned because close in to explosions the wave amplitude decreases inversely with distance, not with the square root of the distance. This is consistant with the dispersive mode of propagation in which the wavelength is not constant but increases with distance. The transition from one mode to the other is gradual. Also, see brief discussion of dispersion in Appendix C.

4. Penney's Crater Assumption

Penney in his paper on Gravity Waves[5] has tried an ingenious description of the surface crater. The wave system is released from rest at time zero from a configuration given by

$$\xi(r) = \frac{2D^4}{3}\left\{\frac{1}{(D^2+r^2)^{3/2}} - \frac{3D^2}{(D^2+r^2)^{5/2}}\right\}$$

(This configuration applies to only one position of the explosive charge, namely that depth, D, at which the ensuing maximum bubble just reaches the plane of the free surface above it.) The first

term in $\xi(r)$ describes the maximum contour of the dome formed by the expanding bubble. The volume of this dome above the former free surface is equal to the volume of the spherical cavity beneath it, namely $4/3\pi D^3$. The second term replaces the spherical cavity with another one of the same volume and of the same class as the surface dome. If $r = D\sqrt{2}$, r being horizontal distance from a point in the undisturbed plane directly over the charge, then $\xi(r) = 0$. For greater values of r the value of ξ is small but positive, so that the expression for ξ describes an open crater if we subtract the second term from the first. In practice it takes time for the dome to fall back into the bubble, and during that time the bubble is filling in from beneath. However, we can look on the crater as a closed cavity or an open one; its mathematical description is the same if we neglect the time of collapse. Using this and other considerations Penney calculated that the explosion of 2,000 tons at optimum depth would create a wave system, the leading part of which was a trough that would be roughly 30 feet deep at a distance of 1,000 feet. The optimum depth was described as the depth at which the maximum bubble became tangent to the plane of the original undisturbed surface. The optimum depth for 2,000 (long) tons is approximately 300 feet depending on the fraction of the total energy which is assumed to be retained in the bubble. We shall assess in a later section (Conclusion) how good an estimate this was.

This paper also contains the suggestion that the explosion of a charge at a depth D less than its optimum depth will produce a wave

system which is exactly the same as a charge of less weight, for which the optimum depth is D. This implies that if a charge is at optimum depth or less, the wave system cannot be enlarged by increasing the charge weight at the same depth. The bigger the charge the more blows out, and the wave system is the same. This statement neglects the effect of increasing air blast on the wave formation.

5. Kirkwood's Basic Theory

The Kirkwood and Seeger theory[6] is also plagued by the bubble behavior near either rigid or free surfaces. The expression for maximum radius is invalid in these cases but is used as a means of estimating bubble volume. However, in treating the case of a charge on the bottom, the calculated bubble volume is arbitrarily divided by two to compensate for energy loss into the bottom. Although the volume of gases is the same in these two cases (free water and bottom), one must remember that the volume of the bubble is thousands of times greater than the original charge volume and is more dependent on the distribution of energy than on the original gas volume. In the case of free water, the theory proceeds quite elegantly from a simple spherical source and its image in the rigid bottom, to a solution for a complete potential function Φ which satisfies the free surface boundary condition. The strength of the source is dV/dt where V is the volume of the spherical bubble as a function of time. The initial configuration of the sea is flat and

at rest. Quoting from Kirkwood and Seeger, "The evaluation of the integrals involved in Φ for an actual gas globe is straightforward, but lengthy. It is convenient to introduce, therefore, a simplifying assumption, the value of which must be tested by analysis of the experimental data. If the period, τ, of the first pulsation of the gas globe is much less than the time interval after the explosion, it is reasonable to suppose that $V(t) = \overline{V}$ for $0 \leq t \leq \tau$ where the constant $\overline{V}$ is some average volume for the period τ." This simplification which then wiped out a term involving dV/dt was entirely reasonable, although it is amusing that none of the subsequent experiments was carried out in free water where the theory could have been properly tested. Now for the first time we have a theory in which the period of the gas globe oscillation appears explicitly. If this period is zero, there is not time for anything to happen and the waves are zero.

The theory reduces to the following basic formula for the wave pressure in dimensionless variables:

$$p_{z'_E}(r',z',t') = pgh(1-z') + \frac{\rho g}{2\pi h^2}\overline{V}\, G_{z'_E,\,\tau'}(r',z',t')$$

where $G_{z'_E,\,\tau'}(r',z',t') \equiv G_{z'_E}(r',z',t') - G_{z'_E}(r',z',t'-\tau')$

$$\text{and } G_{z'_E}(r',z',t') \equiv \int_0^\infty \frac{\cosh \beta z' \cosh \beta z'_E}{\cosh^2 \beta} \cos \omega' t' \; {}_0(\beta r')\beta d\beta$$

with origin in bottom,

h = water depth; z_E is charge position above bottom.

r = horizontal distance, z = vertical distance measured upward.

t = time; τ = explosion bubble period.

$$r' = \frac{r}{h},\ z' = \frac{z}{h},\ z'_E = \frac{z_E}{h}.$$

$$t' = t\sqrt{\frac{g}{h}}\ ;\ \tau' = \tau\sqrt{\frac{g}{h}},\ \omega' = \omega\sqrt{\frac{h}{g}}.$$

$$\omega = \frac{2\pi}{T}\ ;\ \beta = kh = \frac{2\pi}{\lambda}h$$

$$\omega' = (\beta \tanh \beta)^{\frac{1}{2}} \text{ (Same as found in Appendix A)}$$

The integrals for G have been evaluated by the Mathematics Tables Project under the Applied Mathematics Panel of the NDRC and are published in NavOrd Report No. 401. Most of the tables are also published in the Underwater Explosion Research Compendium Volume II, pages 707-760. The tables are computed for $z'_E = 0$, i.e., charge on the bottom. Kirkwood and Seeger remark that the G values are not sensitive to the value of z'_E, having calculated G for $z_E = \frac{1}{2}$ and 1.

It is apparent that there are two major factors which influence the magnitude of the waves -- first, the value of τ which determines how much the basic function $G_{z'_E}(r',z',t')$ will be reduced by a short bubble expansion, and second the quantity $\overline{V}$ which will depend on the charge quantity, the water depth, the charge depth, proximity to surface or bottom and the time over which the value is to be averaged. In comparing experiment with theory, it is clear that the expression given at the end of the Kirkwood and Seeger report[6] is applicable only to the nonblowout case. Gross divergences between it and the measurements for charges blowing out are not a refutation of the theory.

If the charge is on the bottom, $z_E = 0$. If $z' = 0$, then the basic formula gives pressure variations as observed at the bottom. If $z' = 1$, then the formula gives the variations in surface displacement, or wave height, η.

6. Influence of Bubble Period

It will be desirable to estimate the change required by the finite value of τ',. According to the theory, the wave produced by a disturbance of zero duration (i.e., no disturbance, $\tau' = 0$) is null. The wave produced by the disturbance of longest duration, $\tau' = \infty$, is determined from the function G_o. For intermediate values of τ', the waves are computed from

$$G_{o,\tau'} = G_o(r',z',t') - G_o(r',z',t'-\tau')$$

The amplitudes thus generated are usually smaller than the G_o ones but not always.

One way to visualize the effect of the bubble period on wave formation is to plot G_o vs t' at a given distance on transparent paper and to prepare a duplicate plot. By placing the duplicate under the original and transposing it to the left by an amount equal to τ', we have the function $G_o(t'-\tau')$. The difference in the two curves is $G_{o,\tau'}$. For example, Figure 10 is a plot of $G_o(10,1,t')$ made from the table for this particular distance. In order to obtain the time variation of the surface displacement at a reduced distance of 10 when a charge is exploded on the bottom, it is

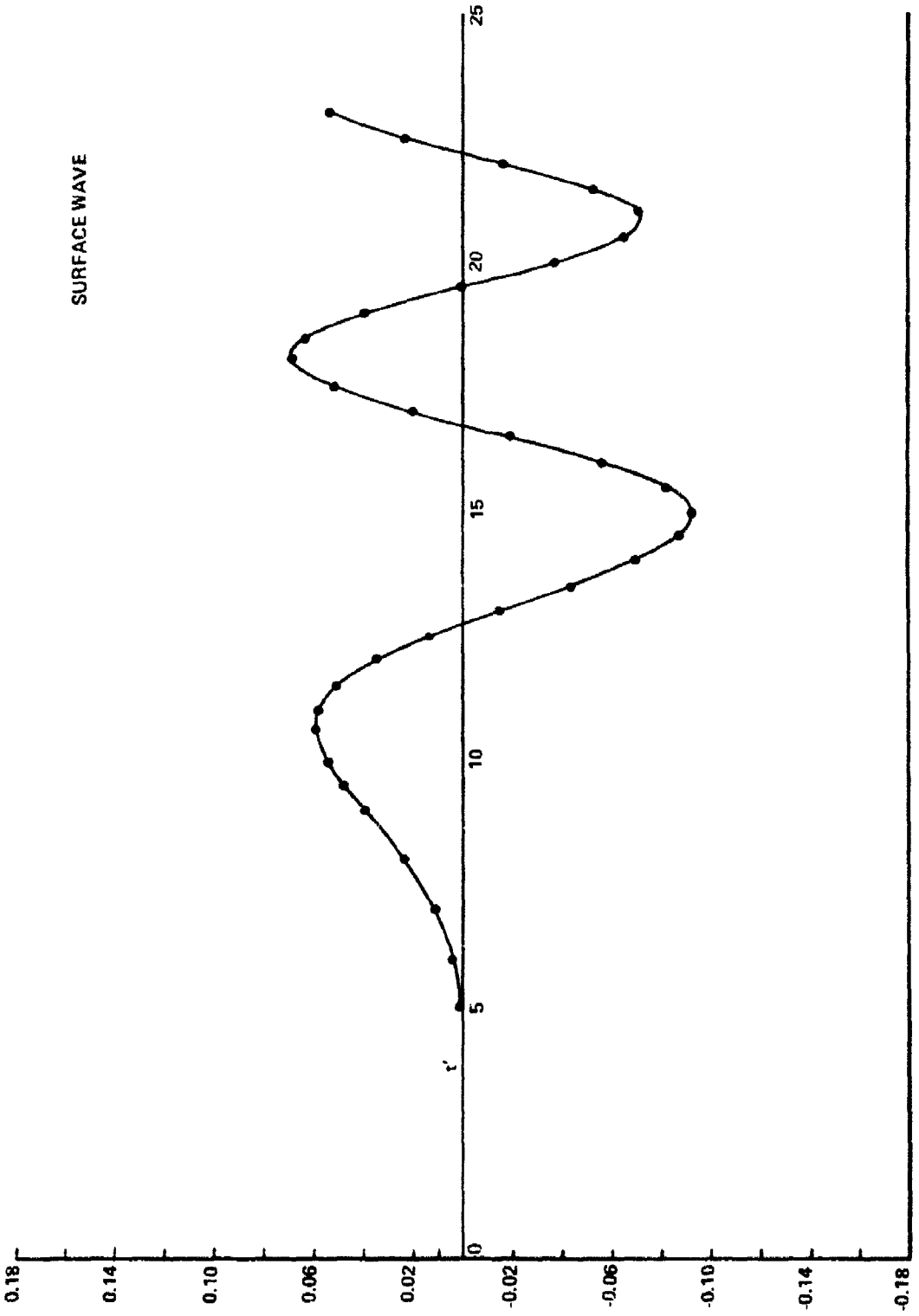

FIG. 10 $G_0(10, 1, t')$ vs t' (EXAMPLE)

necessary to displace this graph to the left by an amount equal to τ', thus obtaining $G_o(10,1,t'-\tau')$ and then to subtract this curve from the previous one obtaining $G_{o,\tau'}(10,1,t')$. More useful is the observation first made by R. W. Spitzer[9] that the value of $G_{o,\tau'}$ for the first minimum is proportional to τ'. This is not true if τ' is too large, but does hold for τ' up to the value 1.1 and probably further as the tables in Appendix D show. The values of $G_{o,\tau'}$ for the first and second maxima, and the first and second minima are tabulated at successive scaled distances and for increasing values of τ' in Appendix D. The durations of the first and second crests and troughs are also tabulated. These tables which were computed, I believe, by the BuOrd Group on Theory of Explosives, are useful for analysis and prediction of waves from up to a ton of explosive. For very large explosions the values which pertain are those for $\tau' = \infty$.

As an example of the use of these tables, we note that the sum of the first minimum and the second maximum pressure on the bottom is proportional to the magnitude of the trough to crest wave height on the surface. Hence, we expect $r' \times \Sigma G$ to be constant if the waves are dispersive and $\sqrt{r'} \times \Sigma G$ to be constant if the waves are of long wavelength.

r'	ΣG if τ' = ∞	$\sqrt{r'}$ x ΣG	ΣG if τ' = 1	r' x ΣG
5	.1299	.290	.1442	.720
10	.0960	.302	.0844	.844
15	.0758	.294	.0583	.870
25	.0529	.264	.0351	.870
50	.0311	.221	.0162	.810
500	.00388	.087	.00095	.475

We note that columns three and five are fairly constant (except at r' = 500) which is to say for values of τ' up to 1 the waves are short and dispersive. For τ' very large, i.e., very big explosion, waves are long and hence nondispersive.

7. Arrival Times

From the tables in Kirkwood and Seeger UER Volume II, one can identify the arrival times of various events such as the first crest, surface and bottom,, the first trough surface and bottom and the second crest surface and bottom. These are plotted in Figure 11. The surface and bottom events travel together. The first crest fits the relation r' = t' from which we find r/t = $\sqrt{gh}$ which is the velocity of shallow water waves, i.e., where wavelength is long compared with depth. The slight curvature of the other two curves shows that these later waves start out with the shorter wavelengths.

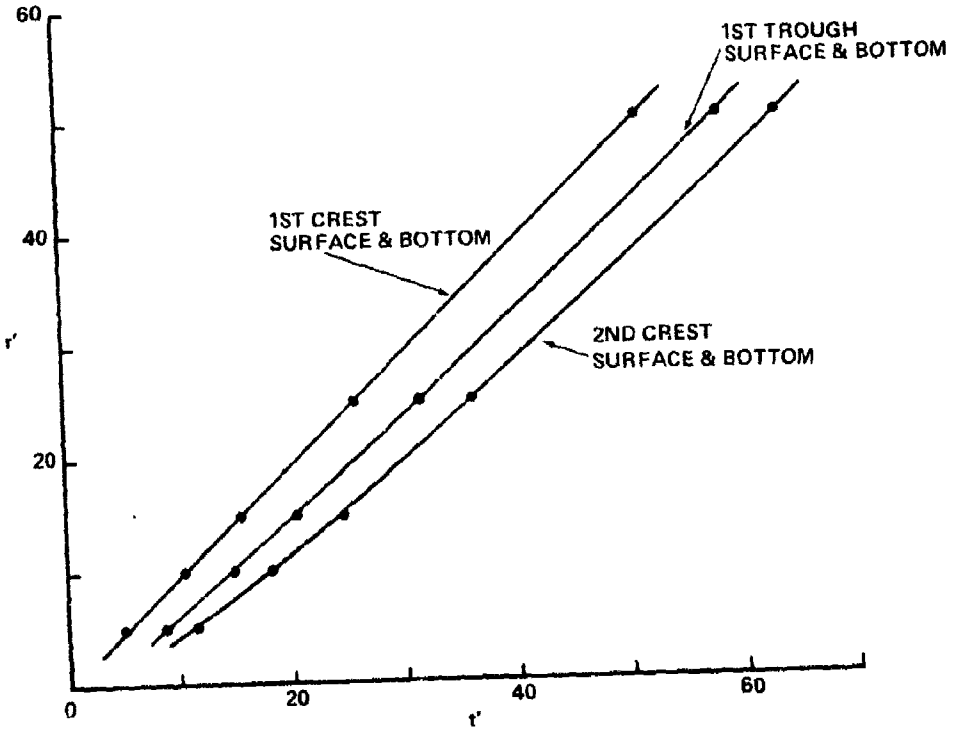

FIG. 11 REDUCED TIME OF ARRIVAL OF CRESTS AND TROUGH.

8. Comparison of Theory with Experiment

The only data we have found taken in free water, i.e., off the bottom and not blowing out, are from Charlesworth's experiments at the Road Research Laboratory and reported in UER Volume II, page 695 under the date February 1945.[10] Charlesworth measured the wave amplitude as a function of time at a point 55 feet away from a series of 32-pound charges of Polar Ammunition Gelignite (equivalent to TNT) detonated at different depths in 15 feet of water. The data taken for the charge at 8-foot depth which is just at the point of breakout, giving maximum waves, were used by A. R. Bryant of the same laboratory to compare with a prediction made using Penney's theory. This is reported in UER Volume II, page 701, dated September 1945.[11] Bryant was able to show almost perfect agreement between theory and experiment for the first two waves. He postulated that disagreement thereafter could be due to detailed differences between the actual shape of the cavity and the assumed shape. He does point out that since the zero of time was not known for the experimental curve it was arbitrarily chosen to give the best fit. In all of Charlesworth's experiments the first thing to arrive is a trough, and this is consistent with the hypothesis that the motion starts from rest by filling in a cavity. Other data, at Solomons and elsewhere particularly for shallow explosions, show that a crest, albeit a low one in some cases, is the first thing to arrive. The theory of Kirkwood and Sceger also predicts an initial crest. For this reason one cannot expect the two theories to agree in minute detail particularly at the beginning of the wave train.

It would be of interest to calculate from the Kirkwood and Seeger theory what would be expected in the Charlesworth experiments. This would require the use of the function $G_{z_E}(r',z',t')$ in which $z_E = \frac{1}{2}$ and $r' = 55/15 = 3.7$. Unfortunately this particular function was not tabulated. The only relevant calculations displayed in Kirkwood and Seeger show that the G functions on the bottom, i.e., $z' = 0$, are virtually the same whether $z_E = \frac{1}{2}$ or zero. We shall assume that the G functions for surface waves, i.e., $z' = 1$, are the same whether the charge is on the bottom or halfway down. We must use the depth of the water not the depth of the charge for scaling purposes, i.e., $r' = 3.7$. The smallest value of r' for which there are any calculations is 5. The amplitude vs time is computed from

$$\text{Amplitude at surface in ft at } r' = 5 \quad = \frac{2 \times 441W}{h^2(h+33)} G_{O,\tau'}(r',1,t'-\tau')$$

NOTE: The value 441 in this formula is obtained using

$$L = 14.0 \left(\frac{W}{h+33}\right)^{1/3}.$$

If we use $L = 13.5 \left(\frac{W}{h+33}\right)^{1/3}$ which is more in line with other data (period observations and so on), then the value in the formula should be 406.

where the factor of 2 has been restored since the charge is not on the bottom, and where h = water depth (15 feet) and W = 32 pounds.

$\tau' = \tau \sqrt{g/h}$ and

$$\tau = \frac{4.36W^{1/3}}{(D+33)^{5/6}} \text{ sec}$$

$$\tau' = 1.26$$

The results are shown in Figure 12 for r' = 5 (Inner Curve). The amplitude has also been multiplied by the ratio of distances in order to estimate the values for r' = 3.7 (Outer Curve). The agreement with respect to period is fair although there is some uncertainty at the beginning, as already remarked upon. The amplitudes do not agree very well at the beginning. Perhaps the agreement may be considered fair in view of all the approximations and enabling assumptions which have been made.

If we take the assumption that the G function is the same whether the charge is halfway down or on the bottom, we can use the bottom function and say that the water is only 8 feet deep. In this case $r' \cong 7$ and we find from Kirkwood and Seeger, Figure 2e and Figure 2g, that $G_o(7,1,t')$ for the maximum of the first positive phase is +.03 and $G_o(7,1,t')$ for the minimum of the first negative phase is -.10. Predicted wave crest is

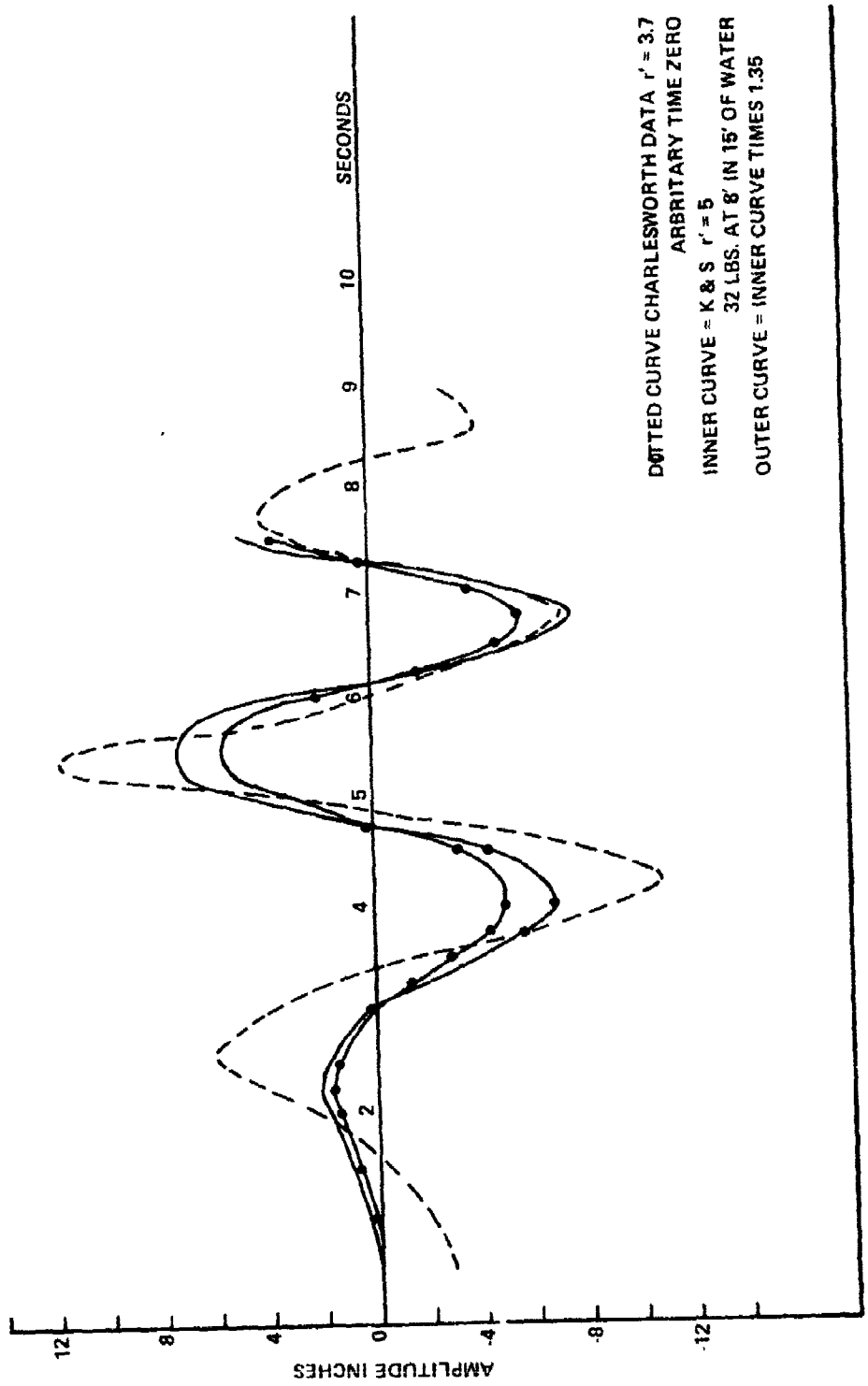

FIG. 12 COMPARISON OF THEORY WITH CHARLESWORTH'S DATA

$$\frac{441 \times 32}{8^2(8+33)} \times .03 = .16 \text{ ft}$$

Similarly the predicted trough is .54 feet.

The experimental measurements presumed for the same waves are .5 feet and .9 feet, respectively. The agreement for crest to trough magnitude is .70 theory vs 1.40 measured. This is in rough agreement with the prediction made before. Note that we have removed the factor of two because the charge was assumed to be on the bottom in order to obtain the calculated functions. Such procedure shows that the theory is more or less self-consistant, but does not improve agreement with experiment. This is the only shot (in free water) that matches the Kirkwood and Seeger assumptions, and it is also the only shot where the experimental result is greater than the theory. It is regrettable that there were not available data from more free water shots so that a better test of the theory could be made.

There are two other shots, one at Woods Hole and one at Solomons in which the charge is on the bottom and where hydrophone data taken on the bottom are available. These shots are of interest because each one is at critical (nonblowout) depth, and one is almost exactly twice the scale of the other.

The data are as follow:

Woods Hole, 300 lbs, depth 20 ft, $\tau' = 1.33$, critical depth 23 ft

Distance	Duration 1st Negative	Period 1st to 2nd min.	Amplitude 1st min.	1st Crest to trough
500 ft	4.3 (theory 4.6)	6.2 sec	-0.8"	1.4"
1000	4.5 (theory 5.5)	7.1	-0.3"	0.7"

Although it was believed at the time that there was good agreement with theory, a calculation based on the (more recent) Kirkwood and Seeger's publication shows that the theory overestimates the amplitudes by 50 to 100%.

Data for the other shot at Solomons (Shot 5) are as follow:

W = 2034 lbs, depth 40 ft, critical depth 42 ft, $\tau' = 1.38$

Distance	Duration 1st Negative	Amplitude 1st minimum	Next Positive Pressure Ampl.
771 ft	7.8 sec	-.94 inches	.94
1860	8.5	-3.6	.38

Values for the amplitude of the first minimum computed from Kirkwood and Seeger theory are -2.25 and -.93 inches. Hence in this case the theory overestimates the measured amplitude at both distances by 150%.

NOTE: For future reference, the surface amplitude on Shot 5 is estimated from the hydrophone data as follows:

Dist.	Trough to Crest Amplitude	Velocity	Measured Period	Calc. λ	cosh $2\pi h/\lambda$	Calc. Surface Trough to Crest
771 ft	1.88"	∿25 ft/sec	∿13 sec	325 ft	1.31	.206 ft
1860	.74	35 ft/sec	13.5 sec	470	1.14	.070 ft

We conclude tentatively that the Penney theory agrees with Charlesworth's data for 32-pound charges in free water placed at a depth equal to .6 maximum bubble radius. The Kirkwood and Seeger theory agrees qualitatively but underestimates the initial phases by about 100%. For depths greater than and less than this, the wave amplitudes are lower as determined experimentally by Charlesworth. However, for two nonblowout cases (Woods Hole and Shot 5 - Solomons) for charges on the bottom, the Kirkwood and Seeger theory overestimates the waves by a factor of 1.5 to 2.4. A possible conclusion from this is that the presence of the bottom reduces the

wave making potential by more than the factor of two already allowed, i.e., that more energy is used in grinding out a crater in the bottom and further that different types of bottom, i.e., at Woods Hole and at Solomons have different attenuations with the latter being the greater. Unless the wave measuring data themselves are faulty, the difference in bottom attenuation is the only postulate for the inability to scale from one explosion to another similar one.

9. Remarks on Scaling and the Influence of the Bottom

The question may be asked: How does one scale from the Woods' Hole experiment to Solomons' Shot 5? Since for these two explosives the maximum bubble radius was approximately equal to the water depth, there was no blowout and therefore the bore method (which see under "scaling methods" Chapter 5), is inapplicable. However in each we have

$$L = 13.5\left(\frac{W}{D+33}\right)^{1/3}$$

L = maximum radius of bubble.

D = Depth of charge.

We have $W_1 = 300$; $D_1 = 20$

$W_2 = 2034$; $D_2 = 40$

Then $L_1 = 24$; $L_2 = 41$

$$\frac{D_1}{L_1} = .85; \quad \frac{D_2}{L_2} = .98$$

According to Charlesworth the wave making efficiency is a function of D/L peaking at about 0.6 and falling off sharply as the charge gets shallower, and gradually as the charge gets deeper. The larger value of D/L may account for some decrease in wave efficiency in the larger explosion. We may expect the wave heights to be proportional to the volume ratio, i.e., $(L_2/L_1)^3$ and inversely proportional to the square of the depth at the same scaled distance. (See Equation (5'), Kirkwood and Seeger's paper[6])

$$\therefore \quad H_2 = \frac{5}{4} H_1$$

and $R_2 = 2R_1$

$$\therefore \quad H_2R_2 = 2.5H_1R_1$$

We now summarize the observations on the two scalable shots:

Source	W lbs	R ft	r'	1st min. Neg. Ampl. on bottom H'	H'R ft^2	Ave. H'R ft^2
Woods Hole	300	500	25	.8"	33.2	29
"	"	1000	50	.3"	25.0	
Kirkwood & Seeger	"	500	25	1.2"	50	50
"	"	1000	50	.6"	50	
Solomons #5	2034	771	19.3	.94	60.4	58
"	"	1860	46.6	.36	55.8	
Kirkwood & Seeger	"	771	19.3	2.25	145	145
"	"	1860	46.6	.93	145	

We can say:

(1) Theory overestimates data for 300 lbs by $\frac{50}{29} = 1.7$

Theory overestimates data for 2034 lbs by $\frac{145}{58} = 2.5$

(2) Theory scales from 300 to 2034 as $\frac{145}{50} = 2.9$

(3) Data scales from 300 to 2034 as $\frac{58}{29} = 2.0$

(4) Scaling as in preceding paragraph goes as 2.5

(5) It is interesting that $\left(\frac{2034}{300}\right)^{\frac{1}{2}} = 2.6$

The next paragraph comments on the rationale for $W^{\frac{1}{2}}$ scaling.

It has been noted by Penney[5] that for example if one scales from one small charge to another at such depths that $D<<33$ for both charges, then $L \sim W^{1/3}$, depths, distances and wave heights scale as $W^{1/3}$. Further, if the charges are large and $D>>33$, and if for example the charges are at depths such that $L = D$ or a fixed multiple thereof, then $D \sim W^{\frac{1}{4}}$, and all dimensions including wave height vary as $W^{\frac{1}{4}}$. All of this follows from the bubble radius formula. Unfortunately in our case, neither of these circumstances existed. It is curious to note that in the breakout case where the bubble cavity is no longer spherical and where the wave heights scale as $W^{1/6}$ from one breakout case to another (see bore scaling in

Baker chapter), all other dimensions going as $W^{1/3}$, the product of HR $\sim W^{1/6}W^{1/3} = W^{1/2}$. This is the same result as for the deep large explosions where HR $\sim W^{1/4}W^{1/4} = W^{1/2}$. The magnitude of the waves will not be the same, presumably the largest occuring for cases where D = .6L.

Charlesworth[10] shows data for 2-ounce and 2-pound charges at depths of about .6L, (3 feet and 1.2 feet), so that these depths can be neglected compared with 33. Nevertheless he shows the wave heights reduced by $W^{1/4}$ rather than by $W^{1/3}$.

One infers that the measurements were as follows:

Weight	Wave Height	Distance	HR
2 oz	.416 ft	13.0 ft	5.41 ft^2
2 lbs	.59	27.6	16.30

Applying $W^{1/3}$ scaling to this the value of HR for 2 pounds inferred from 2 ounces is 5.41 x $(16)^{2/3}$ = 34.2 instead of 16.3 measured. There is no explanation given for this discrepancy, except that Charlesworth notes that the 2-ounce charges seem to be more efficient wave makers. [$W^{1/4}$ scaling gives 21.6. Closer but not strictly applicable.] We can also compare 32- and 300-pound data

fired at 8-foot depth and at the bottom in 16 feet of water, respectively, as quoted by Charlesworth.

We believe the data are:

Weight	Wave Height	Distance	HR
32 lbs	.88 ft	55 ft	48.5 ft
300	1.66	83	138.0

$(\frac{300}{32})^{1/3} = 2.1$ HR = 48.5 x $(2.1)^2$ = 214 (compared with 138 measured)

$(\frac{300}{32})^{\frac{1}{4}} = 3.06$ HR = 48.5 x 3.06 = 149 (compared with 138 measured)

The $W^{1/4}$ scaling from 32 pounds to 300 pounds works better than $W^{1/3}$ scaling and perhaps it should since charge depths are not small compared with 33. It must be remembered that the experimental value

of HR for the charge on the bottom is undoubtedly low. If one were to double it, á la Kirkwood and Seeger, then the cube root scaling would look better.

Again it is forced upon us that a large change in wave making efficiency occurs when the charge interacts with the bottom. The theory is also ambiguous about this. Even the assumption of an equal image source in the assumed rigid bottom is not upheld in the actual situation. We conclude that there is an ambiguity of a factor of two depending on the type of bottom, and how close it is to the charge.

We note in passing that on the Solomons' Shot No. 4 an attempt was made by soundings to determine what had happened to the bottom. The record shows that the water depth at the explosion site was 7 feet greater when probed after the shot. How extensive the bottom crater was or how much work was required to make it are not known.

III ANALYSIS OF SOLOMON'S DATA

The Solomons' data will be discussed in this chapter under three topics: first, bottom pressure or the magnitude of the first negative phase measured by hydrophone data; second, the duration of the first negative phase; and third, the amplitude of the first negative pulse at the surface, and of the following peak.

1. Bottom Pressure (Nonblowout Case)

The hydrophone data for the 40-foot site are plotted in Figure 13. The amplitudes for the blowout shots are all about the same, and those for Shot 5 are considerably lower. We shall wish to discuss the blowout and nonblowout cases separately. Figure 14 is a plot of the dimensionless function $G_o(r'o)$ for various events. These curves are the same for all explosions regardless of depth or size.

The basic Kirkwood and Seeger theory requires the pressure variation on the bottom to be given by

$$p = \frac{\overline{V}}{2\pi h^2} G_{o,\tau'}(r',o,t') \text{ feet}$$

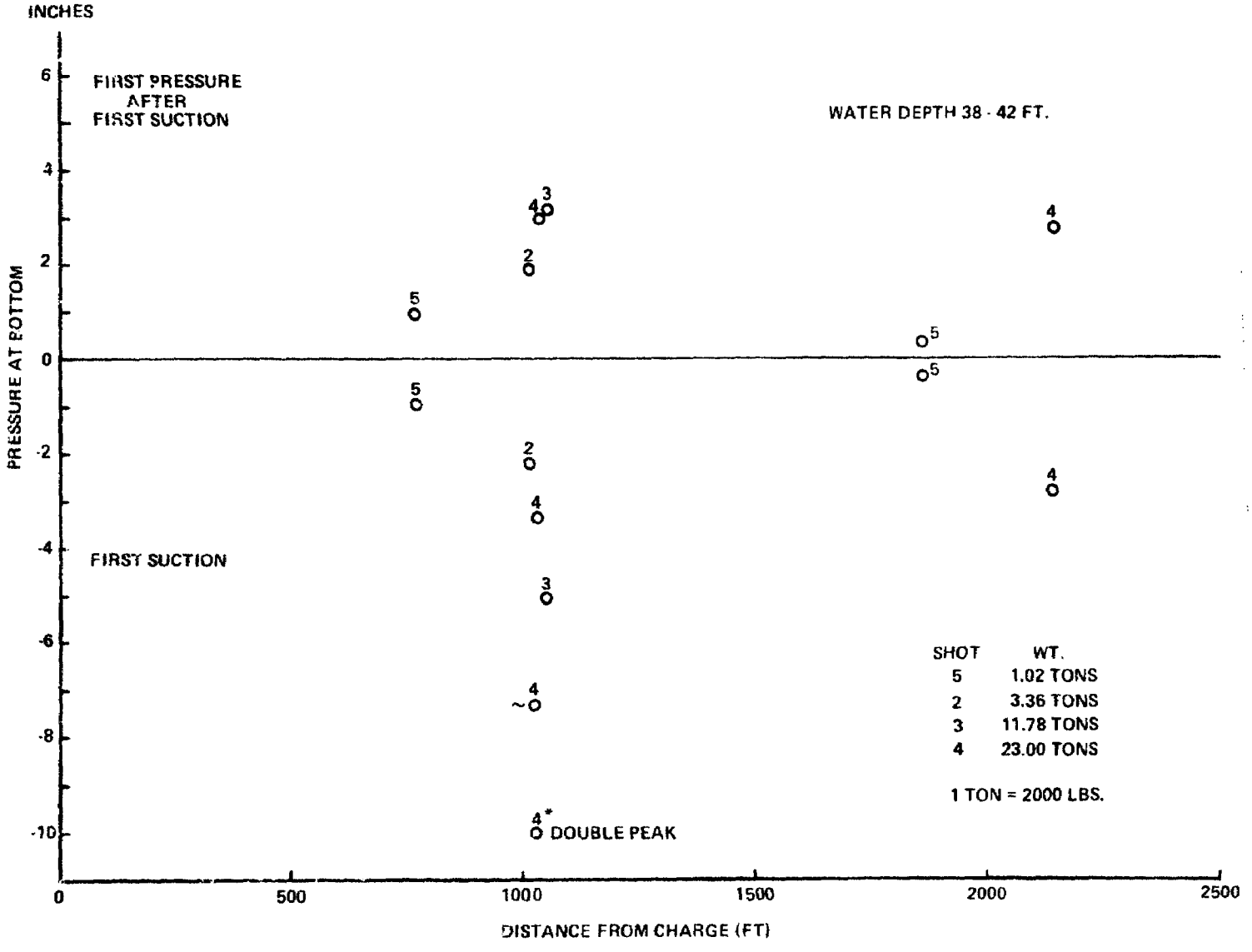

FIG. 13 BOTTOM PRESSURE VS. DISTANCE (SOLOMONS)

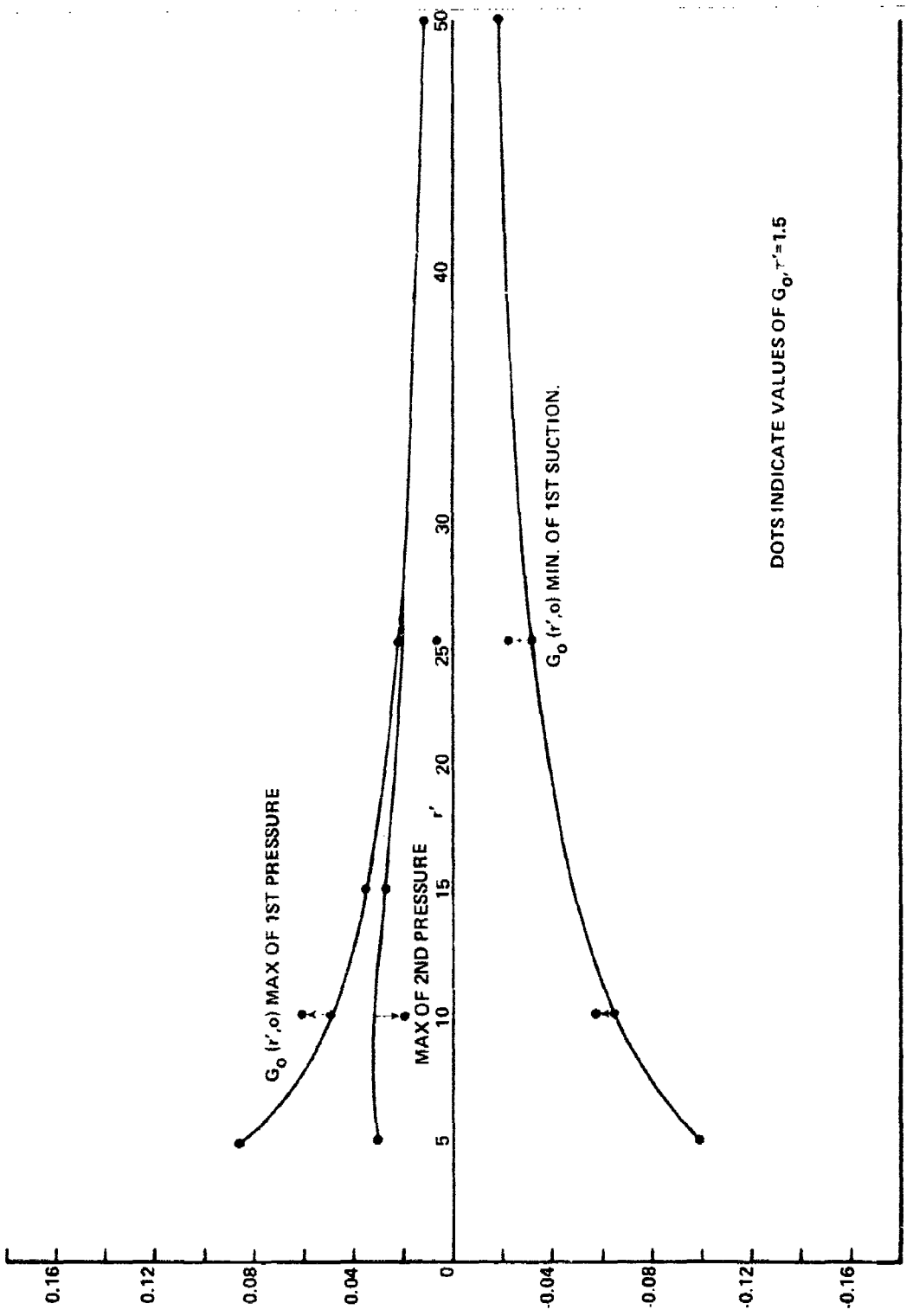

FIG. 14 EXTREMES OF G_0 AT THE BOTTOM

where h = water depth and $\overline{V}$ = "some average volume for the period τ." If the bubble is spherical (charge off the bottom) and of radius a(t) then

$$\overline{V} = \frac{\int_0^{\tau} \frac{4}{3} \pi a^3 dt}{\tau}$$

Now if L is the maximum radius of the expanded bubble, then the work done against ambient pressure by the gases requires that L be proportional to the cube root of W/(D+33).

The proportionality constant depends on the energy per pound of the explosive and on the fraction of this energy which is retained in the gas globe. We shall take the constant to be equal to 13.5 (W in pounds, D charge depth in feet) which is consistent with 1060 cal/gr explosion energy (1.48×10^6 foot pounds per pound) and 45% energy remaining in the bubble. Therefore, $L = 13.5 \left(\frac{W}{D+33}\right)^{1/3}$.

Kirkwood and Seeger state that the time average over τ of the dimensionless quantity $(a(t)/L)^3$ in free water as calculated by Shiffman and Friedman[12] is 0.4819.

Hence, $\overline{V} = 4/3\ \pi(.4819)L^3$ in free water, no blowout. Kirkwood and Seeger now imply that the volume they are using in the pressure formula is the volume of the bubble associated with the explosion, and that when the explosion is on the bottom the actual volume will be half that for a bubble at the same depth with no bottom present. This is certainly wrong if the bottom is rigid, and may be approximately right if the bottom is mud-deformable and wasteful of energy. At any rate, the $\overline{V}$ substituted into the pressure formula is equal to

$$\frac{1}{2} \times \frac{4}{3} \pi \times .4819\ L^3,$$

and then

$$p = \frac{1}{3} \frac{.4819\ L^3}{h^2} G_{o,\tau'}(r',o,t') \text{ feet}$$

This should work for a charge on a mud bottom but not blowing out.

2. Spitzer's Formula for Moderate Charges

It was noted early by R. W. Spitzer[9] that $G_{1\ min}$, which is the value of $G_\tau(r',o,t')$ at the bottom of the first trough is almost exactly proportional to τ', although this is necessarily limited to values of τ' small compared with t', and also typically less than 1 or 1.5. This proportionality holds at each reduced distance. If the ratio $G_{1\ min}/\tau'$ is plotted against $1/r'$, one obtains a good straight line passing through the origin. Spitzer fits this line with the relation

$$\frac{G_{1\ min}}{\tau'} = \frac{.42}{r'}$$

Hence,

$$p_{1\ min} = \frac{\bar{V}}{2\pi h^2}\,\frac{.42\tau'}{r'}\ \text{ft} = \frac{4.6\bar{V}\tau}{rh^{3/2}}\ \text{inches}$$

or for charge on the bottom (halving the volume)

$$p_{1\ min} = \frac{4.64\tau L^3}{rh^{3/2}}\ \text{inches}$$

(provided $\tau' < 1.5$).

Values calculated for nonblowout cases are shown in Table 7. The agreement may be said to be fair. If the value of τ' is large, it is necessary to go back to the tables[6a] and find the value of G_o. The value of τ is determined simply from:

$$\tau = \frac{4.36\ W^{1/3}}{(D+33)^{5/6}} ,$$

$$\tau' = \sqrt{\frac{g}{h}}\ \tau .$$

Elaborate corrections to τ caused by proximity of the bubble to a rigid plane or a free surface are mostly insignificant and are herein ignored.

We may conclude that for the three nonblowout cases cited, the theory predicts the observed amplitudes to within a factor of two.

3. Bottom Pressure (Blowout Case); Other Estimates of Volume

If there is blowout what should be the value of $\bar{V}$? It is clear that the blind use of the previous formula grossly overestimates the bottom pressure because a large part of the

Table 7

First Negative Phase (First Trough)

Pressure on the Bottom, Hydrophone Data

All Charges on the Bottom, a_o = Charge Radius

Shot No.	W lbs	h ft	a_o ft	L ft	a_{max} ft	r ft	r'	τ sec	τ'	$G_{o,\tau'}$	Calculated p_1 inches	Calculated p_2 inches	Calculated p_3 inches	Observed p inches
Nonblowout														
Woods Hole A	300	40	.91	21	23	250	6.2	.81	.72	.044	.56	-	-	.30
Woods Hole B	300	40	.91	21	23	500	12.5	.81	.72	.023	.28	-	-	.25
Solomons 6	2025	100	1.71	33	42	1484	14.8	.99	.56	.014	.11	-	-	.23
Blowout														
Solomons 2	6724	37.5	2.56	62	57	1007	26.9	2.4	2.1	.022	7.0	3.2	1.6	2.2
" 3	23534	39	3.88	96	81	1048	26.9	3.5	3.1	.022	25	7.5	1.6	5.1
" 4	46000	42	4.86	115	96	1028	24.5	4.4	3.9	.023	39	10.5	1.8	7.3
" 4	46000	42	4.86	115	96	2140	51	4.4	3.9	.012	20	5.5	1.0	2.8
Critical Depth														
Solomons 5	2034	41	1.72	41	42	765	18.7	1.5	1.3	.030	2.4	-	2.4	1.0
" 5	2034	41	1.72	41	42	1860	45	1.5	1.3	.012	1.2	-	1.2	.42

NSWC/WOL/MP 76-15

calculated volume is in a sphere or hemisphere which is above the water level. The estimate of the proper volume to use is difficult. It is also necessary to know the cavity volume as a function of time. This will depend in part on whether the explosion products are above or below atmospheric pressure when the breakthrough occurs. As a general rule the explosion products when adiabatically expanded to a radius of ten times the charge radius have reduced their pressure to about one atmosphere. The formation of the bubble will depend on how much work the gases have done when they reach the surface. Calculations of this have shown that most of the kinetic energy which the water will acquire has been imparted in the expansion to the first few charge radii. (For example, at 2 radii 78%, at 3 radii 87% ...) It does not appear worth while to pursue this line of reasoning.

However, crudely, one can show the effect of various simplifying assumptions about the volume. Remembering that

$$p = \frac{\bar{V}}{2\pi h^2} G_{o,\tau}, \text{ ft}$$

we have, as before,

$$p = p_1 \text{ when } \bar{V} = \bar{V}_1 = \frac{2}{3}\pi(.4819)L^3$$

(Volume has been reduced by factor of two for charge on bottom.)

If the cavity is a cylinder of radius L and altitude h, then

$$p = p_2 \text{ when } \bar{V} = \bar{V}_2 = \frac{1}{2}\pi(.4819)L^2h$$

(assuming the same time averaging factor and bottom loss)

If the cavity is a hemisphere with radius equal to h, then

$$p = p_3 \text{ when } \bar{V} = \bar{V}_3 = \frac{2}{3}\pi(.4819)h^3.$$

Hence,

$$\frac{p_2}{p_1} = \frac{3}{4}\frac{h}{L} \text{ and } \frac{p_3}{p_1} = \left(\frac{h}{L}\right)^3.$$

In the blowout cases it is necessary to adopt a procedure for estimating τ. The value is taken as the period which would result if the charge were placed at a depth equal to its maximum bubble

radius. τ is computed also using that same value for h, not the actual depth. The critical depth is plotted as a function of W in Figure 15.

The various quantities for the blowout shots are also shown in Table 7.

We conclude that for the one shot (Shot 5) at critical depth, namely for which L = h, the theory overestimates the observation by a factor of about 2½. For the three blowout cases the observations lie between the cylinder and the hemisphere predictions. One might suppose therefore that the actual cavity volume is somewhere between the two. The low observations on all the Solomons shots except Shot 6, whether in blowout or critical mode are possibly attributable to the muddy river bottom at the 40-foot site. Shot 6 is the only one where the observation exceeded the prediction, and also the only one fired in a different location -- somewhere in Chesapeake Bay. If the bottom there was swept clean and was rocky, it is possible that the troublesome factor of two should be restored to the theory in which case we would achieve almost perfect agreement for this shot.

4. The Duration of the First Negative Phase

The duration of first negative is given by examining the sign of G_τ (reference 6a) and determining the reduced time, call it τ',

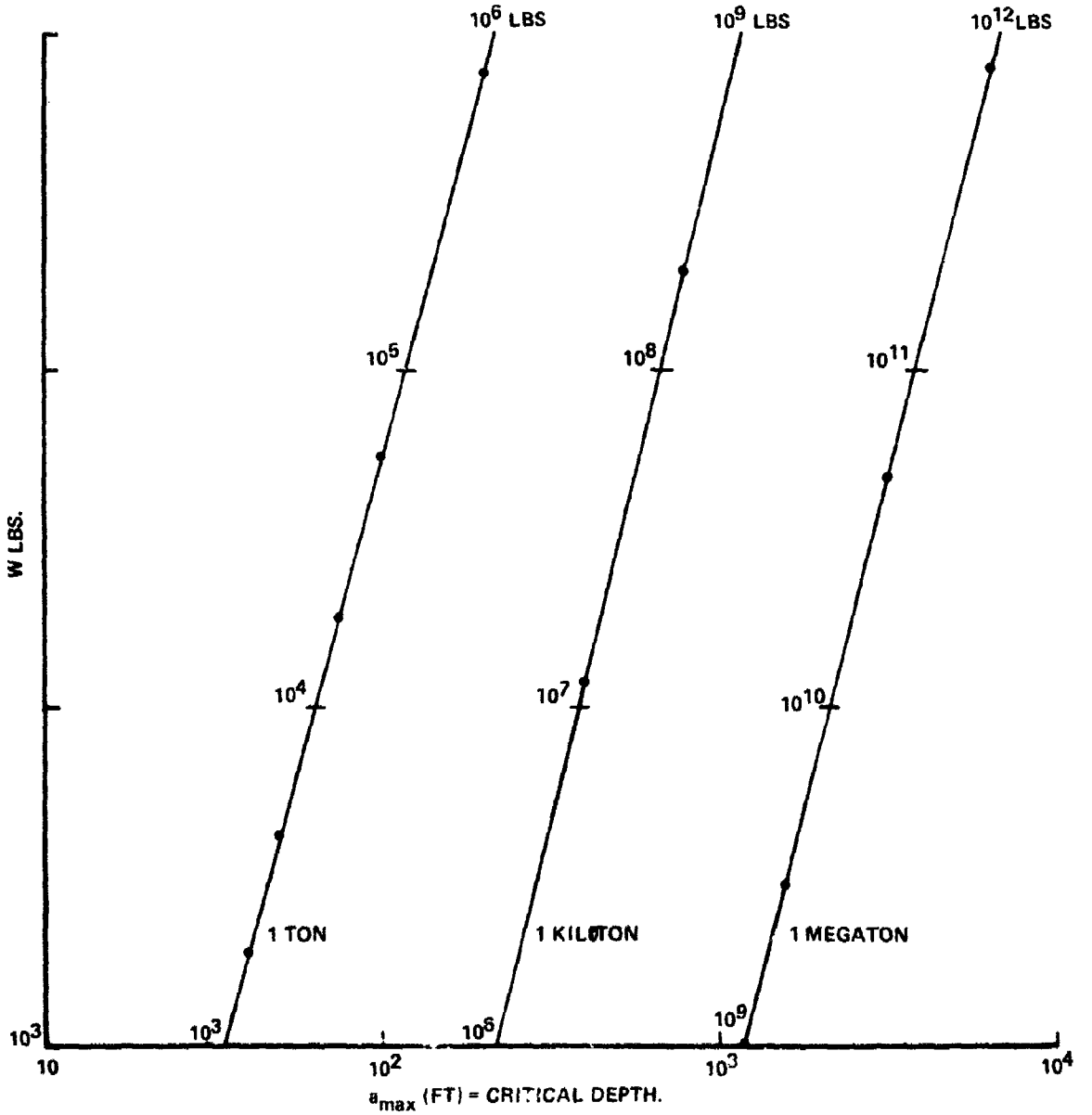

FIG. 15 MAX BUBBLE RADIUS EQUAL TO DEPTH.

between the value of t' when the first zero occurs and the second zero. The reduced value $T' = T\sqrt{g/h}$. This time is determined by G and τ and is dependent on W only through the dependence of τ on W. In the case of blowout one suspects that the value of τ to be used depends on how long it takes the cavity to fill in. Such time is probably longer than the bubble oscillation formula gives. Indications of this come from considering the volume flow when a dam breaks.[13] In any case the value of T' is very insensitive to charge size or bubble period. In determining the durations we are able to use surface photography as well as hydrophone data. The data show excellent agreement with theory. The first suction duration increases gradually with distance and is quite independent of charge weight.

The Solomons' data are plotted in Figure 16. In Figure 17 are plotted in dimensionless form all negative phase duration data available from the shots discussed in the previous section. Data marked with a H come from the hydrophone records; all other data come from surface photography. The durations on Shots 5 and 6 which were critical or nonblowout are longer than theory. On the other hand, the Woods Hole nonblowout cases have shorter durations than theory. There is no ready explanation for these differences. The dashed curve in Figure 17 represents a visual fit to the calculated duration points. It also coincides with a curve which would represent the calculated durations assuming a fixed value of τ' equal to $\sim$1.0. If the value of T' obtained from the basic function,

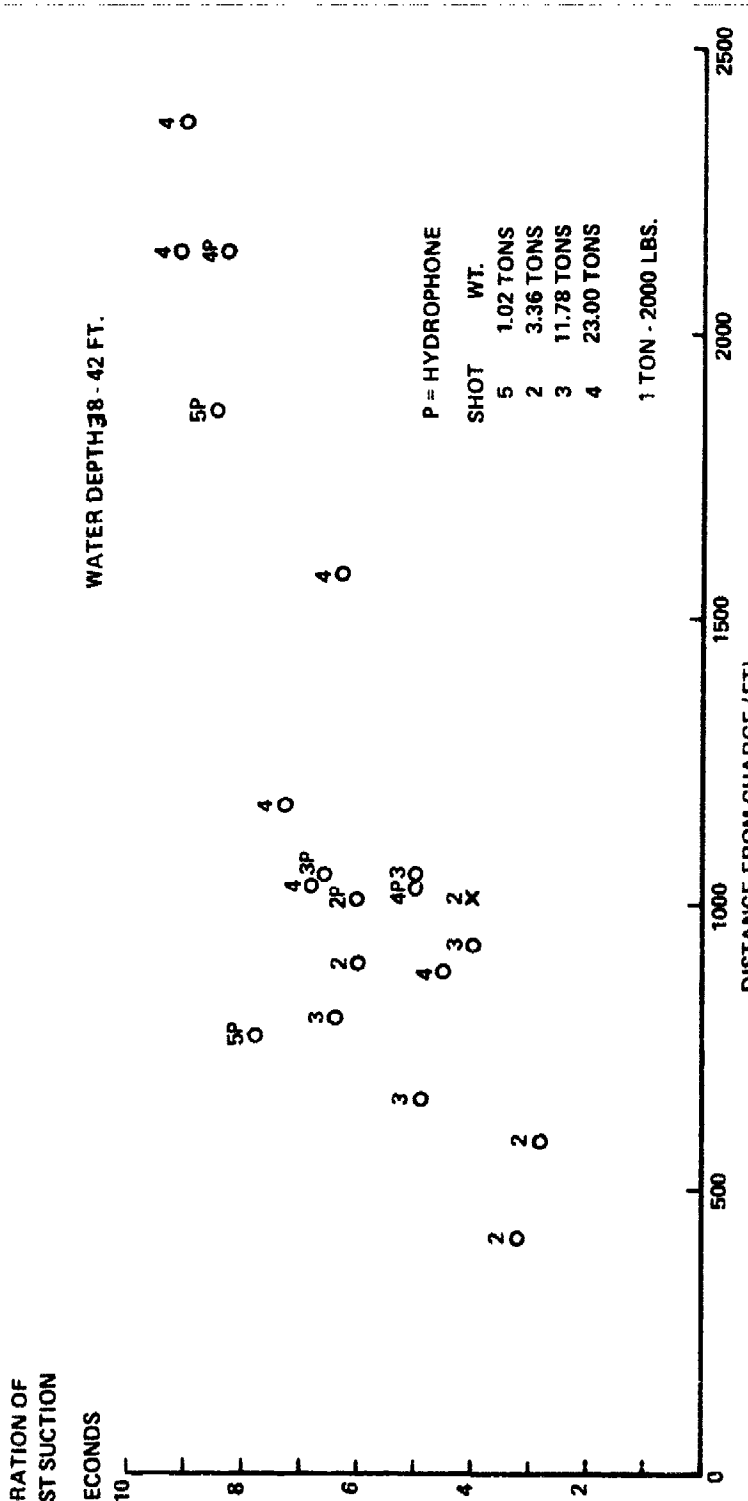

FIG. 16 DURATION OF FIRST SUCTION VS. DISTANCE.

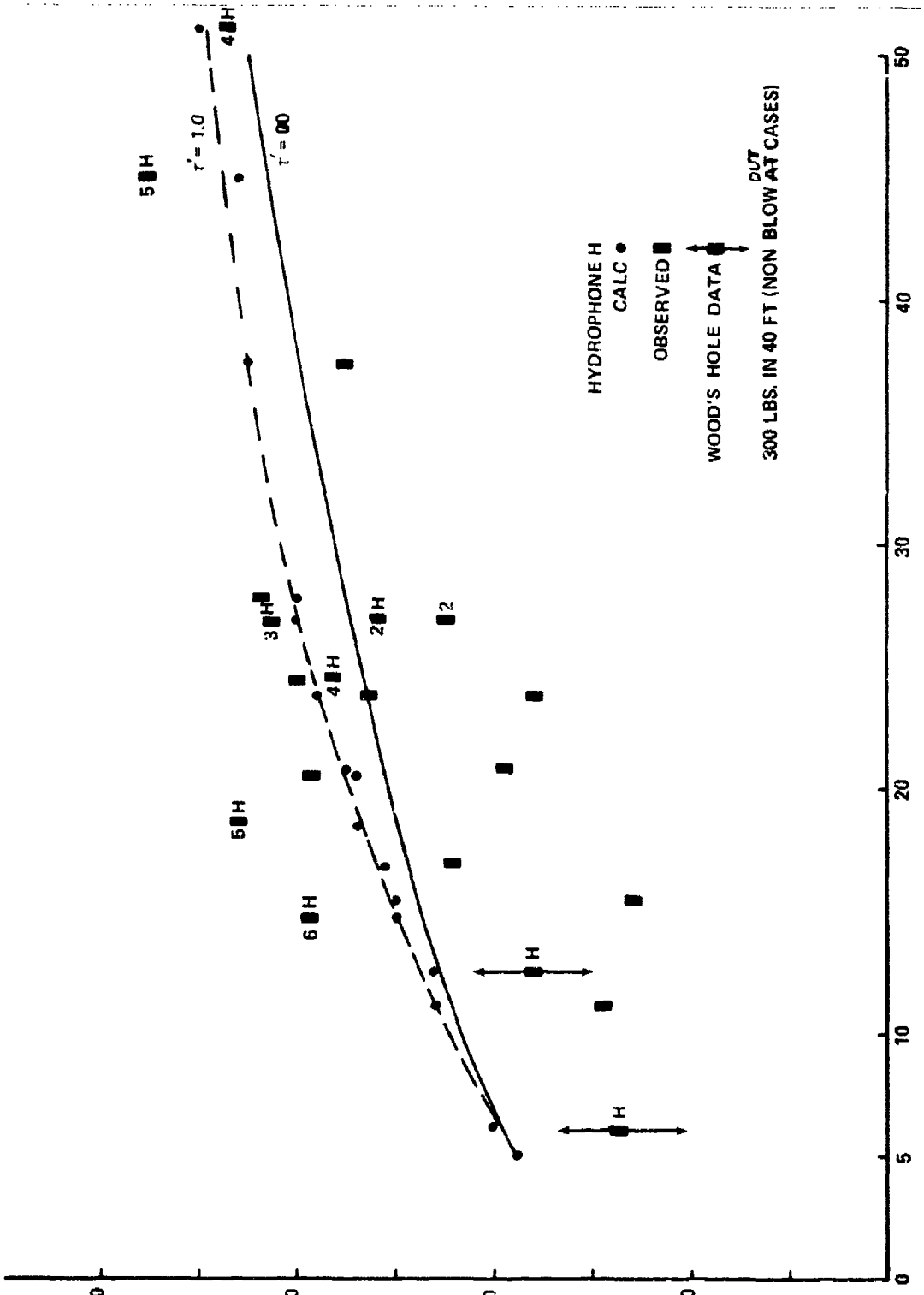

FIG. 17 SCALED DURATION OF FIRST NEGATIVE PHASE

$G_o(r',o,t')$, is plotted (call it T_∞), we obtain the solid line. This is physically equivalent to letting r' become so large that the value of G associated with it is neglected.

The theory can be summarized within one percent over the range of distance r', from 5 to 50 by the fitted relation,

$$T'_\infty = 2.43\ r'^{1/4},$$

This is the same as $T = .46(rh)^{1/4}$ seconds, (r, h in feet). If the charge is small enough there may be no observable waves, yet this relation defines the duration of the first trough even if it cannot be seen.

Taking the calculated duration as a standard, the average percent deviation of observed duration vs. calculated is -8%, i.e., the calculated is slightly in excess of the observed durations. This agreement is much more satisfactory than the amplitude situation where the uncertainties of each experiment have a much larger influence.

5. Surface Amplitudes, Trough and Succeeding Crest (Blowout Cases)

The two previous summaries complete the data and analysis related to mine sweeping applications. In this section the surface waves will be considered which are of interest in connection with very large explosions.

In Figure 18, the surface amplitudes directly observed at Solomons by pole photography are plotted against distance. We have here the first trough followed by the second crest, which is usually larger than the first crest.

In order to calculate these quantities it is necessary to use the function $G_o(r',1,t')$, tabulated in reference 6a. The extremes of $G_o(\tau = \infty)$ at the surface have been plotted in Figure 19, as well as indications of the value of G_o when $\tau' = 1.5$. For the three plotted shots in Figure 18, the values of τ' are 2.1, 3.1 and 3.9. These G values as well as the observed and calculated amplitudes are shown in Table 8. The functions for $\tau' = \infty$ have been used for estimating amplitudes.

As before (p. 68), we have, charge on bottom,

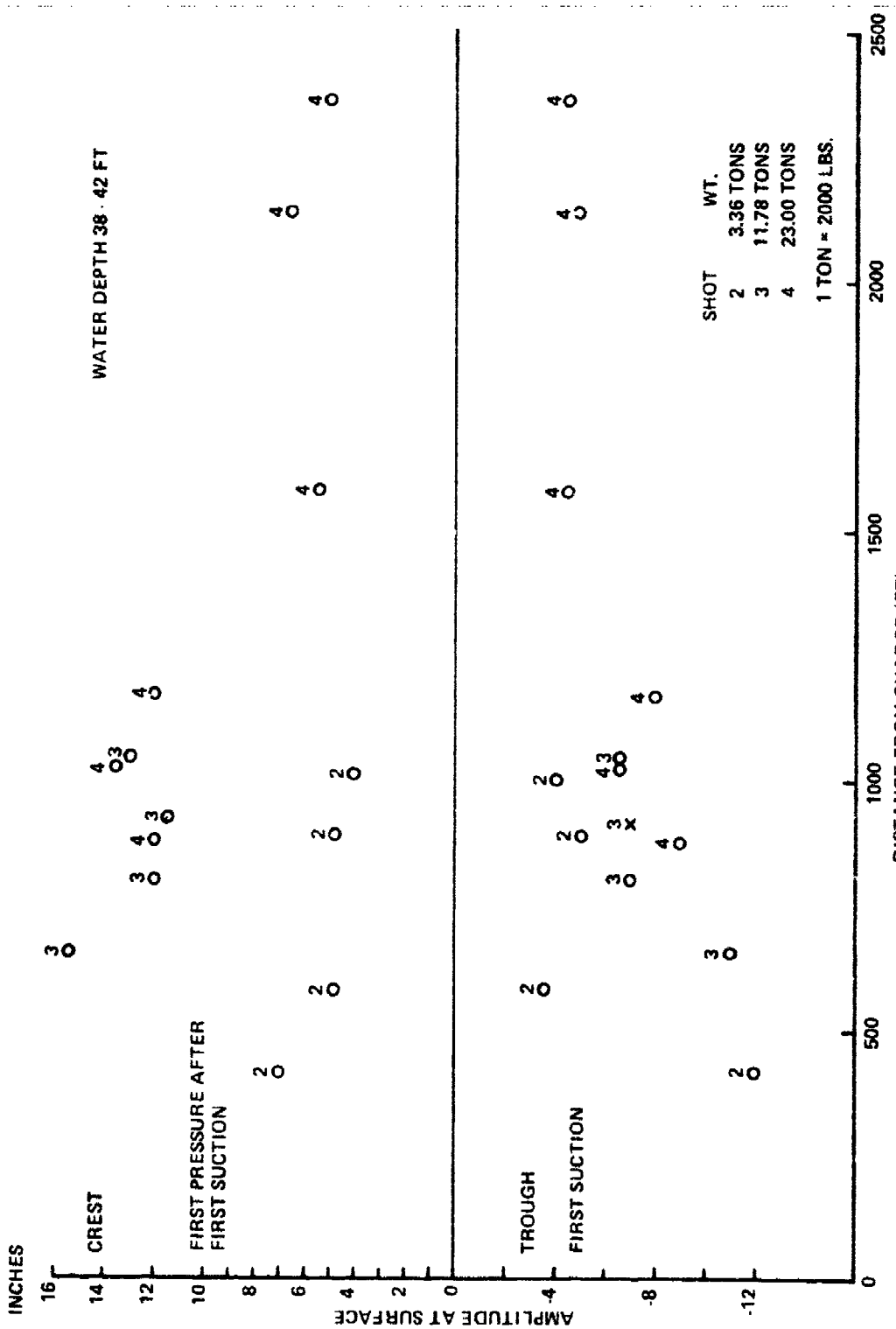

FIG. 18 SURFACE AMPLITUDE VS. DISTANCE

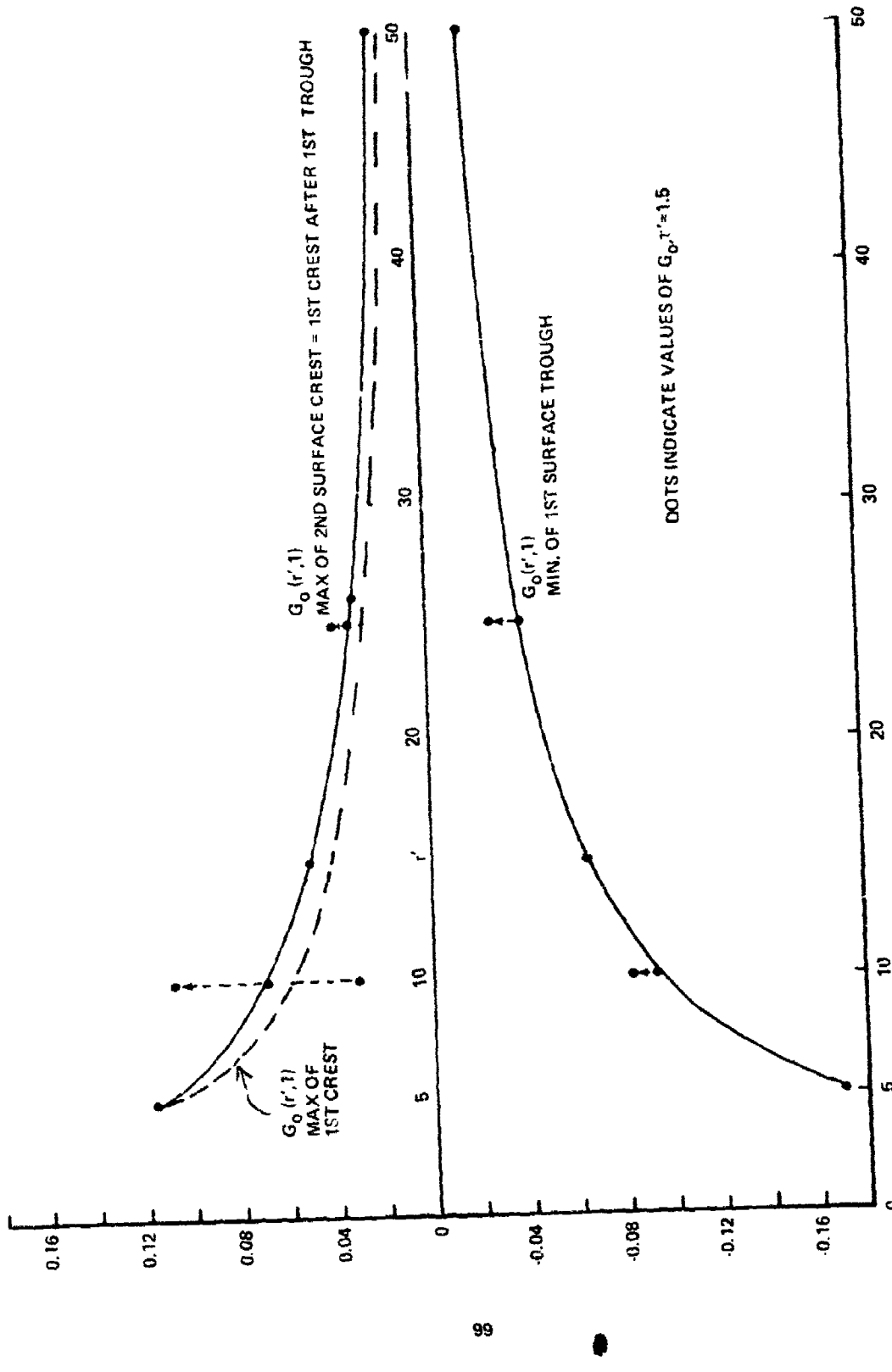

FIG. 19 EXTREMES OF G_0 AT THE SURFACE.

$$p_{1\ min} = 1.92 \frac{L^3}{h^2} G_{(1\ min)} \text{ inches}$$

and

$$p_{2\ max} = 1.92 \frac{L^3}{h^2} G_{(2\ max)} \text{ inches.}$$

We find as before that this calculation for the blowout cases grossly overestimates the amplitudes of the surface waves. If we reduce these in the ratio of $(h/L)^3$ corresponding to the hemispherical bubble, the resulting amplitudes are too small by a factor of 2 or 3. We shall see in the final chapter that the cylindrical assumption is a near approximation for blowout cases.

Table 8 Surface Amplitudes from Pole Photography

Shot	r ft	Observed p_1 min First Trough in.	Observed p_2 max First pressure After first Trough in.	r'	Calculated First min $G_o(r',1)$ $\tau = \infty$	Calculated Second max $G_o(r',1)$ $\tau = \infty$	Calculated p_1 min inches	Calculated p_2 max inches
2	419	-12	7.0	11.2	-.085	+.065	-27.4	21
at 37.5 ft	581	-3.6	4.8	15.5	-.062	.050	-20	16
6724 lbs	895	-5.1	4.8	23.9	-.040	.032	-13	10
L = 61.6 ft	1007	-4.0	4.0	26.9	-.036	.029	-11	9.3
3	659	-11.0	15.4	16.9	-.058	.045	-65	51
at 39 ft	801	-7.0	12.0	20.5	-.047	.038	-53	43
23,534 lbs	928	-7.0	11.5	23.8	-.040	.032	-45	36
L = 96.5 ft	1048	-6.5	13.0	26.9	-.036	.029	-41	33
4	879	-9.0	12.0	20.9	-.046	.038	-80	66
at 42 ft	1028	-6.6	11.5	24.5	-.040	.032	-70	56
46,000 lbs	1170	-8.0	12.0	27.9	-.035	.028	-61	49
L = 115.0	1579	-4.5	5.5	37.6	-.027	.020	-47	35
	2140	-5.0	6.6	51.0	-.021	.016	-37	28
	2363	-4.6	5.0	56.0	-.021	.016	-37	28

IV THE BAKER SHOT AT BIKINI

1. Introduction

On July 25, 1946 (local date) a nominal 20 kiloton bomb was exploded at mid-depth in 180 feet of water in Bikini lagoon. A question of intense interest was what sort of waves would be produced and how big would they be. Estimates and predictions were made by many of the participants using different methods. The sources of uncertainty as we have seen were many. For example, the Kirkwood and Seeger theory did not apply directly to the blowout case, and it was not clear how one should correct for this. Another problem was how to scale up small explosions to big ones. The charge size was so large that an uncertainty between using say $W^{1/3}$ and $W^{1/4}$ resulted in a factor of $W^{1/12}$ or 4.3 in predicted wave height. And finally the various small scale experiments done at different depths and in different places were difficult to compare. In view of this it was necessary to take certain risks in the placement of instruments and cameras, balancing the chance of getting insufficient data against the chance of being wiped out. The easy solution of course was to cover all possibilities, but then the costs became higher.

2. Penney's Bore Theory

On July 24, 1946, W. G. Penney prepared a memorandum in which he proposed a new mechanism for explosive wave making in shallow water, derived a new scaling law for such cases and predicted the Baker wave heights by scaling up relevant small scale experiments, making predictions which turned out to be nearly exact. His own statement is so concise that I quote from it:

"Theories of the wave forming mechanism of explosions below the water surface are not entirely convincing nor do they give a good description of the waves in the early breaking stage.

Visual observation and photographic studies suggest that the mechanism for an explosion near the surface is that a volume of water is hurled away from the charge, a wall of outwardly moving broken water progressively sweeps up the still water just outside; the height of this "wall" or "bore" decreases quite quickly and degenerates into a wave. Soon, by the normal processes of dispersion of cylindrically expanding waves from a finite central disturbed area, a wave train is established. The suggestion is made here that the wave train is caused by the cylindrical bore. This is in contrast to earlier theories which attributed the waves to the filling in of a cavity and the subsequent palsations of the water surface. While the later waves may have their origin in such a cause, the first two waves, which on the scale of charges of 2000

lbs or less, are much the greatest, leave the center well before th return flow to the center has developed.

The model proposed here has a scaling law different from that of the reflux to the crater, and the wave heights calculated on the "cylindrical bore" model are much smaller than those on the cavity model. Possibly, the implication is that the crater waves, which come later, perhaps waves number 4, 5, ..., at one mile from the Baker atomic bomb at Bikini will be larger, say by a factor 2 or 3 than the earlier ones. [Note, they weren't].

The "cylindrical bore" model assumes that the explosion of a mass of explosive W removes some water into the air and gives to an annulus of water still in the main body of water an outward impulse. This water then establishes a bore which picks up still water, thus reducing the mass velocity of the bore, and hence its height. The bore degenerates into waves, by the mechanism of the Cauchy-Poisson generation of surface waves from a distribution of surface elevation and impulse."

The situation is depicted as follows:

The conservation of mass requires $u = \frac{HU}{D+H}$.

This together with the conservation of momentum gives

$$U = \sqrt{\frac{g(D+H)(2D+H)}{2D}}$$

Note that if $H \ll D$, this reduces to $U_o = \sqrt{gD}$. If H is not negligible, then $U > U_o$. It may be shown that as long as H is not negligible, the bore provides a mechanism for energy dissipation.

Suppose two explosions are made with charges W and W_1 where $W = n^3 W_1$ and linear dimensions, depth of water, depth of charge, horizontal radius to any observation point are all chosen in the ratio n to 1. At corresponding points and times the particle velocities must be equal. That is $u(R,t) = u_1(R_1,t_1)$.

Since $u = H\sqrt{\frac{g(2D+H)}{2D(D+H)}}$

we have

$$H = H_1\sqrt{\frac{(2D_1+H_1)D(D+H)}{(2D+H)D_1(D_1+H_1)}}$$

Since $D = nD_1$,

$$H = \sqrt{n}\, H_1 \sqrt{\left(\frac{2\,D_1 + H_1}{D_1 + H_1}\right)\left(\frac{n\,D_1 + H}{2n\,D_1 + H}\right)}$$

This is an equation for H convenient for iteration. The approximate solution, holding well for H and H_1 small compared with D_1, is

$$H = \sqrt{n}\, H_1$$

Hence, the bore heights (and consequently wave heights at all distances) are in the ratio of $\sqrt{n}$, i.e., $W^{1/6}$.

3. An Energy Argument

A rather simpler argument based on energy conservation indicates the same conclusion for wave height scaling. Consider a subsequent single wave of height H_1 emanating from the original bore formation. Its potential energy is proportional to $\lambda_1 R_1 H_1^2$ where λ_1 is the "wavelength" and R_1 is the distance from the explosion. This energy is proportional to W_1. If we move to another scale, we must have

$$\frac{\lambda}{\lambda_1}\,\frac{R}{R_1}\,\frac{H^2}{H_1^2} = n^3$$

If now $\frac{\lambda}{\lambda_1} = n$, since $\frac{R}{R_1} = n$, we have $\frac{H}{H_1} = \sqrt{n}$. There are two cases to be distinguished. If the wavelength is small compared with the depth, then the medium is dispersive and the value of λ increases with R on a given scale. In this case assuming $\lambda \sim R$, we have

$$\frac{HR}{H_1 R_1} = n^{3/2} \quad .$$

If the wavelength is long compared with the depth, then the medium is nondispersive and the value of λ is constant as R increases on a given scale. In this case, we have

$$\frac{H^2 R}{H_1^2 R_1} = n^2$$

Cylindrical waves from explosions start out in the dispersive mode. As we shall see the Baker data fit the dispersive mode, since HR is constant rather than $H\sqrt{R}$.

The great advantage of the foregoing considerations is that one can go from one scale to another without having a detailed view of the phenomena which are taking place. If we are fortunate enough to have an experiment that is scaled to the event which it is desired to simulate, then predictions can be made easily. In the case of Bikini Baker there were two sets of experiments which had been scaled to the event. These are referred to as the NEL data,[14] and the O'Brien data[15]. The bore height quoted in Table 9 refers to the wave height above the undisturbed level. It is therefore necessary to double this value in order to make comparison with the wave measurements at Baker. Doubling is only approximately correct, since in many cases the crest is not equal to the following trough.

The Bikini Baker wave measurements are summarized as follows in "The Effects of Atomic Weapons" p. 99[16]. They are quoted only as crest to trough heights.

Let H = max height in feet from crest to following trough and R = distance from the explosion in feet. Then the Baker data fit the following relation.

$$HR = 94{,}000, \text{ within } 8000 \text{ feet.}$$

This will be presumed to be the best fit for all data obtained at these distances. [Beyond 8000 feet the empirical equation (HR)·9 = 42,700 is given.]

The explosion at Baker occurred in 180 feet of water at mid-depth. The equivalent charge radius was 45 feet and so the water was presumably completely removed just as if the charge had been on the bottom. In fact it is possible that a greater fraction of the charge energy went into wave making than if it had been resting on the bottom (because of less damage to the bottom). This consideration, however, will be ignored, and we will assume that a high explosive scaled experiment with the charge on the bottom is equivalent to one with the charge at mid depth. In either case the water is completely removed from a cylindrical volume surrounding the charge. In the scaled NEL & O'Brien experiments quoted, it is not positively stated whether the charges were on the bottom, but it is assumed that they were. The information is summarized in Table 9.

Table 9 High Explosive Results Scaled to Baker

	Original Data						Scaled To 20 kt			
Source	W_1	D_1 charge	D_1 water	R_1 ft	H_1^1 inch	n	D ft	R ft	H^1 ft	RH^1
NEL	2040 lbs.	83 inch	same	161	24	27	187	4350	10.4	45,250.
	278	40.5	"	82	15.5	52.4	177	4300	9.4	40,500.
	44	23	"	46	12.5	95.5	183	4400	10.2	45,000.
O'Brien	1000.	60	"	330	9.6	34.2	171	11300	4.67	52,500.

These shots were at a depth of four charge radii. In the absence of definite information it will be assumed that the charges were on the bottom. The nature of the bottom is not known and presumably would make a difference, that is, a rocky hard bottom would not absorb energy as much as a soft mud bottom and would therefore make for larger waves. Furthermore, the positive phase height is quoted, H_1^1, and we are forced to double it to compare with the Baker quoted value which goes from crest to trough. It is clear however that the

bore scaling applies because the depths are all the same when stated in terms of charge radii, and are in the blowout region where the bubble radius formula does not apply. Hence all dimensions are scaled as $n = \left(\frac{W}{W_1}\right)^{1/3}$ and wave heights are scaled as $\sqrt{n}$. This produces for the NEL average HR = 87,200 and for O'Brien, HR = 105,000. The corresponding measurement for Baker is HR = 94,000. This agreement can be taken to mean the nuclear explosion underwater behaves like a conventional explosion of the same yield, as far as mechanical effects at a distance are concerned. It may also be assumed that the mid depth explosion of a nuclear bomb in such shallow water resolves itself into the same situation as a high explosive of the same energy sitting on the bottom. There also may be a compensating effect i.e., that the nuclear explosion at 2 equivalent charge radii from the surface lost the same fractional energy to the atmosphere that the high explosive at the depth of 4 charge radii lost to the bottom in making a crater. In this way the scaling up of the high explosive experiment leads to a correct prediction of the nuclear experiment in this very shallow situation. The agreement of prediction with later observation within 2% is truly remarkable.

5. A Speculative Adjustment to Make Scaling Applicable

We have seen that the "bore" scaling works well when the dimensions of the experiment are in scale. If, however, we apply "bore" scaling to say Shot 4 of the Solomons' data, where n = 9.3,

we find that the predicted wave heights are too small and the depth is too large. That is, the scaled up depth is 370 feet and the average value of HR is 4900 (crest to trough). If the same weight had been fired at Solomons' in 20 feet of water, then the scaled up depth would have been 185 feet and presumably (except for mud absorption) the height-distance product would have been larger. This in fact seems backward, that by decreasing the depth we would expect an increase in wave height. There may be a physical reason for a possible effect of this sort within limits of course. It is related to the behavior of the gases as they escape from the water in the shallow explosion case. In brief, if the explosion is deep, the gases have to work against the static pressure including the atmosphere. If the explosion is shallow, the work against the atmosphere is cancelled when the gases break out. If a large fraction of the available energy has been converted (i.e., if the explosion is not too shallow) to kinetic energy in the water, then it is possible that a cavity can be formed with a larger radius than L. The range of depths of charge within which this is possible is quite small, probably between two and about eight charge radii. Such a larger cavity would produce a higher bore and a larger wave.

To review, if there is no blowout, the maximum bubble size is determined by the work done against the total hydrostatic pressure including atmospheric.

The pressure inside the bubble at its maximum size is very low, perhaps .1 atm. In the case of blowout the pressure inside the cavity at some stage in the expansion phase becomes atmospheric. Consequently, the expansion can proceed without doing any work against the atmosphere. The resulting size of the crater will then depend on how much kinetic energy the water was able to absorb before blowout.

Let L = max radius in feet.

Experimental data on periods show that 45% of the energy remains in the bubble. Then,

$$L = 13.5 \left(\frac{W}{D_c + 33}\right)^{1/3}$$

where D_c = depth of charge below surface.

$$\text{Let } n^3 = \frac{W}{W_1} = \frac{L^3}{L_1^3} \frac{D_c + 33}{D_{c_1} + 33} \text{ (for no blowout)}$$

For the blowout case we have $L > D_c$. Let D = depth of water. We wish to estimate the maximum crater radius, a. The work done to produce the crater and the elevated annulus is $\rho g \pi a^2 D \frac{D + C}{2}$

where C is the height of the annulus above sea level. This work is equal to that part of the explosion energy not sent off in the shockwave. If the explosion is deep enough to allow the underwater shock to be formed - say two charge radii or more, then we can assume that 45% of the energy is available for crater formation. This energy is imparted very early to the water as kinetic energy. Hence, try writing

$$\rho g \pi a^2 D \frac{D + C}{2} = .45W \times 1.48 \times 10^6$$

[A detonation energy of 1060 cal per gram is equivalent to 1.48 x 10^6 ft lbs energy per lb of explosive.]

In the above $\rho = 2$, $g = 32$.

$$a^2 D(D+C) = 6650W$$

If D>C, we may approximate a by

$$a = \sqrt{\frac{6650\ W^{1/2}}{D}} = 81.5 \frac{W^{\frac{1}{4}}}{D}$$

If on the other hand C is of the order of D, then $a = 57 \frac{W^{\frac{1}{4}}}{D}$. Values of a obtained from either of these relations for small values of D are of course too large to represent any real cavity radius. In fact, they suggest that the value of energy assigned to

the crater formation is much too large, recalling that not 45% of the explosive energy shows up in waves but only perhaps 1/100 of that. Nevertheless, the temptation is strong to believe that if we change the depth of this shot from 40 feet to 20 feet, whatever the value of a was will increase by a factor of two. Hence, the volume removed from the crater will be greater by a factor of two because volume is proportional to a^2 times depth. If the energy available for waves is likewise doubled, the wave heights at the same distance would then increase by $\sqrt{2}$. We infer that if we had fired the 46,000 lbs in 20 feet instead of 40 feet the HR product could have been 2460 instead of 1740, and the scaled up value from this would be HR = 70,000 for 20 kt in 180 feet of water.

It must be admitted that this is pure speculation, and that a scruting of Charlesworth's shallow data does not confirm the notion.

Whatever the merits of this discussion it is clear that there is a change of regime when charge depth is progressively less than the critical depth. The cavity changes from an expanding sphere to an expanding ring of some sort. In the first case one can scale from one size to another and we will have $L \sim n^{2/3}$ (for D>>33) or $L \sim n$ (for D<<33). In the second case the radius of the cylindrical cavity will scale as $n^{1/2}$.

6. Use of Kirkwood and Seeger's theory To Make Adjustments

Another way to adjust the data of a given shot to conditions from which bore scaling may be done is to use the Kirkwood and Seeger theory. In other words, if for Shot 4 (Solomons) the value of HR is 1740, what should it be if the same weight were exploded in 20 feet of water instead of 40 feet?

We know that

$$H \sim \frac{\overline{V}\, G}{D^2} \quad .$$

Using the cylindrical model we have $\overline{V} \sim L^2 D$.

Hence. $$\frac{H_{20}}{H_{40}} = \frac{L_{20}^2}{D_{20}} \frac{D_{40}}{L_{40}^2} \frac{G_{20}}{G_{40}}$$

The value of L_{40} for this shot is 116 feet; $L_{20} = 127$. At a given distance, say R = 1000 feet, in the original shot, $r^1 = \frac{1000}{40} = 25$; whereas if the depth is only 20 feet, then we must evaluate the G function at $r^1 = 50$. Since H is the sum of the first trough and the next crest, we must find the G values for these, for $r^1 = 25$ and $r^1 = 50$. Fortunately, the tables exist for just these values. We find,

G_{40}: $G_o\ (25,1)_{1\ min} = -.0400$; $G_o\ (25,1)_{2\ max} = .0318$

G_{20}: $G_o\ (50,1)_{1\ min} = -.0207$; $G_o\ (50,1)_{2\ max} = .0169$

Hence,

$$H_{20} = H_{40} \left(\frac{127}{116}\right)^2 \frac{40}{20} \frac{.0207 + .0169}{.0400 + .0318}$$

$$H_{20} = H_{40} \times 1.26$$

We conclude that if the same charge had been fired in 20 feet of water the waves would have been 26% higher at the same distance. Hence the value of HR would be 2190 feet^2 and the corresponding bore scaled prediction for Baker would be 2190 x $n^{3/2}$ = 62,000.

This result is fairly close to the preceding estimate. Both depend on guesses as to the proper value of volume to use. The beauty of a properly scaled experiment is that all such speculations are avoided. It is nevertheless unfortunately necessary to have to make such deductions in the absence of scalable data.

7. The Cavity at Baker

"The Effects of Atomic Weapons"[16], p. 40, states that the greatest radius of the "plume" at Baker was 1000 feet. The plume is described as the entrained water which was propelled upward by the escaping gases (mostly steam) from the explosion itself. The plume overtook and exceeded the spray dome at a height "of a few thousand feet." The spray dome, caused by the reflection of the underwater shock wave from the water surface, had a radius probably less than 1000 feet. Its radius estimated from dome formation investigation (Effects p. 97) is about 800 feet. The radius at which the dome degenerates into the travelling slick is of course not precisely determined. The base surge appeared at a radius of 1230 feet at 10 seconds after the burst (Effects p. 106). The expression for spherical bubble radius (Section 5) gives a value of L = 930 feet which is curiously of the same magnitude as the plume or column diameter. Although this formula (for L) does not apply to the blowout case, it appears to give a reasonable estimate of the cavity radius which was presumably less than the plume radius but must have been considerably more than the depth. There is another clue to the possible estimation of the maximum cavity size. The bubble period for the nonblowout case is given by

$$\tau = \frac{4.36W^{1/3}}{(D+33)^{5/6}} \text{ sec.}$$

where D = depth of charge below surface.

In case of blowout, use this to estimate time for bubble to reach its maximum radius. This time should be approximately $\tau/2$. The filling of the cavity is by a different process (similar to the breaking of a dam).

In the case of Baker,

$$\frac{\tau}{2} = 13.6 \text{ sec}$$

This is about the time of maximum diameter of the water column. See p. 104 of Effects of Atomic Weapons. In other words, the maximum diameter of column occurs at approximately the same time and in the same size as is calculated from the nonblowout formulae. This may be due to the fact that a large transfer of energy to the water occurs in the very early stages of the explosion expansion. The subsequent size of the bubble is determined by expansion against ambient pressure. It is possible that the energy communicated to the water in the shallow cases is less than in the deep cases because of blowout, but that the ambient pressure against which the expansion occurs is less because of the shallower head of water, and because there is no work done against the atmosphere as there is in the self contained (deep) case. Consequently these effects are

contrary and compensating so that the apparent agreement in the Baker case between the deep formulae predictions and the observations is better than one would originally have guessed.

8. Other Baker Predictions

We have found elsewhere that the Kirkwood and Seeger theory over estimates by 100% the single observation to which it applies, namely a nonblowout (critical depth) experiment done in midwater (not on the bottom) by Charlesworth using a 32-pound charge. In predicting wave heights for Baker, Kirkwood and Seeger in a memorandum to O'Brien, dated 29 June 1946, overestimated the wave heights by a factor of 6 to 8 at distances between 5000 and 10,000 feet. If in their prediction they used the final formula of their later paper, they overestimated the source volume, by a factor of about 7, i.e., the ratio of $4/3\ \pi\ L^3$ to $\pi\ L^2 D$. A new calculation based on their subsequent paper overestimates the trough to crest wave height by a factor of 12. It is not known how the volume was estimated.

V CONCLUSIONS

In this chapter we shall summarize the data, discuss the scaling and review the procedure for estimating waves for a given situation.

1. Data Summary

We have seen first that the wave height (trough to crest) multiplied by the distance is a constant for a given explosion provided we are not too far away. At great enough distance we expect that H R will be constant. Table 10 shows the HR values observed for the three Solomon's shots where surface measurements were made.

Table 11 shows averaged products of wave height x distance for all data previously discussed. Figure 20 represents the data scaled up in all cases by simply multiply the measured H x R by $\sqrt{\frac{40 \times 10^6}{W}}$.
As we have seen this works for different reasons for both blowout and deep shots. It seems that the blowout data obtained for freewater explosions and for bottom shots (Solomons) corrected to

Table 10 Wave Height x Distance, Solomons

The following table shows the constancy of HR for each of the three Solomons shots:

Shot No.	R ft.	Trough to Crest Height inches	HR inch ft.	Avg. values RH (ft^2)
2.	419	19	7950	
	581	8.4	4900	630
	895	10.0	8950	
	1007	7.4	7450	
3.	659	26.5	17500	
	801	19.0	15200	1470
	928	18.5	17200	
	1048	19.5	20500	
4.	879	21	18500	
	1028	20	20600	
	1170	20	23400	1740
	1579	10	15790	
	2140	11.5	24600	
	2363	9.5	22400	

Table 11 Data Summary: Wave Height x Distance, All Shots

Source		W lbs.	D ft.	Depth in charge radii	$\frac{D}{L}$	HR ft^2 Surface trough to crest	$\frac{40\times10^6}{W}$	Scaled up HR ft^2	Remarks
	2	6700	40	15.5	.66	630.	77.5	49,000.	Surface photography
	3	23500	40	10.3	.44	1470.	41.0	60,000.	"
Solomons	4	46000	40	8.2	.34	1740	28.2	49,000.	"
	5	2034	40	23.4	1.00	145.	140.	20,300.	Hydrophones corrected to surface ampl.
	6	2025	100	58.5	3.00	158	140.	22,100.	"
Woods Hole		300	20	11.0	.83	75	366.	27,200	Hydrophones corrected to surface ampl.
NEL		2040	83"	4.00	.138	322x2	140	90,000.	Surface photography
		278	40.5"	3.80	.128	106x2	379	80,200.	"
		44	23"	4.00	.131	4.8x2	931	89,500.	"
O'Brien		1000	5	3.7	.125	264x2	200	106,000	Surface photography
Charlesworth		32	8	18.5	.67	82	1120	92,000	In 15 ft of water surface photography
		"	2	4.6	.15	69	"	77,000	"
		"	3	7.0	.23	71	"	79,000.	"
		"	4.75	11.0	.37	60	"	67,000.	"
		"	6.5	15.0	.51	78	"	87,000	"
		"	9.5	22.0	.76	85	"	95,000	"
		"	18	42.0	1.56	32	"	36,000	Charge on bottom in gravel pit
Baker		40×10^6	90	2.0	.087	94,000	1	94,000	Water depth 180 ft

The quantity L is computed from $L = 13.5\ (\frac{W}{D+33})^{1/3}$ for all cases including blowout cases (for which the formula strictly does not apply but gives a good estimate).

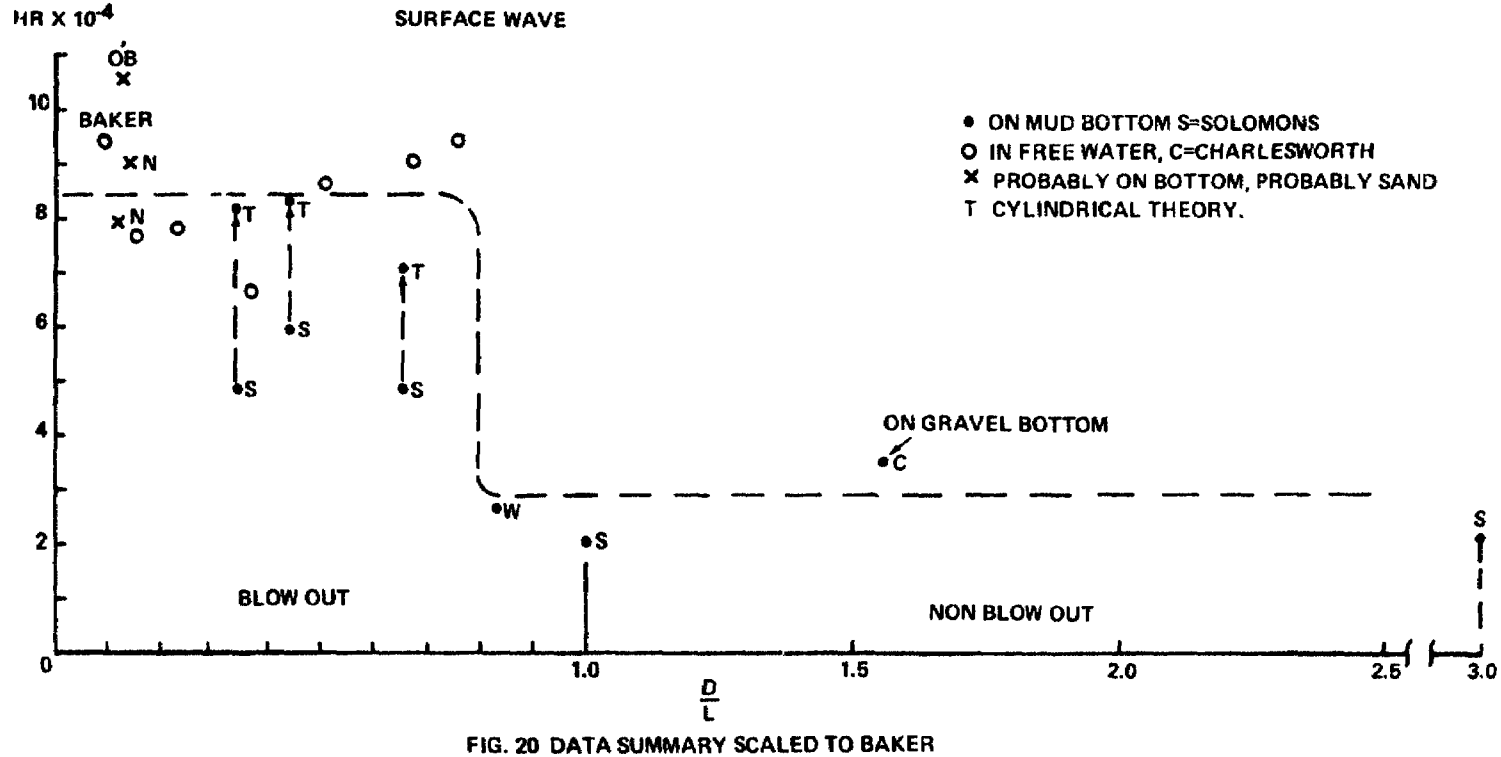

FIG. 20 DATA SUMMARY SCALED TO BAKER

free water all give a value of between 80,000 and 90,000 feet^2 when scaled up to Baker.

An estimate is made using the Kirkwood and Seeger theory with cylindrical volume calculation for the three Solomons' shots that were blowouts, i.e., for which L>D. We have:

Shot No.	L	$\frac{4}{3}\frac{L}{D}$	Theory* HR(spherical volume)	Theory HR cylindrical	Measured HR	Ratio
2	61.6	2.0	1820 ft^2	910	630	1.44
3	96.5	3.2	6500	2040.	1470.	1.38
4	115.0	4.0	11600.	2900.	1740.	1.67

*From Table 8 calculated values.

It can be seen that the cylindrical volume overestimates the results by only 38 to 67%. Perhaps these remaining differences can be attributed to the uncertainties of the mud bottom. If that were assumed, for example, then one could claim that the blow out results should be given by the cylindrical theory. Then for Baker scale the HR values for Shots 2, 3, and 4 if they had been done at middepth should be 71,000, 84,000 and 82,000. The nonblowout, bottom, shots give a mean value of about 30,000. The conclusion is indicated that charges on the bottom even at optimum depth produce waves which are

1/2 to 1/3 the height of waves produced by the same charges off the bottom in the same water depth.

2. Kirkwood and Seeger Summary

According to Kirkwood and Seeger, the amplitude of a wave is equal to $\frac{1}{2\pi h^2} \overline{V}$ x related G value.

$\overline{V}$ is the time average of the bubble volume.

For deep explosions not on the bottom,

$$\overline{V} = \frac{4}{3} \pi \ (.4819) \ L^3$$

where

$$\overline{a^3(t)} = .4819 \ L^3$$

$$\therefore \text{Amp} = .321 \ \frac{L^3}{h^2} \ G \text{ ft.}$$

For nonblowout explosions on the bottom, Kirkwood and Seeger say that the value of $\overline{V}$ to use in calculating amplitude is half as

large, i.e., $\frac{2}{3}\pi(.4819)\ L^3$. Hence for charge on the bottom the amplitude is

$$\text{amp} = .1606\ \frac{L^3}{h^2}\ G \text{ ft.}$$

If charge is at a blowout depth but not on the bottom, "a better approximation is the volume of a cylinder if a height equal to the depth of the water and a radius slightly less than the maximum spherical globe in an unbounded liquid," (6). Actually one should consider the time average of the volume averaged over its life. This is hard to do in the blowout case because we don't know the volume mode of expansion or collapse. At any rate take the volume expression as $\overline{V} = \pi\ h\ \overline{L}^2$. If $L \sim \sin \omega t$ for example, then $\overline{V} = .5\ \pi h L^2$. One could take this time average factor to be the same, i.e., .4819. If the charge is on the bottom one could, to be consistent with the previous calculation, assert that the volume was half what it would be if the charge were at the same depth in deep water.

Then

$$\overline{V} = .4819\ \frac{\pi h L^2}{2}$$

and

$$\text{amp} = \frac{1}{2\pi h^2} .4819 \frac{\pi h L^2}{2} \quad G;$$

Half cylindrical on bottom.

also

$$\text{amp} = \frac{1}{2\pi h^2} \frac{2}{3} \pi .4819 L^3 \quad G;$$

Half spherical on bottom.

$$\text{Ratio } \frac{\text{spherical}}{\text{cylindrical}} = \frac{2}{3} \frac{L^3}{(\frac{h}{2}) L^2} = \frac{4}{3} \frac{L}{h}$$

The volume for Baker and hence the predicted wave height is overestimated by a factor of 7 (h = 180, L = 930) by using the spherical rather than the cylindrical expression.

3. Scaling (Impulsive, Bore, Deep, Blowout)

Surface waves in water are a gravity controlled phenomenon. When we change from one scale to another, for example by chosing a different charge weight, the value of gravity is unchanged. The linear dimensions change in the ratio of $n = (\frac{W}{W_1})^{1/3}$. This

includes the charge radius, charge depth, water depth, and distance. Time however goes as $\sqrt{n}$ in order for g to remain constant from one scale to another. This requires wave velocity to scale as $\sqrt{n}$. Wave displacement and the particle velocity associated with it, however, may have various scaling laws depending on the method of wave formation. To see how this comes about let us start with the case of waves produced by a downward impulsive loading of the water surface (such as would be caused by an airburst over water). It has been shown by the Applied Mathematical Group N.Y.U. ($\sim$1946), by Penney (Gravity Waves, etc.) that the wave amplitude in this case is proportional to the sixth root of the charge weight ratio. This can be illuminated by the following simplified argument. Let the vertical wave displacement be represented by $\eta = A \sin \omega t$. The particle velocity then is $\dot{\eta} = A\omega \cos \omega t$. On the two scales these velocities are equal. This is because the impulse to an area varies as n^3 and the mass of water affected also varies as n^3. Hence all initial velocities are the same. Note that for the initial loading phase gravity is not a part of the process and time scales in the same manner as distance. It is for this reason that the initial particle velocity acquired by the water is the same on all scales. Returning, then, to the ensuing wave motion we have,

$$A_n \omega_n = A\omega$$

The wave velocity is proportional to $\sqrt{\text{Depth}}$, gravity being unchanging, and hence scales as n. Hence it follows that time must scale as $\sqrt{n}$. Therefore, ω scales as $\frac{1}{\sqrt{n}}$ and from the above relation λ scales as $\sqrt{n}$. Note that wave velocity being proportional to wavelength times frequency requires that λ scale as n. Therefore, all lengths scale as n except the wave height which goes as $\sqrt{n}$ or $W^{1/6}$. It is this very fact which allows the particle velocities on different scales to be equal, since time also scales as $\sqrt{n}$. For the case of impulsive loading, if the charge weight is increased the wave amplitude increases as the square root of the linear dimension or the sixth root of the charge weight.

If we now put the charge into the water in a blowout position, we see that the bore forming mechanism is somewhat analogous to the previous instance except that the loading is horizontal instead of vertical. Water is pushed outward by the explosion gases, and the outward velocity impulsively acquired is the same on the different scales. This outward movement causes the bore front to form in the same fashion as a shock front forms in a shock tube. The conservation laws (mass and momentum only) applied to this formation require the bore height and hence ensuing wave heights to vary as $\sqrt{n}$, when we go from one scale to another. After the wave system is formed, time scales as the square root of the linear scale factor as is generally required for all gravity waves.

Let us now consider the nonblowout case and ask how wave heights should change when charge weight is changed from one nonblowout case to another. We take the Kirkwood and Seeger theory to be a valid expression for wave height for this situation and can write

$$\text{Amplitude} \sim \frac{\bar{V}}{h^2} \times \text{related G function} \sim \frac{L^3 G}{h^2} \sim \frac{W G_T\ (r^1, z^1, t^1)}{h^2\ (D+33)}$$

If we change charge weight, G is unchanged except for the effect of W on τ. Consider the critical case in which L = D and, in addition, they both are large compared with 33. Then $L^3\ D \sim W$ or $D^4 \sim W$ and $D \sim W^{1/4}$ or $n^{3/4}$. Let m be proportional to $W^{1/4}$. If depth is scaled according to m, time as $\sqrt{m}$, wave velocity as $\sqrt{m}$, distance as m, then,

$$\text{Amplitude} \sim m \quad .$$

We have seen that if the charges are not too large, i.e., the value of τ^1 is limited (less than about 2), then the G function at a given distance is proportional to τ^1. G is also inversely proportional to r^1. This leads to an expression for wave height such that

$$H \sim \frac{\bar{V}}{h^2} \frac{\tau^1}{r^1}$$

Since $\tau^1 \sim \sqrt{\frac{g}{h}} \frac{W^{1/3}}{(D+33)^{5/6}}$, we find that

$Hr \sim m^2$ and wave heights vary as $m = W^{1/4}$ at corresponding distances for deep explosions (neglecting 33 compared with D) where W is of the order of one ton or less. All distances scale as $W^{1/4}$ and time scales as $W^{1/8}$.

Let us now look at the blowout case or the relatively shallow explosion in which the spherical bubble volume is to be replaced by a cylindrical crater of radius L and depth h. In this case for large charges we have

$$\text{amplitude} \sim \frac{W^{2/3}}{h(D+33)^{2/3}} \quad G$$

If G is unchanged, i.e., if τ is very large and if D>>33, then

$$\text{according to this, the amplitude} \sim \frac{n^2}{n \cdot n^{2/3}} = n^{1/3} \quad .$$

If D<<33, amplitude would vary as n.

These relations are incorrect since they are at variance with bore scaling which is quite straightforward. They fail because the whole postulate of a simple spherical source assumed in the Kirkwood and Seeger development is invalidated by the interference of surface and bottom in the blowout case. The bore scaling does not describe the wave forming process; it merely identifies corresponding situations and lets whatever happens on one scale repeat itself on another. The Kirkwood and Seeger scaling for the deep explosion or explosion at critical depth predicting wave heights as $W^{1/4}$ at corresponding $W^{1/4}$ distances should be correct. We note that the cylindrical formula is consistent with wave heights and distances scaling as $W^{1/4}$. However, as the depth is diminished, we expect to go over to the bore scaling regime, and the cylindrical formula does not give any indication as to what depth at which this occurs. It is impossible to scale from a nonblowout case to a blowout case or vice versa.

Scaling may then be done from one blowout case to another, scaling wave heights as $W^{1/6}$, other distances as $W^{1/3}$ and time as $W^{1/6}$. Scaling may also be done from nonblowout to nonblowout, scaling wave heights as $W^{1/4}$, other distances as $W^{1/4}$, and time as $W^{1/8}$. Wave velocity in the one case, goes as $W^{1/6}$ and in the other as $W^{1/8}$.

4. Energy Consideration for Deep or Shallow Scaling

The potential energy of a cylindrically spreading wave is proportional to the wavelength, the distance from the center and the square of the wave height. This quantity should therefore be proportional to the charge weight.

Hence in all cases $W \sim r\lambda_o H^2$ initially. Now with bore or impulsing loading scaling we have $r \sim \lambda_o \sim n \sim W^{1/3}$; $H \sim \sqrt{n} \sim W^{1/6}$. With deep explosion scaling we have $r \sim \lambda_o \sim H \sim W^{1/4}$. The interesting thing is that in either case we have $rH \sim W^{1/2}$. This makes it possible to compare the shallow and deep cases at the same charge level simply by using $W^{1/2}$ for the product.

If the wavelength is sufficiently long that there is no dispersion, then λ_o is independent of r. If there is dispersion, then λ_o = const x r. In one case $H\sqrt{r}$ is constant for a given explosion. In the other, HR is constant. We have seen that in the early stages of explosive wave making the waves are short enough for dispersion to occur. Later, the waves attenuate so that if they achieve a constant wavelength, they may be too small to measure. Whether there is or is not dispersion makes no difference to the scaling laws which are determined by the wave formation process.

5. Prediction of Waves

Knowing the charge weight, depth and water depth how can the waves resulting from an explosion be predicted? The first step is to compute L and determine whether the explosion is in the blowout region or not. Figure 21 illustrates the two regimes and shows the appropriate formula. If the explosion is in the blowout region, determine the value of the HR product in feet by multiplying 13.5 by the square root of the charge weight in lbs. [This comes from Figure 20 where HR for $W = 40 \times 10^6$ is taken as 85,000 $feet^2$ ± 5%]. This product will estimate the trough to crest wave height at any chosen distance R feet, particularly if the charge is not on the bottom. If the charge is on the bottom then the wave height estimated by this procedure should be reduced by about one-third. (Multiply by 2/3). If the explosion is in the nonblowout region, one can calculate HR for this case by multiplying 4.8 by $W^{1/2}$. This will estimate H for any given R for a charge in the nonblowout regime on the bottom,,. If the charge is not on the bottom the estimate for H should be increased by a factor of 1.5 (multiply by 3/2).

For the nonblowout case it is also possible to make the estimate without having recourse to previous experimental data, through the use of the Kirkwood and Seeger theory. If the charge is about 2000 lbs. or less, it is possible to express $G_\tau 1$ as proportional to τ^1. From the tables in Kirkwood and Seeger, a

detailed calculation of $G_\tau 1$ at the first minimum (trough) and at the next maximum, (crest) on the surface as a function of τ^1 shows that we can write,

$$G_\tau 1_{min} = \frac{-.48\ \tau^1}{r^1}$$

and

$$G_\tau 1_{max} = \frac{+.66\ \tau^1}{r^1}$$

The trough to crest height is

$$H = \frac{\overline{V}}{2\pi h^2}(-G_\tau 1_{min} + G_\tau 1_{max}) = \frac{1.14\ \overline{V}}{2\pi h^2}\ \frac{\tau^1}{r^1}\ \text{ft.}$$

or

$$H = \frac{1.0\ \overline{V}}{h^{3/2}}\ \frac{\tau}{r}\ \text{ft.}$$

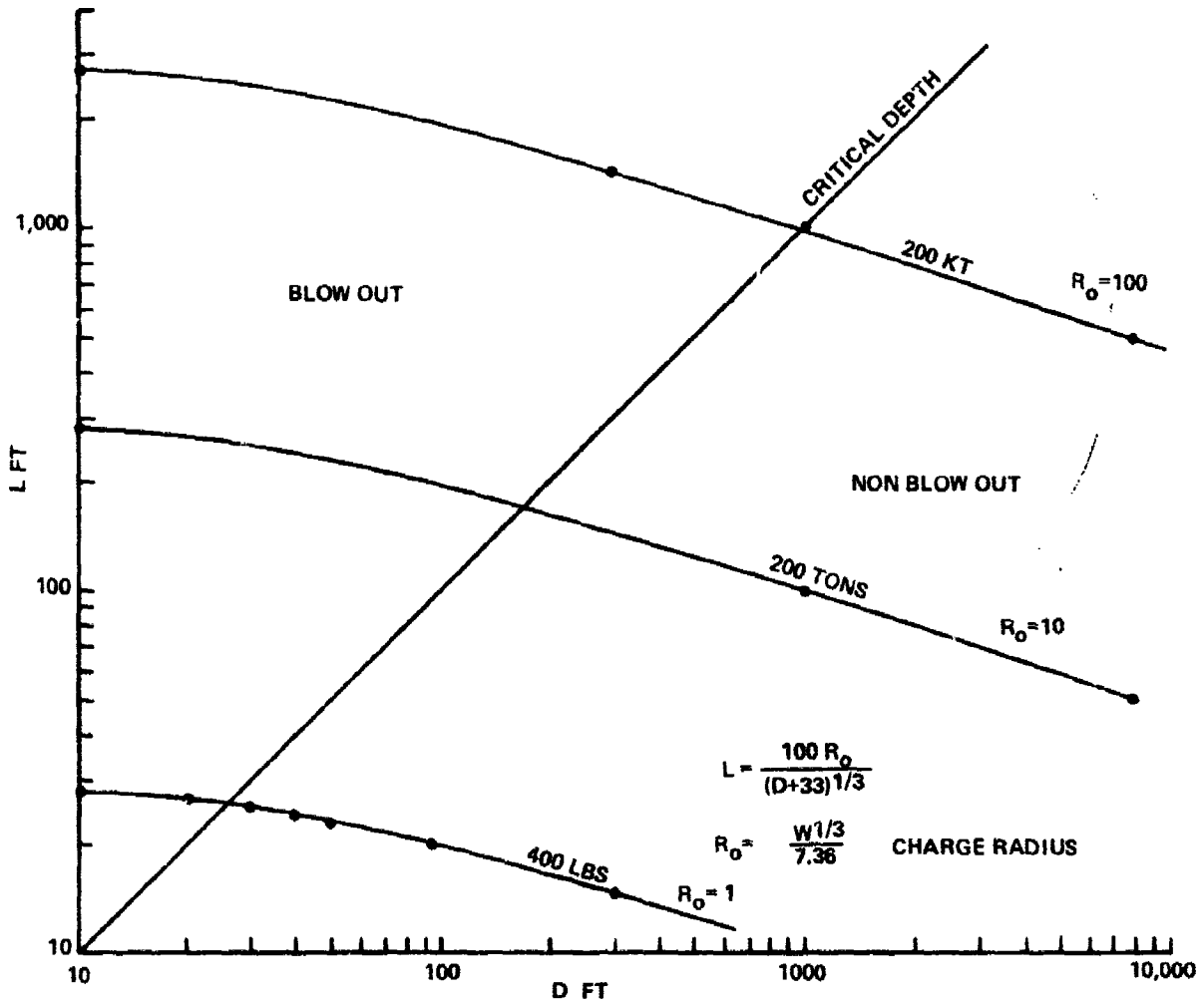

FIG. 21 BUBBLE RADIUS VS. DEPTH

For much larger charges the value of G approaches a maximum which is shown by the extremes plotted in Figure 19. These values should be used in the previous expression for H.

In general it may be said that the phenomena are complex, and that the theory which deals with most of the cases is also complex and difficult to apply in a simple manner. Predicted durations of positive or negative phases are awkward to make but quite accurately reflect the observations. Amplitudes on the other hand are subject to uncertainty because of bottom interference. Estimates however can be made with some confidence within a factor of two using ab initio Kirkwood and Seeger calculations for the nonblowout case (spherical volume) and for the blowout cases (cylindrical volume).

6. Correction Factor

Let the ratio of the calculated value of amplitude to the observed value at a distance, computed by the Kirkwood and Seeger theory, be called a correction factor. This factor becomes larger as more of the explosive energy blows out. In Figure 22 we have plotted the correction factor against D/L, where D is the depth of the charge. In all cases except Baker itself the charge was actually on the bottom. The numbers have been taken from Table 8 and elsewhere in this report. The curve may be used to adjust calculated values to values that would be expected to be observed. "Calculated" here means using the original spherical volume formula

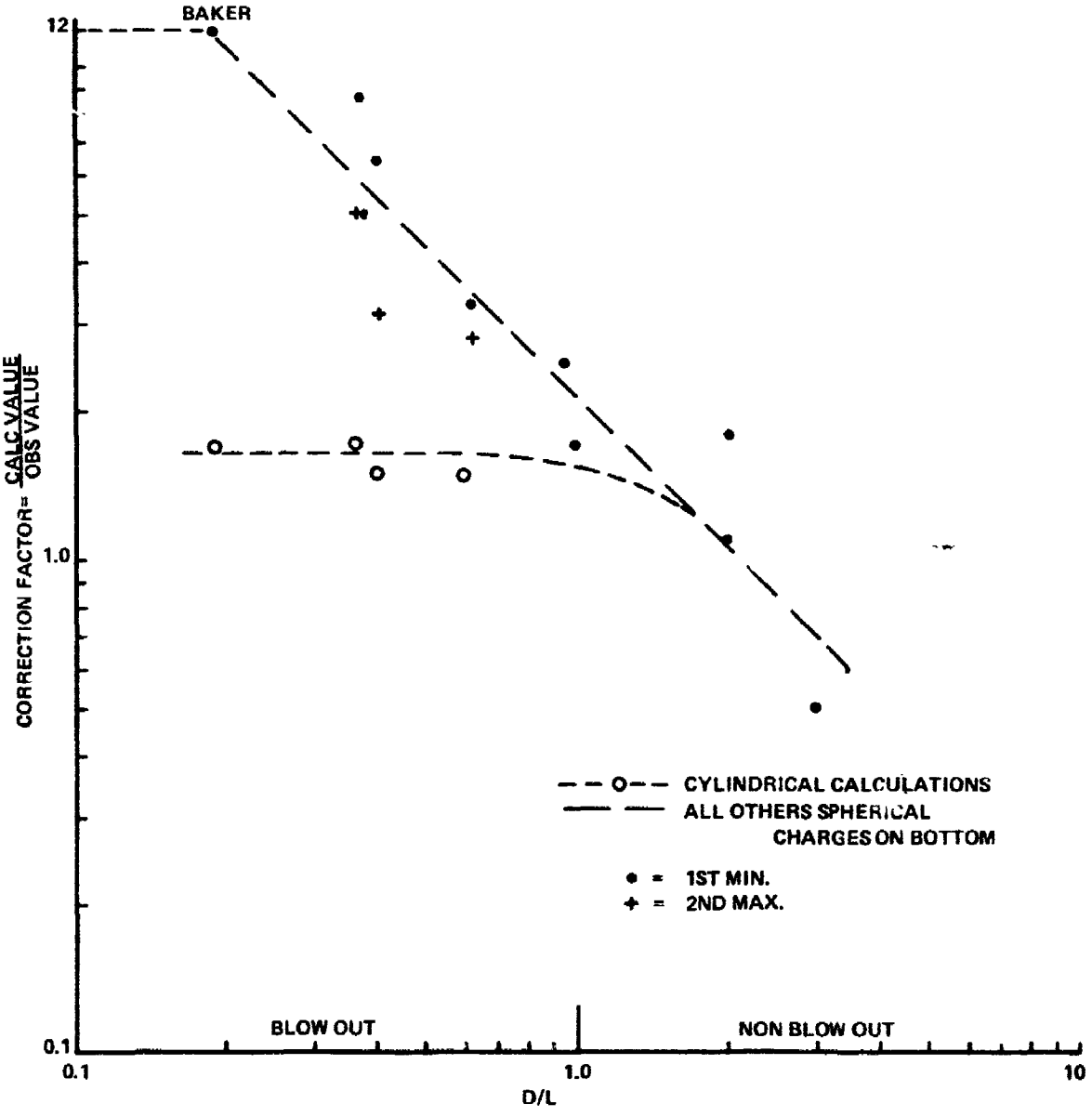

FIG. 22 CORRECTION FACTOR VS. $\frac{D}{L}$

for all depths. The dotted line in the graph for the blowout region has been adjusted for the smaller cylindrical volume. If a charge at depth D is not on the bottom, then the expectation is that the waves will be bigger than if it were on the bottom. The theory would restore the troublesome factor of two in this case. Unfortunately, we do not have enough data with charges off the bottom to establish what will happen.

7. Estimate for Critical Depth Case for a Large Explosion

It is, however, possible to use the theory to make reasonable estimates in nonblowout cases. As an example, suppose one wished to calculate the height of the second crest when 1 megaton is exploded at critical depth for wave making. Such a depth may be seen from Figure 15 to be a_{max} = 1400 feet. If we have L = h = a_{max}, then ρ_{2max} = .1606 a_{max} G_{2max} ft or ρ_{2max} = 223 G_{2max} feet (charge on bottom).

From Figure 19 we can construct the following:

r' =	5	10	15	25	50	500
G_{2max} =	.1156	.0694	.0497	.0318	.0169	∿.0019
Calculated height, ρ_{2max} =	25.8 ft	15.5	13.3	7.1	3.76	0.42

r	=	7000 ft	14,000	21,000	35,000	70,000	700,000
r	=	1.17 nautical miles	2.33	3.5	5.8	11.7	116.5

According to Figure 22 these calculated heights are about twice what would be observed.

If water depth is greater than the charge depth, say $>2a_{max}$, then the factor of 2 in the bubble volume should be restored. However, the values of G are approximately doubled (for half the values of r'), and the doubled depth requires division by four. Consequently, the waves should be about the same height at the same distance whether the charge is halfway down or on the bottom, as long as its depth is the same neglecting additional energy absorption by the bottom. The theory predicts that the first crest is 3 to 25% lower than the second crest as distance increases. The available data on the first crest are insufficient to confirm or deny this prediction. We shall therefore take the second crest as the largest predicted crest. Figure 22 shows that for critical depth the spherical theory overestimates by a factor of about 2.0. Hence the wave height at say 14,000 feet should be $\frac{15.5}{2.0}$ x 2 (trough to crest) or 15.5 feet. This gives HR = 15.5 x 14,000 = 218,000 $feet^2$ which is only 2.5 times the value of the corresponding product for Baker. However, if a megaton were placed at a depth of 2 charge radii in water 4 radii deep, then we would have a situation exactly scaled to

Baker with 50 times the charge weight. The water depth would be 660 feet, and the HR product would be 85,000 x $\sqrt{50}$ or 600,000. We then predict that at a given distance the wave height (trough to crest) would be 7 times that observed at Baker and in fact nearly 3 times (2.8) higher than the same charge would produce if placed at the "critical" depth of 1400 feet.

By arguments of this sort one can estimate the wave effects from large explosions. It is hoped that the estimate will remain academic!

8. Ocean Impact of an Asteroid

If a spherical asteroid of radius of say 100 feet were to crash into the deep ocean, what sort of wave disturbance would be created? There would, of course, be a huge splash followed by the formation of a water crater and thereafter the production of surface waves. Consider that the kinetic energy of the asteroid on impact may be treated as the explosion of a weight of explosive (TNT) at rest having the same energy. For example, an asteroid of radius 100 feet, specific gravity 5, and impact velocity of 7 miles/sec would have 2.8×10^{16} ft/lbs of kinetic energy. This can be equated to 1.9×10^{10} lbs of explosive, (1.48×10^{6} ft/lbs per lb of explosive) or very close to 10 megatons. The critical depth for such an explosion is 2500 feet (Figure 15). The charge radius would be 362 feet. The chief uncertainty is at what depth the energy could be

considered released. This will depend on the body shape. The worst case would be to assume a Baker geometry. Hence the water depth will be presumed to be at least 4 charge radii (to match Baker) or greater than say 1500 feet deep. An estimate of the waves may then be made by setting,

$$HR = 85{,}000 \left(\frac{1.9 \times 10^{10}}{4 \times 10^{7}}\right)^{1/2} = 1.85 \times 10^{6} \text{ ft}^2.$$

If R is in nautical miles, H in feet we have

$$HR = 307.$$

This also says that if a 10 megaton event were to occur, in water 1500 feet deep the trough to crest wave height at a distance of ten miles would be 31 feet in water of uniform depth. If such a wave were to impinge on a beach or shore line, the resulting breaking wave could be as much as 2 or even 3 times higher depending on the bottom contour. If the water were shallow enough so that there were no dispersion, then the waves would fall off as $\frac{1}{\sqrt{R}}$ rather than as $\frac{1}{R}$, and hence would be 40% higher at twice the distance. In other words, if the waves got out to 10 miles at a height of 31 feet, they

could arrive at 20 miles at a height of 21 feet rather than 15.5 feet. The impact of a 10 megaton equivalent asteroid would have a rather local effect as far as waves are concerned on a global scale. The trough to crest height would probably be less than ten feet at 40 miles from impact point.

REFERENCES

1. Thorade, H., "Probleme der Wasserwellen," Henri Grand, Hamburg 1931, Corrected Translation by Beach Erosion Board reproduced (J. R. Davis, Jr.) as NOLM 5310, April, 1944.
2. Landau and Lifshitz, "Fluid Mechanics," Section 12, Pergamon Press 1959.
3. Cauchy 1815, "Memoire sur la Theorie des Ondes," Mem. de l'Acad. Roy. des Sciences, Paris.
4. Poisson 1816, "Memoire sur la Theorie des Ondes," Mem. de l'Acad. Roy. des Sciences, Paris.
5. Penney, W. G., "Gravity Waves Produced by Surface and Underwater Explosions," March 1945, Underwater Explosion Research, Vol. II, pp. 679-693.
6. Kirkwood, J. G. and Seeger, R. J., "Surface Waves from an Underwater Explosion," Journal of Applied Physics, Vol. 19, pp. 346-360, April 1948. Also (6a), the same paper in Underwater Explosion Research* Vol. II, "The Gas Globe," pp. 707-760, containing tables of the functions $G_o(r',o,t')$ (bottom) and $G_o(r',1,t')$ (surface) vs. reduced time for selected values of r'. These integrals had been computed by the Mathematics Tables Project under the Applied Mathematics Panel of the National Defense Research Committee by G. Blanch and A. N. Lowan.

*A Compendium of British and American Reports published in 1950 by ONR; Editors, G. K. Hartmann and E. G. Hill.

7. Coulson, C. A., "Waves, a mathematical account of the common types of wave motion," Oliver and Boyd Ltd, 1941.

8. Lamb, H., "Hydrodynamics," 6th revised edition 1932 New York, Dover Publications, 1945.

9. Spitzer, R. W., "Production of Surface Waves by Underwater Explosion," (Distributed and Lumped Charges) UERL draft 29 Nov 1944. WHOI

10. Charlesworth, G., "Surface Waves Produced by Firing Underwater 32-lb. charges of Polar Ammon. Gelignite at Various Depths," UER Vol. II, pp. 695-700.

11. Bryant, A. R., "Surface Waves Produced by Underwater Explosion - Comparison of the Theory of W. G. Penney with Experimental Results for a 32-lb charge." UER Vol. II, pp. 701-706.

12. Shiffman, M. and Friedman, B., "Studies on the Gas Bubble Resulting from Underwater Explosions," Underwater Explosion Research Vol. II, pp. 245-320.

13. Stoker, J. J., "Water Waves," p. 337, Interscience Publishers, Inc., New York, 1957.

14. Focke, A. B., Naval Electronics Laboratory, San Diego, Field Communication (1946).

15. O'Brien, M. P., University of California, Field Communication (1946).

16. "The Effects of Atomic Weapons" June 1950. U.S. Govt. Printing Office, Washington, 25, D.C.

Gravity waves in cylindrical coordinates. The argument is reproduced here because it is difficult to find in one place. Assume cylindrical symmetry. $\nabla^2\phi = 0$, where ϕ = velocity potential

or

$$\frac{\partial^2\phi}{\partial r^2} + \frac{1}{r}\frac{\partial\phi}{\partial r} + \frac{\partial^2\phi}{\partial z^2} = 0$$

Assume separation of variables,

then $\phi = RZ$

$$\phi = J_o(kr)\ (Ae^{kz} + Be^{-kz}) \quad .$$

Chose origin in rigid bottom. Depth of water = h.

Boundary conditions:

At the bottom, (1) $\left(\frac{\partial\phi}{\partial z}\right)_{z=0} = 0$

Bernoullis equation, neglecting the square of the particle velocity, is

$$\frac{p-p_a}{\rho} = \frac{\partial \phi}{\partial t} - g(z-h)$$

This equation comes from integrating Euler's equation of motion.

At the surface, (2) $(\frac{\partial^2 \phi}{\partial t^2} + g \frac{\partial \phi}{\partial z})_{z=h} = 0$, i.e., pressure at surface is constant.

The first boundary condition requires A = B.

Hence $\phi(r,z) = A_1 J_o (kr) \cosh kz$, where $A_1 = 2A$.

Try $\phi(r,z,t) = A_1 J_o (kr) \cosh kz \cos \omega t$; where $\omega = \frac{2\pi V}{\lambda}$

Then second boundary condition gives

$$\omega^2 = gk \tanh kh$$

to interpret k, note that if kh is small, we have $\omega^2 = gk^2h$

or $(\frac{2\pi}{\lambda} V)^2 = gk^2h$

or $k = \frac{2\pi}{\lambda}$ if $V^2 = gh$ as is known for shallow water waves.

To find displacement amplitude ζ at any point, z,

$$\frac{\partial \zeta}{\partial t} = - \frac{\partial \phi}{\partial z} = - A_1 \, k \, J_o \, (kr) \, \text{sink} \, kz \cos \omega t.$$

or $\zeta = -A_1 \dfrac{k \, J_o \, (kr)}{\omega} \sinh kz \sin \omega t;$

at $\zeta = \eta$, (Surface amplitude) $z = h$,

$$\therefore \eta = -A_1 \frac{k \, J_o \, (kr)}{\omega} \sinh kh \sin \omega t$$

From Bernoullis equation,

$$\frac{p - p_a}{\rho} = -\omega \, A_1 \, J_o \, (kr) \cosh kz \sin \omega t - g(z-h).$$

The static pressure at any point z is $p_o + \rho g \, (h-z)$

Hence excess pressure due to waves at any point z is

$$\frac{\Delta p}{\rho} = - \omega \, A_1 \, J_o (kr) \cosh kz \sin \omega t$$

Combining expressions for Δp and η, we find:

$$\eta = \frac{\Delta p}{\rho g} \frac{\cosh kh}{\cosh kz}$$

If we write $|\Delta p| = \frac{\Delta p}{\rho g}$, i.e., pressure in linear units, η in linear units.

$$\eta = |\Delta p| \frac{\cosh kh}{\cosh kz}$$

If $|\Delta p|$ is measured on the bottom where z=o, we have the simple relation, $\eta = |\Delta p| \cosh kh$ which holds for a train of cylindrical or plane waves of wavelength $\lambda = \frac{2\pi}{k}$.

APPENDIX B

Energy in surface waves. [Ref. (8), p. 369]

Kinetic + Potential energy per unit area = $\frac{\rho g a^2}{2}$ ft lb/ft^2

where a = surface amplitude; p = 2 slug/ft^3; g = 32 ft/sec^2.

The area covered by this is that covered by the wave whose amplitude is a. It is necessary therefore in computing the total wave energy to know how many waves there are, their wavelengths and their amplitudes. Since we do not have a measurement of the wave pattern everywhere at the same instant, we will take the pattern as it passes a point of observation, namely pole 16, Shot 4 Solomons. There we find that six major waves went by followed by about six smaller waves. The first positive disturbance arrived at the pole 2140 feet from the explosion after approximately 60 seconds. Hence its average velocity was about the same as the shallow water wave velocity for very long waves ($\sqrt{40g}$ = 36 ft/sec). We shall assume this velocity in order to estimate the wavelengths.

$$E/\text{Area} = \frac{2 \times 32}{2} \frac{a^2}{144} = .222a^2 \text{ ft lbs/ft}^2$$

(a in inches).

Wave energy calculated for Shot 4 Solomons.

Wave number (1st crest is No. 1.)	1	2	3	4	5	6	7	8	9-12
Amplitude (1/2 crest + trough)	3"	2"	5.5"	5.5"	5.5	5.5	5.5	3.5"	2.5
Period (crest to crest)	12 sec	8.0	8.0	7.0	6.7	6.0	6.0	5.7	4.7
Wavelength = 36 x Period	430 ft	290	290	250	240	216	216	205	169
E ftlbs/ft^2 =.222 a^2	2.0	.89	6.66	6.66	6.66	6.66	6.66	2.7	1.39
Area = $2\pi(2140)\lambda$ ft^2	5.77 x 10^6	3.9 x 10^6	3.9 x 10^6	3.36 x 10^6	3.22 x 10^6	2.9 x 10^6	2.9 x 10^6	2.75 x 10^6	2.26 x 10^6
E x A ft. lbs x 10^{-6}	11.5	3.5	26.0	22.4	21.5	19.3	19.3	7.5	3.2

Total wave energy in 12 waves = 143.8×10^6 ft/lbs.

Charge wt of 46,000 lbs has total energy of $46{,}000 \times 1.48 \times 10^6$ ft/lbs. or $68{,}000 \times 10^6$.

$\therefore$ Total wave energy is approx $\frac{143.8}{68000}$ = .21% of total energy.

A similar calculation for Shot 2 at pole 12:1007 ft. from 6700 lbs.

Wavelength	188 ft.	139	112	103	94.5	93	91	87.5	87.5	91.5
Amplitude = 1/2 wave height	3.35"	2.20	.6	1.0	2.0	2.6	3.75	5.0	3.75	2.2
Area = $2\pi(1007)\lambda$	11.8 $\times 10^5$	8.8 $\times 10^5$	7.1 $\times 10^5$	6.5 $\times 10^5$	5.9 $\times 10^5$	5.9 $\times 10^5$	5.7 $\times 10^5$	5.5 $\times 10^5$	5.5 $\times 10^5$	5.7 $\times 10^5$
$\frac{\text{ExA ft lbs} \times 10^{-5}}{.222}$	133.	42.	2.5	6.5	23.6	40.	80	138	77	28

Total wave energy in 10 waves = 571×10^5 ft/lbs x .222 = 127×10^5 ft/lbs.

Total energy is $6700 \times 1.48 \times 10^6$ ft/lbs.

Fraction in waves = $\frac{127 \times 10^5}{10^{10}}$ or .127% of total energy.

"The Effects of Atomic Weapons"[16], p. 102, finds the wave energy at Baker to be between 0.3 and 0.4 percent of the nominal (20 kt) energy.

The fraction of the total energy which goes into wave making is so small that it is perhaps not surprising to find large changes in this fraction with small changes in depth. The estimates made here for Solomons' Shots 2 and 4 are not accurate but do indicate the same order of magnitude as found at Baker with a progressively larger fraction of the energy going into waves as the relative depth is diminished.

APPENDIX C

Dispersive Medium - Yes & No?

If $\lambda >> 2\pi h$, then the velocity of all such waves is equal to gh and this is their maximum velocity. All such wavelengths travel at this same velocity and hence the medium is nondispersive. However, if λ is not $>> 2\pi h$, i.e., if λ is of order of $2\pi h$ (or less than $2\pi h$) than the longer waves travel faster than the shorter waves. If wavelength is small or water is deep, then $V^2 = \frac{g\lambda}{2\pi}$ and medium is dispersive. Consider three successive peaks in a wave system, travelling from left to right in deep water.

If the distance from 1 to 2 is greater than from 2 to 3, the peaks 1 and 2 will separate faster than 2 and 3 because the wavelength and hence velocity associated with 1 and 2 are greater than those associated with 2 and 3.

If a set of waves starts out with a large wavelength or separation between the first few peaks, and a small separation between the later peaks, then the first ones should separate from the later ones. If a set of waves all have the same wavelength, then they should travel at the same speed and not show a growing separation. If we start out with a group of different wavelengths, then the longer ones will separate from the shorter ones, provided they all are comparable to $2\pi h$ or less. All of these remarks are contained in the expression for wave velocity,

$$V^2 = \frac{g\lambda}{2\pi} \tanh \frac{2\pi h}{\lambda}$$

where λ = wavelength, and h = water depth. This expression holds for plane waves or cylindrically spreading waves, and is a result of the linear wave equation derived from neglecting the square of the particle velocity in the equation of motion. It holds for wave amplitude small compared with water depth, and assumes that the upward component of the acceleration of the water particles has a negligible effect on the pressure due to the wave which depends only on the wave amplitude. The expression does hold for the "shallow water" case as well as for the deep water case, i.e., for the nondispersive case and the dispersive case. The expression is in fact the arbiter of the choice.

If $\frac{2\pi h}{\lambda}$ is small, then $\tanh \frac{2\pi h}{\lambda} \to \frac{2\pi h}{\lambda}$

Hence $V = \sqrt{gh}$ for λ large compared with h.

If $\frac{2\pi h}{\lambda}$ is large, then $\tanh \frac{2\pi h}{\lambda} \to 1$.

Hence $V = \sqrt{\frac{g\lambda}{2\pi}}$ for h large compared with λ.

The latter is called the deep water case. The former is called the shallow water case (even when it refers to tides in the ocean).

APPENDIX D

Maximum and Minimum Values of G and Durations on the Bottom as a Fcn of τ', or Table Showing Influence of Bubble Period on Amplitude and Duration.

	$G_{o,\tau'}(r',o,t'_m)$				Duration $T^{\perp}$			
	Maximum		Minimum		Maximum		Minimum	
τ'	1st	2nd	1st	2nd	1st	2nd	1st	2nd
				r' = 5				
.059	.0018	.0042	-.0047	-.0025	5.05	2.90	3.82	2.26
.1	.0029	.0071	-.0079	-.0042	5.05	2.91	3.81	2.26
.2	.0059	.0142	-.0158	-.0084	5.05	2.90	3.87	2.26
.3	.0088	.0213	-.0237	-.0125	5.15	2.90	3.82	2.29
.4	.0117	.0282	-.0315	-.0165	5.26	2.90	3.75	2.28
.5	.0146	.0351	-.0393	-.0205	5.25	2.90	3.81	2.28
.6	.0175	.0419	-.0469	-.0244	5.30	2.91	3.81	2.27
.7	.0203	.0486	-.0545	-.0281	5.34	2.91	3.82	2.28
.8	.0232	.0551	-.0620	-.0318	5.39	2.91	3.82	2.28
.9	.0260	.0615	-.0694	-.0352	5.44	2.91	3.82	2.28
1.0	.0288	.0676	-.0766	-.0386	5.48	2.92	3.83	2.28
1.1	.0315	.0736	-.0837	-.0417	5.53	2.92	3.83	2.28
∞	.0858	.0311	-.0988	-.0296	6.98	2.09	3.76	2.61
				r' = 10				
.059	.0008	.0027	-.0025	-.0021	10.35	3.37	4.48	2.73
.1	.0014	.0046	-.0042	-.0036	10.35	3.37	4.48	2.74
.2	.0028	.0091	-.0084	-.0071	10.41	3.37	4.47	2.79
.3	.0042	.0136	-.0125	-.0106	10.46	3.37	4.47	2.73
.4	.0055	.0180	-.0166	-.0142	10.51	3.37	4.47	2.73
.5	.0069	.0224	-.0207	-.0175	10.56	3.37	4.47	2.73
.6	.0083	.0268	-.0247	-.0209	10.60	3.37	4.48	2.73
.7	.0097	.0311	-.0288	-.0242	10.65	3.37	4.48	2.72
.8	.0111	.0354	-.0328	-.0274	10.69	3.38	4.49	2.68
.9	.0124	.0396	-.0368	-.0305	10.74	3.37	4.49	2.73
1.0	.0137	.0437	-.0407	-.0336	10.79	3.37	4.49	2.73
1.1	.0150	.0476	-.0447	-.0365	10.83	3.37	4.50	2.73
∞	.0495	.0315	-.0645	-.0301	12.59	2.66	4.27	2.83
				r' = 15				
.059	.0005	.0019	-.0017	-.0017	15.55	3.66	4.98	3.08
.1	.0009	.0032	-.0028	-.0028	15.50	3.70	5.03	3.07
.2	.0018	.0064	-.0055	-.0056	15.60	3.70	4.98	3.07
.3	.0027	.0096	-.0083	-.0084	15.65	3.69	4.99	3.06
.4	.0035	.0128	-.0110	-.0111	15.70	3.70	4.98	3.07
.5	.0044	.0160	-.0137	-.0138	15.75	3.72	4.97	3.05
.6	.0052	.0191	-.0164	-.0164	15.79	3.72	4.98	3.06
.7	.0061	.0222	-.0191	-.0190	15.84	3.71	4.99	3.05
.8	.0069	.0252	-.0218	-.0216	15.89	3.72	4.98	3.06
.9	.0078	.0282	-.0244	-.0241	15.93	3.73	4.98	3.06
1.0	.0086	.0312	-.0271	-.0266	15.98	3.74	4.98	3.05
1.1	.0095	.0340	-.0297	-.0290	16.03	3.74	4.98	3.05
∞	.0349	.0274	-.0484	-.0265	18.01	3.03	4.69	3.09
				r' = 25				
.059	.0004	.0012	-.0009	-.0011	27.70	4.25	5.84	3.54
.1	.0006	.0021	-.0016	-.0019	25.75	4.26	5.82	3.52
.2	.0011	.0040	-.0032	-.0037	25.80	4.21	5.82	3.55
.3	.0016	.0061	-.0048	-.0055	25.80	4.21	5.86	3.56
.4	.0021	.0081	-.0063	-.0073	25.87	4.23	5.83	3.56
.5	.0026	.0100	-.0079	.0090	25.90	4.22	5.86	3.56
.6	.0031	.0120	-.0095	-.0108	25.95	4.22	5.86	3.55
.7	.0036	.0139	-.0110	-.0125	25.98	4.25	5.87	3.54
.8	.0041	.0158	-.0126	-.0142	26.03	4.24	5.87	3.55
.9	.0046	.0176	-.0141	-.0159	26.08	4.23	5.87	3.56
1.0	.0050	.0195	-.0156	-.0176	26.13	4.27	5.86	3.53
1.1	.0055	.0213	-.0171	-.0192	26.18	4.24	5.86	3.56
∞	.0220	.0207	-.0322	-.0207	28.62	3.55	5.36	3.51

APPENDIX D (Continued)

Maximum and Minimum Values of G and Durations on the Bottom as a Fcn of τ', or Table Showing Influence of Bubble Period on Amplitude and Duration.

	$G_{o,\tau'}(r',o,t'_m)$				Duration T^1			
	Maximum		Minimum		Maximum		Minimum	
τ'	1st	2nd	1st	2nd	1st	2nd	1st	2nd
				r' = 50				
.059	.0001	.0006	-.0004	-.0006	51.15	5.20	7.05	4.35
.1	.0002	.0010	-.0007	-.0010	51.20	5.10	7.05	4.35
.2	.0005	.0019	-.0014	-.0019	51.25	5.20	7.02	4.29
.3	.0007	.0029	-.0021	-.0029	51.30	5.20	7.03	4.32
.4	.0009	.0038	-.0028	-.0038	51.35	5.20	7.00	4.35
.5	.0011	.0047	-.0035	-.0047	51.50	5.20	6.90	4.33
.6	.0013	.0056	-.0042	-.0057	51.45	5.20	7.00	4.33
.7	.0015	.0066	-.0049	-.0066	51.50	5.21	7.00	4.33
.8	.0017	.0075	-.0055	-.0075	51.50	5.21	7.05	4.32
.9	.0019	.0084	-.0062	-.0084	51.57	5.22	7.03	4.33
1.0	.0021	.0093	-.0069	-.0093	51.63	5.22	7.02	4.32
1.1	.0023	.0102	-.0075	-.0102	51.65	5.23	7.05	4.31
∞	.0117	.0130	-.0181	-.0132	54.61	4.40	6.53	4.25
				r' = 500				
.1	.00001	.00006	-.00004		502.90	10.65	14.70	
.2	.00002	.00012	-.00008		503.25	10.70	14.35	
.3	.00003	.00017	-.00012		503.23	10.70	14.40	
.4	.00005	.00023	-.00016		503.30	10.75	14.35	
.5	.00006	.00029	-.00019		503.35	10.65	14.45	
.6	.00007	.00035	-.00023		503.40	10.70	14.40	
.7	.00008	.00040	-.00027		503.50	10.65	14.40	
.8	.00009	.00046	-.00031		503.60	10.70	14.30	
.9	.00010	.00051	-.00035		503.65	10.65	14.35	
1.0	.00011	.00057	-.00038		503.65	10.60	14.40	
1.1	.00012	.00063	-.00042		503.65	10.68	14.42	
∞	.00128	.00177	-.00211		510.18		13.34	

DISTRIBUTION

Lockheed Missiles and Space Company
320 Logue Avenue
Mountain View, CA 94040
Attn: Dr. William F. Whitmore

Martin Marietta Aerospace
Orlando Division
Post Office Box 5837
Orlando, FL 23805
Attn: Mr. T. E. Dolan

Martin Marietta Aerospace
1800 K Street NW
Washington, DC 20006
Attn: Mr. J. Sullivan

U.S. Naval Institute
Annapolis, MD 21402

National Academy of Sciences
2101 Constitution Ave NW
Washington, DC 20418
Attn: Lee Hunt

National Academy of Sciences
Naval Studies Board
21st and Pennsylvania Ave
Washington, DC 20418

Director
Naval Historical Center
Washington Navy Yard
Washington, DC 20390
Attn: VADM E. Hooper

VADM Frederick L. Ashworth, USN
Sunlit Hills
Route #3
P.O. Box 90T
Santa Fe, NM 87501

RADM Alexander S. Goodfellow, USN
409 First Street
Coronado, CA 92118

Dr. William B. Graham
Head, Engineering Sciences Dept.
RAND Corporation
1700 Main Street
Santa Monica, CA 90406

Dr. William Q. Jeffers
Senior Scientist
McDonnell Douglas
Research Laboratories
P.O. Box 516
St. Louis, MO 63166

Dr. John F. Moore
1121 Denmark Road
Plainfield, N.J. 07062

Mr. John A. Saxten
135 Via Concha
Aptos, CA 95003

Professor Jerome Smith
Associate Professor
Aeronautical Engineering
Princeton University
Princeton, NJ 08540

Goodyear Aerospace Corporation
1210 Massillon Drive
Akron, OH 44315
Attn: W. F. Johnson

Gould, Inc.
Advanced Technology Group
18901 Euclid Avenue
Cleveland, OH 44117
Attn: T. E. Lynch

Harry Diamond Laboratories
(AMXDO-SAB)
Washington, DC 20438
Attn: M. B. Ginsberg

Honeywell, Inc.
600 N. 2nd Street
Hopkins, MN 55343
Attn: J. O. Voss

I. E. DuPont De Nemours & Co. Inc.
Wilmington, DE 19898
Attn: L. M. Magner

Lockheed Ocean Laboratory
3380 N. Harbor Drive
San Diego, CA 92101
Attn: RADM L. D. Coates, USN (Ret)

Presearch, Inc.
8720 Georgia Avenue
Silver Spring, MD 20910
Attn: G. L. Brubaker
T. C. Cox
J. R. Penny
CAPT D. E. Hihn, USN (Ret)

The Rand Corporation
1700 Main Street
Santa Monica, CA 90406
Attn: Dr. M. M. Balaban
J. W. Higgins
Dr. J. E. Neufer

Government Plans and
Systems Development
RCA Corporation (108-113)
Borton Landing Road & Marne Highway
Moorestown, NJ 08057
Attn: BGEN F. P. Henderson, USMC (Ret)

Leland Stanford Junior University
Stanford University
7100 Serra Street
Stanford, CA 94305
Attn: Drw D. B. DeBra

Thiokol Chemical Corporation
Elkton Division
Elkton, MD 21921
Attn: O. D. Reed

TRACOR, Inc.
6500 Tracor Lane
Austin, TX 78721
Attn: D. R. Sanders

TRACOR Marine, Inc.
P.O. Box 13107
Port Everglades, FL 33316
Attn: Dr. M. L. Collier

U.S. Steel Corporation
600 Grant Street, Rm 2175
Pittsburgh, PA 15219
Attn: M. A. Burello

Commandant
15th Naval District
FPO New York 09580

Commandant
Naval District Washington
Washington Navy Yard
Washington, DC 20390

Applied Research Laboratories
The University of Texas at Austin
P.O. Box 8029
Austin, TX 78712
Attn: Dr. C. M. McKinney
B. F. Weiss

ARINC Research Corporation
2551 Riva Road
Annapolis, MD 21401
Attn: F. C. Townley

Automation Industries, Inc.
Vitro Laboratories Division
14000 Georgia Avenue
Silver Spring, MD 20910
Attn: CAPT N. B. Atkins, USN (Ret)

Bendix Corporation
Electrodynamics Division
11600 Sherman Way
North Hollywood, CA 91605
Attn: F. Geldert

Bendix Corporation
1730 K Street, NW
Washington, DC 20006
Attn: F. L. Lundquist

Burroughs Corporation
P.O. Box 517
GVL - DS&SSG
Paoli, PA 19301
Attn: R. M. Tillman

Booz-Allen Applied Research, Inc.
4733 Bethesda Avenue
Bethesda, MA 20014
Attn: C. F. Willard

Edo Corporation
2001 Jefferson Davis Highway
Arlington, VA 22202
Attn: R. N. Flath

General Electric Company
P.O. Box 1122
Farrell Road Plant, Bldg 1, Rm M8
Syracuse, NY 13201
Attn: F. G. Spann

Commandant Industrial College
of the Armed Forces
Fort Lesley J. McNair
Washington, DC 20315

Officer in Charge
Naval Air Reserve
ASW Tactical School
Naval Air Station
Willow Grove, PA 19090

Commanding Officer
Naval Air Reserve Unit
Naval Air Facility
Washington, DC 20390

Commanding Officer
Naval Amphibious School, Little Creek
Naval Amphibious Base
Norfolk, VA 23521

Commanding Officer and Director
Atlantic Fleet ASW Tactical School
Norfolk, VA 23511

Commanding Officer
Fleet Anti-Submarine Warfare School
San Diego, CA 92147

Director Naval Weapons
Engineering Support Activity
Washington Navy Yard
Washington, DC 20390

Commandant
1st Naval District
495 Summer St.
Boston, MA 02210

Commandant
3rd Naval District
Flushing and Washington Aves.
Brooklyn, NY 11251

Commandant
4th Naval District
Philadelphia, PA 19112

Commandant
5th Naval District
Norfolk, VA 23511

Commandant
6th Naval District
Naval Base
Charleston, SC 29408

Commandant
8th Naval District
New Orleans, LA 70146

Commandant
9th Naval District
Building 1
Great Lakes, IL 60088

Commandant
10th Naval District
FPO New York 09551

Commandant
11th Naval District
San Diego, CA 92132

Commandant
12th Naval District
Treasure Island, Building 1
San Francisco, CA 94130

Commandant
13th Naval District
Seattle, WA 98115

Commandant
14th Naval District
Box 110
FPO San Francisco 96610

Commander Hawaiian Sea Frontier
Box 110
FPO San Francisco 96610

Commander Western Sea Frontier
Treasure Island
San Francisco, CA 94130

Commander Amphibious Force
U.S. Pacific Fleet
San Diego, CA 92155

Commander
Antisubmarine Warfare Force
U.S. Pacific Fleet
FPO San Francisco 96610

Commander
U.S. Naval Forces, Japan
FPO Seattle 98762

Commander
U.S. Naval Forces, Korea
APO San Francisco 96301

Deputy Commander Operational Test
and Evaluation Force, Pacific
Naval Air Station, North Island
San Diego, CA 92135

Commander Mine Flotilla 3
U.S. Pacific Fleet
FPO San Francisco 96601

Commander Amphibious Group 1
FPO San Francisco 96601

Commander Submarine Squadron 1
FPO San Francisco 96601

Commander Fleet Air Wing 1
FPO Seattle 98768

Commander Fleet Air Wing 2
FPO San Francisco 96601

Commander Fleet Wing 10
FPO San Francisco 96601

Director
Institute for Defense Analyses
400 Army-Navy Drive
Arlington, VA 22202

Chief of Research and Development
Department of the Army
Washington, DC 20315

Commander Army Material Systems
Analysis Agency
Aberdeen Proving Ground, MD 21005

Commandant
Armed Forces Staff College
Norfolk, VA 23511

Commanding Officer
Fleet Intelligence Center, Europe
Box 18, Naval Air Station
Jacksonville, FL 32212

Commanding Officer
Fleet Weather Facility
Washington, DC 20390

Commander in Chief
U.S. Pacific Fleet
FPO San Francisco 96610

Commander, Amphibious Training
Command, U.S. Atlantic Fleet
Naval Amphibious Base, Little Creek
Norfolk, VA 23521

Commander Amphibious Force
U.S. Atlantic Fleet
Norfolk, VA 23520

Commander Antisubmarine Warfare Force
U.S. Atlantic Fleet
Norfolk, VA 23511

Commanding General
Fleet Marine Force, Atlantic
Norfolk, VA 23511

Commander
Mine Warfare Force, U.S. Navy
Charleston, SC 29408

Commander
Mine Warfare Command, U.S. Navy
Charleston, SC 29408

Commander Naval Air Force
U.S. Atlantic Fleet
Naval Air Station
Norfolk, VA 23511

Commander Operational Test and
Evaluation Force
Norfolk, VA 23511

Commander Service Force
U.S. Atlantic Fleet
Norfolk, VA 23511

Commander Submarine Force
U.S. Atlantic Fleet
Norfolk, VA 23511

Commander, Naval Inshore
Warfare Command, Atlantic
Naval Amphibious Base, Little Creek
Norfolk, VA 23521

Commander Submarine
Development Group 2, Box 70
Naval Submarine Base, New London
Groton, CT 06340

Commander Mine Squadron 10
U.S. Atlantic Fleet
FPO New York 09501

Commander Submarine Squadron 4
U.S. Atlantic Fleet
FPO New York 09501

Commander, Nuclear Weapon
Training Group, Pacific
Naval Air Station, North Island
San Diego, CA 92135

Commander
Naval Ship Research and
Development Center
Bethesda, MD 20034
Attn: Undersea Warfare Research and
Development Planning Council

Commanding Officer
Naval Ship Research and
Development Center
Annapolis, MD 21402

Commander in Chief
U. S. Naval Forces, Europe
FPO New York 09510

Commanding Officer
Naval Coastal Systems Laboratory
Panama City, FL 32401
Attn: G. Gould
Undersea Warfare Research and
Development Planning Council

Commanding Officer
Naval Torpedo Station
Keyport, WA 98345

Commander
Naval Undersea Center
San Diego, CA 92132
Attn: Undersea Warfare Research and
Development Planning Council

Commanding Officer
Naval Underwater Systems Center
Newport, RI 02840
Attn: Undersea Warfare Research and
Development Planning Council

Commander
Naval Undersea Center
3202 E. Foothill Boulevard
Pasadena, CA 91107

Commander
Naval Weapons Center
China Lake, CA 93555

Commanding Officer
Naval Weapons Station
Yorktown, VA 23491

Officer in Charge
Navy Tactical Doctrine Activity
Washington Navy Yard
Washington, DC 23090

Defense Documentation Center
Cameron Station
Alexandria, VA 22314 12

U.S. Liaison Officer to Supreme
Allied Commander, Atlantic
Norfolk, VA 23511

U.S. National Military
Representative
Supreme Headquarters
Allied Powers, Europe
APO New York 09055
Attn: US DOCO

Commander in Chief
U.S. Atlantic Fleet
Norfolk, VA 23511

Commander Second Fleet
Norfolk, VA 23511

Commander Sixth Fleet
FPO New York 09501

Commander Seventh Fleet
FPO San Francisco 96601

Commanding Officer
Fleet Intelligence Center, Atlantic
Norfolk, VA 23511

Commandant
National War College
Washington, DC 20305

Commanding Officer, Naval Reserve
Officer Corps Training Unit
University of Kansas
Lawrence, KS 66044

Director of Central Intelligence
Washington, DC 20505

Director
Defense Intelligence Agency
Washington, DC 20301

Commander, Naval Air Development
Center, Johnsville
Warminster, PA 18974
Attn: Undersea Warfare Research and
Development Planning Council

Commanding Officer
Naval Ammunition Depot
Colts Neck, NJ 07722

Commanding Officer
Naval Ammunition Depot
Hawthorne, NV 89415

Commanding Officer
Naval Ammunition Depot
FPO San Francisco 96612

Commanding Officer
Naval Civil Engineering Laboratory
Port Hueneme, CA 93043

Commander
Naval Electronics Laboratory Center
San Diego, CA 92152
Attn: Undersea Warfare Research and
Development Planning Council

Commanding Officer
Naval Explosive Ordnance Disposal
Facility
Indian Head, MD 20640

Officer in Charge
Naval Mine Engineering Facility
Yorktown, VA 23491

Commander
Naval Oceanographic Office
Washington, DC 20390
Attn: Undersea Warfare Research and
Development Planning Council

Commanding Officer
Naval Ordnance Station
Louisville, KY 40214

Commanding Officer
Naval Ordnance Systems Support
Office, Atlantic
Bldg. 62, Norfolk Naval Shipyard
Portsmouth, VA 23709

Director
Naval Research Laboratory
Washington, DC 20375
Attn: Undersea Warfare Research and Development Planning Council

Commander, Naval Safety Center
Naval Air Station
Norfolk, VA 23511

Commanding Officer
Naval Intelligence Support Center
4301 Suitland Road
Washington, DC 20390

Commander
Naval Ship Engineering Center
Prince George's Center
Hyattsville, MD 20782

Commander in Chief
DOX, Headquarters SAC
Offutt Air Force Base
Nebraska 68113

Commander
Army Materiel Command
Washington, DC 20315

Commanding General
Army Munitions Command
Picatinny Arsenal, Bldg 62N
Dover, NJ 07801

Commandant
U.S. Coast Guard
400 Seventh Street, SW
Washington, DC 20591

Commanding General, Marine Corps
Development and Education Command
(Mobility and Support Division)
Quantico, VA 22134

Director
Applied Physics Laboratory
University of Washington
Seattle, WA 98105
Attn: Undersea Warfare Research and Development Planning Council

Commandant
U.S. Army Engineer School
Combat and Training Development
Concepts and Studies Division
Fort Belvoir, VA 22060

Director
Ordnance Research Laboratory
Pennsylvania State University
State College, PA 16801
Attn: Undersea Warfare Research and Development Planning Council

Director
Scripps Institute of Oceanography
P.O. Box 1529
La Jolla, CA 92037
Attn: Undersea Warfare Research and Development Planning Council

Director
Defense Advanced Research Projects Agency/TTO
1400 Wilson Boulevard
Arlington, VA 22209

Director
Woods Hole Oceanographic Institute
Woods Hole, MA 02543
Attn: Undersea Warfare Research and Development Planning Council

Superintendent, Naval Academy
Annapolis, MD 21402

Superintendent
Naval Postgraduate School
Monterey, CA 93940

Commanding Officer
Naval School Explosive Ordnance Disposal
Indian Head, MD 20640

Commanding Officer
Fleet and Mine Warfare Training Center
Charleston, SC 29408

Commanding Officer
Naval Training Device Center
Orlando, FL 32813

President
Naval War College
Newport, RI 02840

Director
Defense Research and Engineering
Department of Defense
Washington, DC 20301

Assistant Secretary of Defense
(Systems Analysis)
Department of Defense
Washington, DC 20301

Assistant Secretary of the Navy
(Research and Development)
Navy Department
Washington, DC 20350
Attn: Dr. Sam Kosloff

Director of Navy Laboratories
Crystal Plaza Bldg. 5
Department of the Navy
Washington, DC 20390

Oceanographer of the Navy
The Madison Building
732 North Washington Street
Alexandria, VA 22314
Attn: W. H. Hymes

Chief of Naval Operations
Navy Department
Washington, DC 20350
Attn: Mine Desk

Chief of Naval Material
Navy Department
Washington, DC 20350

Project Manager
Mine Warfare Project (PM-13)
Department of the Navy
Washington, DC 20360

Chief of Naval Research
800 North Quincy Street
Arlington, VA 22217
Attn: Chief Scientist (ONR-102)

Commander
Naval Air Systems Command
Washington, DC 20360
Attn: AIR-530
AIR-5305A (L. E. Wheat)

Commander
Naval Electronic Systems Command
Washington, DC 20360

Commander
Naval Sea Systems Command
Washington, DC 20360
SEA-0332 1 SEA-09G32 2

Director and Chief
Center for Naval Analyses
1401 Wilson Boulevard
Arlington, VA 22209
Attn: Dr. J. R. Pipal

Project Manager
Deep Submergence Systems Project
Department of the Navy
6900 Wisconsin Avenue
Chevy Chase, MD 20015

Officer in Charge
Strategic Analysis Support Group
Applied Physics Laboratory
Silver Spring, MD 20910

Director
Strategic Systems Project Office
Washington, DC 20390

Library Branch
Technical Information Center
U.S. Army Engineer Waterways Experiment
Station
Vicksburg, Mississippi 39180

Defense Nuclear Agency
Washington, DC 20305

New York University
360 Lexington Avenue
New York 10017